
Technical Report 2006-02

PUGET SOUND
NEARSHORE
PARTNERSHIP

The Geomorphology of Puget Sound Beaches

Prepared in support of the Puget Sound
Nearshore Partnership (PSNP)

October 2006

David Finlayson, University of Washington



RESTORING OUR
ECOSYSTEM HEALTH



Technical subject matter of this document was produced by the Puget Sound Nearshore Partnership which is entirely responsible for its contents. Publication services were provided by Washington Sea Grant, with financial support from King Conservation District. Copyright 2005, University of Washington. This document may be freely copied and distributed without charge.

Acknowledgements

I thank Harold Mofjeld for reviewing the tide and sea-level information in this report and for suggesting that I read Pugh's book which greatly helped me; Hugh Shipman, Ralph Haugerud and Guy Gelfenbaum for many suggestions over the years, which helped me write the geology and geomorphology chapters; and my Ph.D. committee, Jeff Parsons, Miles Logsdon, Andrea Ogston, Charles Simenstad and Joan Oltman-Shay, who helped shape the material in this report in numerous ways. Special thanks are due to Jeff Wheeler and the staff of Cama Beach State Park, who graciously allowed me to deploy instruments on one of the most beautiful beaches on Puget Sound. I thank Charles Simenstad at the University of Washington and Marcus Duke and the staff of Washington Sea Grant for editing and preparing this report for publication.

This report was supported by the Puget Sound Nearshore Ecosystem Restoration Project and the U.S. Army Corps of Engineers. Research funding was obtained from Washington Sea Grant and the School of Oceanography, University of Washington.

Citation:

Finlayson, D. 2006. The geomorphology of Puget Sound beaches. Puget Sound Nearshore Partnership Report No. 2006-02. Published by Washington Sea Grant Program, University of Washington, Seattle, Washington. Available at <http://pugetsoundnearshore.org>.

Cover: Storm event at Cama Beach, Camano Island. Photo by David Finlayson.

Contents

Executive Summary.....	iv
1. Introduction	1
2. Geology	3
2.1. Large-Scale Morphology.....	3
2.2. Sediment Character and Supply.....	7
2.3. Sea-Level History and Neo-Tectonics	7
3. Waves.....	9
3.1. Wind Patterns in the Pacific Northwest	9
3.2. Wind and Wave Observations at Cama Beach.....	10
3.3. Wave Hindcasting	12
4. Water Levels.....	17
4.1. Tides	17
4.2. Surge	19
4.3. Mean Sea-Level	21
5. Beaches	24
5.1. General Characteristics	24
5.2. Puget Sound Beaches.....	29
5.3. Cama Beach	31
5.4. Longshore Transport Observations.....	39
5.5. Secondary Features.....	40
6. Conclusions.....	42
6.1. Tidal Distribution Curve.....	42
6.2. Role of Extreme Storm Events.....	42
References	43

List of Figures

2.1. Reconstruction of the Puget Lobe of the Cordillern Ice Sheet at glacial maximum ca. 16,500 cal yr before present.....	3
2.2. Digital elevation model of the Great Bend region of southwest Hood Canal.....	4
2.3. Nearshore bathymetry and topography of Piner Pt. on the southwest corner of Maury Island.....	4
2.4. Combined bathymetry and topography of Brace Pt. south of the Fautleroy (Vashon) ferry terminal, Seattle.....	5
2.5. A small creek delta near Lofall, northern Hood Canal.....	5
2.6. Bathymetry and topography of Duwamish Head, Seattle.....	6
2.7. Oblique view looking northwest at Possession Pt., southernmost Whidbey Island.....	6
2.8. The Clinton ferry terminal, Whidbey Island.....	6
2.9. Littoral cells and the direction of net shore drift for southern Whidbey Island.....	7
2.10. Relative sea-level curves for Puget Sound.....	8
3.1. Weather patterns of the Pacific Northwest.....	9
3.2. Location of Cama Beach, Washington.....	11
3.3. Time series of wind and tide observations at Cama Beach for October 2002 to May 2005.....	12
3.4. Significant wave height, significant wave period, and penetration statistics as a function of wind speed for observations at Cama Beach between September 2002 and November 2004.....	13
3.5. Probabilities of annual maximum wind speed at West Point, Seattle.....	14
3.6. Mean storm significant wave height and period for Puget Sound and Juan de Fuca Strait.....	16
4.1. An example of mixed semidiurnal tides from Elliott Bay, Seattle.....	18
4.2. Hourly tide-level histogram and associated tidal datum for Seattle between 1983 and 2001.....	18
4.3. Tidal range for Puget Sound and Hood Canal interpolated from the Puget Sound Tide Channel Model.....	19
4.4. Extra-tropical cyclone off the west coast of North America, March 3, 1999.....	19
4.5. Wind, air pressure, and tidal characteristics during an extra-tropical cyclone over the Pacific Northwest between March 1 and 6, 1999.....	20
4.6. Subtidal sea-surface levels across western Washington for 1999.....	21
4.7. The relationship between annual mean water levels and annual mean air pressures at Seattle (1984–2003).....	21
4.8. Monthly surge probability calculated by subtracting the predicted tide from the observed water level for Seattle over the period 1983–2001.....	22
4.9. Monthly subtidal SSL at Seattle and the Southern Oscillation Index for 1983–2001.....	22
4.10. Annual maximum water level above mean lower low water for Seattle.....	23
4.11. Monthly mean sea-level for Seattle.....	23
5.1. Example of a mixed sand and gravel beach foreshore.....	24
5.2. Example of a composite profile with a distinct break in slope and a break in sediment grain size between the upper foreshore and the low-tide terrace.....	24
5.3. Comparison of high-tide and low-tide wind waves.....	25
5.4. Beach seepage face, Cama Beach, Camano Island and seep-induced rilling of the low-tide terrace, Kitsap Memorial State Park, Hood Canal.....	27
5.5. Eelgrass on the low-tide terrace, Cama Beach; oyster bed on Kitsap Memorial State Park, Hood Canal.....	28

5.6. Large woody debris accumulated on the storm berm at Keystone Spit, Whidbey Island.....	29
5.7. Profile change model for low-energy beaches	30
5.8. Profile response to erosional conditions on macro-tidal, low-energy beaches	30
5.9. Location map of beaches studied in the Puget Lowland	31
5.10. Intertidal beach profiles for 23 locations in Puget Sound grouped according to shape characteristics.....	33
5.11. Cross-sections of the accretion and erosion beach segments at Cama Beach.....	34
5.12. Cross-shore profile changes at Cama Beach, August 2002–May 2005.....	35
5.13. Normalized volume change per-unit-area by profile at Cama Beach, August 2002–May 2005	36
5.14. Evolution of the upper foreshore at Cama Beach through time.....	37
5.15. Measured wind speed, wind direction, significant wave height, water level, and surge at Cama Beach during near-gale conditions, October 15–20, 2003.....	38
5.16. Vertical distributions of water level, cumulative wave energy, and profile elevation change from September 7, 2003 through November 8, 2003, at Cama Beach.....	38
5.17. Transverse bars off the west coast of Camano Island.....	40
5.18. Lag stones at Foulweather Bluff	41
5.19. Surface pavements developed on gravel beaches.....	41

List of Tables

2.1. Erosion rates of coastal bluffs on Puget Sound	8
3.1. Peak wind speeds from storms of record in the Puget Lowland, 1950–2002.....	14
3.2. Relative frequency and mean duration of exceedence for wind events in the Puget Lowland from 16 weather stations in Puget Sound for 1996 through 2004.....	16
5.1. Intertidal profile characteristics for 23 beaches in Puget Sound.....	32
5.2. Net longshore drift rates for Puget Sound.	39

Executive Summary

The preservation and restoration of nearshore ecosystems in Puget Sound (including Puget Sound, Hood Canal, Saratoga Passage, Skagit Bay and Port Susan) fundamentally depends on a sophisticated understanding of shoreline geomorphology and the processes that shape the shoreline over space and time. However, the majority of existing literature on beach geomorphology concerns open-coast sandy environments with limited tidal ranges. In contrast, the shorelines of Puget Sound are fetch-limited, composed of a mixture of glacier-derived sands and gravels, and subject to large tidal ranges. Consequently, estuarine beaches such as those found along Puget Sound's shoreline have been, so far, neglected by coastal managers and scientists alike. To date, most efforts to study Puget Sound shorelines have been limited to inventories and a quantitative, process-based knowledge of nearshore morphodynamics has yet to emerge. Preliminary studies suggest that (1) the effects of tidal distributions in concentrating wave action to the upper foreshore effect sediment transport zones and, hence, beach habitat zonation; and (2) infrequent, strong storms (return intervals greater than 1-2 years) are very important in driving the beach morphodynamic system.

The purpose of this report is to synthesize information about the geomorphology and dynamics of Puget Sound's beaches. It summarizes important peer-reviewed literature relevant to these beach environments and assembles background information that should be useful to shoreline managers and scientists alike.

Coastal Geomorphology

Throughout the Pleistocene, the Puget Lowland served as a southern terminus of the Cordilleran Ice Sheet. The advance and retreat of the last ice sheet about 16,000 years ago carved the deep troughs of Puget Sound and filled the lowland with a mixture of glaciogenic sediments. The effects of isostatic rebound and eustatic sea-level rise associated with glacial advance and retreat resulted in large variations in relative sea level over the Holocene that continue today. Regional tectonic forces have also affected relative sea level in some locations. Catastrophic vertical displacements of the marine platform have been identified at a number of east-west striking faults located throughout Puget Sound. The most dramatic of these is a 5- to 7-m vertical displacement of the marine platform in central Puget Sound dated to around 900 to 930 AD.

Modern beaches are formed on narrow, wave-cut platforms notched into the steep walls of the marine basins and channels of the Sound. Typically, the subtidal walls of the basins rise steeply until they reach the nearshore platform at around -4 m to -2 m mean lower low water (MLLW). There, a distinct break in slope forms the base of the platform. The platform rises gradually to the bottom of the coastal bluffs between 6 and 8 m MLLW. Then, the bluffs rise up to another 100 m or more above the beach level. The marine platform is narrow, typically less than 300 m across,

and it is highly three-dimensional with dramatic variation in elevation both along and across shore. The intertidal portion of the platform is the beach, with the lower intertidal and shallow subtidal portion of the platform often being called a "low-tide terrace."

The major source of sediment to the beaches is derived from the erosion and reworking of coastal bluff exposures of till, outwash sediments, and glacialmarine and glaciolacustrine deposits. These deposits often exhibit a variety of sediment facies simultaneously including clay, silt, sand, and gravel. Consequently, the beach sediments derived from these sources are similarly complex with heterogeneous mixtures of pebble gravels and coarse-grained sands being the most prevalent.

Waves

Most beaches in Puget Sound and Hood Canal are isolated from the Pacific Ocean by topography. As a result, waves in these more protected waters are generated locally by wind blowing over the irregular channels and basins of the fjord system; they receive little to no swell from the eastern Pacific. Consequently, (1) the waves have limited fetch and low energy compared with incident waves on the Pacific Coast, and (2) the wave climate is tightly coupled with local wind patterns.

The direction of prevailing wind is south or southwest during the winter and west or northwest during the summer. The strongest winds are southerlies resulting from winter storms moving inland from the eastern Pacific. Periodically during the winter, high pressure over the continent and low pressure on the coast can force air down the Fraser River valley and through the mountain passes, resulting in strong northerly winds over the Puget Sound Basin. Summer winds are slight to moderate northerlies with diurnal sea and shore breezes.

Between September 2002 and May 2005, wind speed, wind direction, wave height, and wave period were monitored nearly continuously at Cama Beach, located on the western shoreline of Camano Island, Saratoga Passage. During this period, the 15-min average wind speed was $2.6 \pm 2.5 \text{ m s}^{-1}$ with peak wind speeds ranging 10–17 m s^{-1} . The corresponding significant wave height and period were $0.24 \pm 0.19 \text{ m}$ and $2.0 \pm 0.8 \text{ s}$, respectively. Interestingly, of the 27,797 total wave measurements collected, only 3,628 (15.9%) recorded significant wave height measurements; more than 80% of the time, the wave conditions were below the signal-to-noise threshold of the wave gage (equivalent to approximately 0.1 m minimum wave height).

Whether the waves at Cama Beach are characteristic for other locations in Puget Sound is not known because no other long-term measurements are available for comparison. However, the fetches and wind climate are similar enough that some generalizations should be broadly applicable to Puget Sound and Hood Canal:

1. Waves in most of Puget Sound (probably excluding Admiralty Inlet) are generated by local winds with little or no energy component from ocean swell.
2. Normal wave conditions are very calm with little or no wave action on the smaller water bodies. Large waves (> 0.4 m significant wave height) only result during infrequent wind storms
3. Waves are fetch-limited: even during the strongest storms, the topographic confines of Puget Sound set a maximum wave height beyond which the waves cannot grow.

Storm wave heights in most channels are probably similar to Cama Beach: that is, small ($H_s < 1$ m) with short periods ($T < 4$ s). They are perhaps larger at the ends of the main Puget Sound Basin, where fetches are longest and steady winds will have greater opportunity to transfer energy to the sea. In this case, assuming a fetch of 40 km and a wind speed of 25 m s^{-1} (a 50-year storm), the estimated significant wave height and period for Puget Sound are 3.8 m and 7.1 s, respectively. Few places in Puget Sound have such a large open-water fetch and sustained wind speeds of 25 m s^{-1} are extremely rare, so these waves are about as large as will ever be observed for wind-waves in Puget Sound.

Water Levels

After waves, tides are the most important natural forcing mechanism regulating the morphodynamics of Puget Sound beaches. The twice-daily rise and fall of mean water level translates the swash zone (the portion of the nearshore region where the beach face is alternately covered by the run-up of the wave swash and exposed by the backwash [Komar, 1998, p. 47]) across the beach profile, governing the amount of time each beach elevation is exposed to wave processes. At the same time, the tides raise and lower the beach groundwater table. The resulting infiltration and exfiltration through the beach is an important component of swash-zone fluid dynamics and foreshore (the sloping portion of the beach profile lying between the upper limit of wave swash at high tide and the break in slope at the low-tide terrace [modified from Komar, 1998, p. 47]) sediment transport. Typical tidal curves in the Sound are not symmetrical. Statistically speaking, water levels are more likely to be observed above mean sea level than below. This fact has implications for sediment transport dynamics as well as the distribution of intertidal habitat.

Actual water level observations in the Sound comprise three components: (1) the gravitational or tidal component, (2) atmospheric pressure effects, and (3) mean sea level. The tidal component of water level observations is entirely predictable (these values are reported in tide tables). Similarly, over short time intervals (< 50 years), mean sea level changes are negligible. However, a change in atmospheric pressure of 1 mb produces a 19.4 mm change in sea level in Puget Sound. When this change in sea level is the result of the passage of a weather system, it is referred to as *surge*; when the change is a result of longer-term climate variations it is referred to as a *meteorological residual*.

An analysis of regional air pressure and water level observations at Elliott Bay from 1983 through 2001 reveals the following patterns in residual water levels:

1. Between December and February, 99% of surges resulted in sea level changes (from those predicted) of between -40 cm and +60 cm.
2. Between May and August, 99% of surges resulted in sea level changes (from those predicted) of between -30 cm and +30 cm.
3. Interannual fluctuations in mean water levels are coupled with climate cycles that affect the eastern Pacific. For example, during El Niño years mean air pressure drops over the region, resulting in a 10–20 cm rise in winter sea levels (over predicted tide levels).
4. The atmospheric pressure effects on sea level are regional in nature, affecting all inland waters of the Pacific Northwest and the eastern Pacific similarly.

At long time intervals (>50 years), mean sea level cannot be considered a constant. The 100-year tide record at Seattle shows that relative sea level is rising at a rate of about $+2 \text{ mm yr}^{-1}$ over the past century, Friday Harbor is rising at about $+1 \text{ mm yr}^{-1}$, and Neah Bay is *decreasing* at -1.6 mm yr^{-1} . Positive values of relative sea level in the Puget Lowland reflect eustatic sea-level rise, while the negative value at Neah Bay indicates that tectonic forces from the subduction of the Juan de Fuca plate beneath North America are uplifting the Olympic coast at a rate in excess of eustatic sea-level rise.

Beaches

Puget Sound beaches exhibit three characteristics simultaneously that are typically treated as separate beach types in the scientific literature: (1) mixed sand and gravel composition, (2) meso- to macro-tidal environments, and (3) low-energy (estuarine) wave environment. Although modern research into beach forms and processes dates back to World War II, most of this research has focused on beach environments that have well-sorted sand, high wave energy, and micro-tidal characteristics. As a result, many conventional beach models are based on assumptions about the wave environment, sediment properties, and transport mechanics that are not appropriate for Puget Sound.

Most beaches in Puget Sound have a composite profile with a narrow, steep foreshore, and a low-gradient, “low-tide” terrace. The break in slope between the upper foreshore and the terrace is typically accompanied by a break in sediment size with coarse-grained sediments found above the break and finer sediments below. The horizontal width of the foreshore is narrow and it often lacks a backshore (the zone of the beach profile extending landward from the sloping foreshore to the point of development of vegetation or change in physiography [sea cliff, dune field, etc.; Komar, 1998, p. 47]), especially when abutting a coastal bluff. The width of the low-tide terrace can extend from a few hundred meters to more than a kilometer before a second break in slope marks a distinct drop into deeper water.

The study of beach dynamics and profile response at Cama Beach State Park, Camano Island, showed that significant elevation changes were infrequent and confined to the foreshore, with little or no change observed on the intertidal portion of the low-tide terrace. The maximum elevation change observed was 0.70 m, but it was more common to see changes <0.15 m. On several surveys, the entire profile registered elevation changes beneath the vertical root mean square (RMS) error of the survey equipment (approximately ± 6 cm).

Between September 7 and November 8, 2003, a series of strong storms occurred at Cama Beach. These events represented the strongest weather observed during the investigation and resulted in the largest changes to the beach profiles. An important feature of the storm was the relationship between tide levels, storm waves, and beach change. During this storm, the strongest winds occurred during high tides. As a result, the largest waves occurred high on the beach foreshore rather than lower on the beach face or terrace. This concentrated erosion and sediment transport into a narrow corridor high on the beach.

On the basis of long-term tidal records and the typical duration of strong storms in the Sound, the observations at Cama Beach were used to develop a conceptual model of low-energy beach response in macro-tidal, mixed-sediment beaches. The model incorporates two main features:

1. An explicit accounting of the effects of the tidal distribution in concentrating wave action and hence, sediment transport, to a narrow vertical corridor located above mean sea level. Sediment transport below this zone may be negligible (on the coarse-grained foreshore, at least).
2. The most important sediment transport events observed at Cama Beach were associated with dominant storms. Dominant storms are sufficiently strong that they generate waves capable of mobilizing beach sediments, but they must occur frequently enough that their cumulative effect on the beach dominates other stronger, but more infrequent storm events. In a low-wave energy environment like Puget Sound, the dominant storm may have a return interval of several years or more but something less than a 50- or 100-year storm, which occurs too infrequently to have dominant geomorphic impact.

Secondary Features

Puget Sound beaches also exhibit many features characteristic of other low energy environments such as (1) longshore and transverse bars, (2) swash bars, (3) vegetation and wrack accumulations, (4) pebbles/shells, and (5) small sand dunes. In addition to these features, Puget Sound beaches are commonly paved with a natural pebble armor layer and cobble lag deposits. Lag deposits are large boulders that have been eroded out of coastal bluffs and deposited on the beach face. There is a certain

size beyond which no wind-generated wave in Puget Sound can mobilize these stones and they become abandoned in place. The beach simply evolves around them. In some places cobbles are sufficiently dense that they form a nearly continuous surface—a cobble lag deposit. These surfaces may not be completely immobile under storm conditions, but they are stable enough that they tend to be heavily encrusted with marine life.

Surface armoring is a related phenomenon that is found on many mixed-sediment beaches in Puget Sound. An armored surface constitutes a nearly homogeneous layer of gravel. Immediately beneath this surface layer, one finds a much more heterogeneous mixture of sand and gravel. The difference between the surface armor and subsurface is mainly the addition of fine-grained material to the mix rather than a loss of coarse clasts (rock fragment or grain resulting from the breakdown of larger rocks). Various mechanisms have been suggested for armoring including (a) gravel overpassing during the backwash, (b) a process similar to kinetic sieving when the bed is fluidized during the swash cycle, and (c) winnowing of fine-grained materials during the decelerating phase of the backwash. In comparison to gravel rivers, there has been almost no research on surface armoring of beaches under oscillatory flow, so determining what effect armoring might have on beach morphodynamics is difficult.

Conclusions

Preliminary studies of the response of beach profiles to incident wave conditions indicate the following:

1. tides play an important role in controlling the vertical level of wave attack on the shoreline, and
2. strong storms are required to mobilize coarse sediments on the beach.

However, much remains to be investigated. For example, it is not yet clear how to convert predictions of incident wave and tide conditions into sediment transport rates (particularly if the beach sediments are coarse-grained). Similarly, tidally induced seepage (from the beach face) probably plays an important role in keeping the intertidal portion of the beach foreshore irrigated during low tides. In addition to habitat implications, the seepage process likely is important for transporting fine sediments from the foreshore to the terrace—even in the complete absence of waves—but no measurements are available for Puget Sound.

Puget Sound is an extraordinary resource to the Pacific Northwest and the beaches of the Sound are an important part of the marine ecosystem. Significant urbanization of the Sound over the coming decades will put development pressure on the shorelines, as well as fundamentally alter upland sediment and water supplies to the beach. If conservation and restoration efforts are going to succeed in preserving a functional littoral system, detailed, quantitative studies of the nearshore morphodynamics will need to become a larger priority than they are at present.

1. Introduction

In the preface to Karl Nordstrom's seminal *Estuarine Beaches* (Nordstrom 1992), he justifies the lack of scientific interest in estuarine beaches as understandable because of the greater value of ocean shores to society. He continues, noting that

The low-energy of estuarine shorelines, the small and isolated nature of the beaches, the low level of investment and the unattractive appearance of many of them have caused them to be neglected both as public resources requiring management and as natural systems worthy of scientific investigation.

In Puget Sound, as in other estuaries throughout the world, our ignorance has come home to roost. By 2020, more than 8 million people are anticipated to live in the Puget Sound/Strait of Georgia region (Transboundary Georgia Basin–Puget Sound Environmental Indicators Working Group 2002). More than 50% of the emergent wetlands and tidal flats in the major deltas of Puget Sound have been lost to diking and in-filling. Between 22% and 37% of the shoreline of the main basin is estimated to have been armored by bulkheads, seawalls, piers, docks, boat launch ramps, jetties, groins, and other structures intruding into intertidal habitats (NearPRISM 2000). Shoreline managers need—and in some cases are mandated—to evaluate and manage the conflicting needs of both the natural and anthropogenic uses of the shoreline.

The intertidal nearshore of Puget Sound is a particularly visible example of coastal management needs driving scientific inquiry. The lower intertidal and shallow subtidal of most of the shorelines of Puget Sound are defined by a narrow, low-gradient platform (low-tide terrace). This is the primary habitat of eelgrass (*Zostera marina*) which, among other important functions, serves as a fish nursery and migratory corridor for many species of endangered salmonids (Phillips 1984, Anonymous 1999). The decline of these fish stocks has promoted the protection of low-tide habitat to the forefront of coastal zone management. As a result, policy makers must balance the requirements of the low-tide environment with traditional commercial and private shoreline interests.

Modern technology such as geographic information systems (GIS) and remote sensing have facilitated fairly extensive inventories of the shoreline and its various habitats; however, quantitative, process-based knowledge about how the system functions, at what rates the system functions, and to what extent modifications to parts of the system affect other areas remains lacking. Even basic environmental data are missing such as regional wave climates, shoreline geology, and nearshore bathymetry.

Most research on Puget Sound shorelines has been conducted by state agencies and local municipalities in the service of management needs. These reports provide some measurements of wave statistics, sediment composition and distribution, and shoreline change monitoring, but they often have not been vetted through a formal peer-review process. In particular, the consulting

reports of Wolf Bauer have heavily influenced local shoreline management regulations as well as introduced a number of unconventional terms into the lexicon of regional shoreline management (i.e., Bauer 1974, 1978).

Four regional shoreline mapping efforts sponsored by the state of Washington bear special mention. The earliest effort is the Coastal Zone Atlas of Washington (Youngmann 1977–1980), which presents 1:100000 scale maps of shoreline geology and littoral drift (among many shoreline themes). The Atlas estimated drift directions using hindcasting methods where historical wind data were used to approximate wave conditions and to model sediment transport directions. Unfortunately, the Atlas often resulted in transport directions contrary to those indicated by geomorphological evidence. This has been attributed to fact that wind conditions along the shoreline may not be represented well by the five wind stations employed upland and that short-term wind records did not provide a reliable basis for establishing long-term drift patterns (Jacobsen and Schwartz 1971, Schwartz et al. 1989).

The second major effort was performed by Dr. Maury Schwartz and his students at Western Washington University. They mapped littoral cells, or net shore-drift cells, and the direction of net shore-drift throughout Puget Sound using geomorphological indicators of long-term patterns of longshore transport (Schwartz et al. 1989). They applied a protocol (Jacobsen and Schwartz 1981) for delineating long-term patterns in littoral drift based on a suite of geomorphological criteria, including the effect of local obstructions to drift, systematic changes in sediment size and bluff morphology, beach morphology, and the shape of coastal landforms (e.g., spit orientation or stream mouth offsets). The study encompassing Island County was later expanded into a published USGS map (Keuler 1988).

The third regional shoreline study is the Washington State ShoreZone Inventory (Berry et al. 2001). ShoreZone characterizes approximately 4,800 km of shorelines statewide. Inter- and supratidal areas were surveyed between 1994 and 2000 using helicopter-based aerial video. These recordings were then used to create geographic data that summarize the physical and biological characteristics of the shoreline. Over 50 parameters describe shoreline geomorphology, vegetation, and anthropogenic development. The inventory is a useful catalog of regional shoreline geomorphology.

The fourth study is the result of the author's recently completed Ph.D. program at the University of Washington (Finlayson 2006). This study was designed to address the morphological and dynamic characteristics of low-energy, mixed-sediment beaches and the extent to which these factors affect intertidal habitat. It is one of the first systematic investigations of beach dynamics in Puget Sound that measured wave and tidal processes in situ as the beach morphology evolved.

This report presents information about the morphology and

dynamics of beaches common to Puget Sound. It attempts to summarize important peer-reviewed literature relevant to this unique environment and gathers together background information that should be useful to engineers and scientists. It was developed from an early draft of the author's Ph.D. dissertation

and interested readers are referred to that document for a more comprehensive and technical presentation of the material, as well as for information about experiments that were not complete at the time this report was prepared.

2. Geology

2.1. Large-Scale Morphology

Puget Sound occupies a structural basin bounded on the west by the Olympic Mountains and on the east by the Cascade Mountains. It is a region of active tectonic stresses driven by the northeastward subduction of the Juan de Fuca plate and the northward migration of the Pacific plate along the San Andreas fault (Wells et al. 1998). Throughout the Pleistocene, the Puget Lowland served as a southern terminus of the Cordilleran Ice Sheet (Figure 2.1) (Bretz 1913, Crandell et al. 1958, Armstrong et al. 1965) where as many as six distinct glacial advances filled the basin with sediment to an elevation of more than 100 m above present sea level (Booth 1994). Puget Sound itself was cut by the last advance of the ice sheet about 16900 calibrated years before present (cal yr BP). The region was ice free and inundated by marine water by 16300 cal yr BP (Booth 1994, Porter and Swanson 1998, Hewitt and Mosher 2001).

The glacial heritage of the Puget Lowland was well known to geologists by the beginning of the 20th century (Bretz 1913) and has been studied nearly continuously since then. While the thick forest canopy of the Pacific Northwest had been a serious hindrance to landscape analysis, recent developments in laser topographic mapping have enabled high-resolution digital elevation models (DEMs) of the Lowland to be constructed free of vegetation and cultural artifacts. The DEMs make it possible to distinguish at least five distinct morphological units (groups of related landforms) that shed light on the geologic history of the Lowland and its 16,000-year post-glacial recovery.

The oldest of the morphologic units (predating the Pleistocene

ice ages) are associated with the bedrock highlands of the Olympic and Cascade mountains (Figure 2.2). The mountain ranges (along with a few isolated foothills) stood well above the ice sheet even during the height of the glaciation. As a result, they do not show the fluted and streamlined topography of the lower elevations. For example, a portion of Dow Mountain (Figure 2.2, northwest corner) was sufficiently high to avoid scour by the ice sheets.

The second major morphological unit is the streamlined surface topography of the Lowland fill. As the last major ice sheet advanced into the region, an outwash plain developed in front of the glacier (Booth 1994). This fill was then overrun by the glacier and buried under the flowing ice. The resulting scour fluted and streamlined the landscape (Goldstein 1994). The strong northeast-to-southwest grain to the topography (Figure 2.2) is caused by the streamlined hills (drumlins) left by the glacier. In most locations the Lowland fill is elevated more than 100 m above present sea level.

The third major morphological unit is associated with the channels of Puget Sound itself. Modern research suggests that the channels were carved by the ice after the deposition of the Lowland fill (Bretz 1913, Crandell et al. 1965, Booth 1994). Various theories have been advanced for the exact mechanism responsible for carving the troughs (i.e., Bretz 1913, Crandell et al. 1965), but the modern consensus centers around massive sub-glacial water flows (Booth and Hallet 1993, Booth 1994). Properly speaking, the troughs are fjords since they were ice-carved, have elongated U-shaped channels, and have over-deepened basins

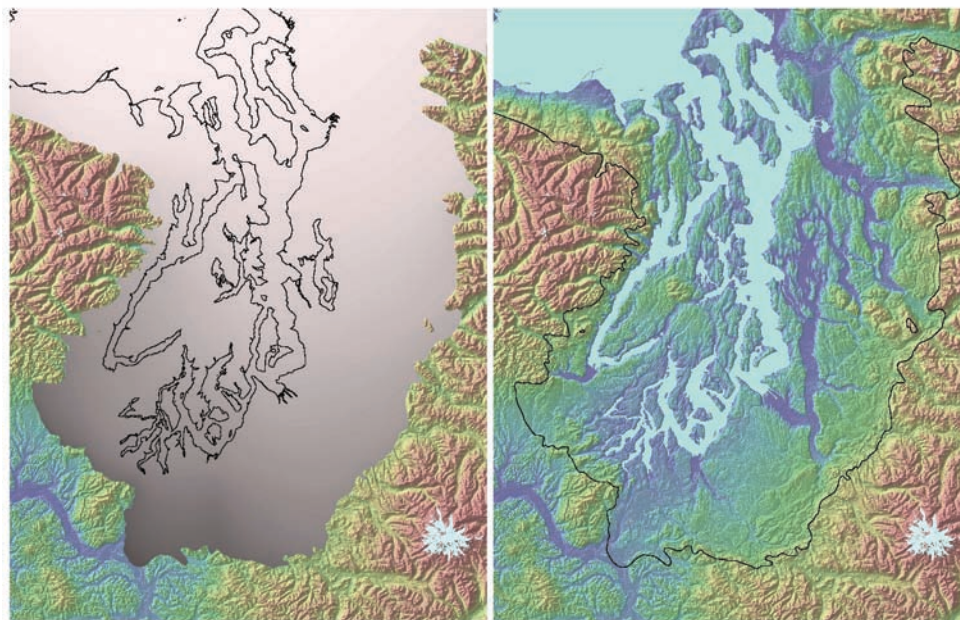


Figure 2.1. Reconstruction of the Puget Lobe of the Cordilleran Ice Sheet at glacial maximum ca. 16,500 cal yr before present (BP) (H. Greenberg, Univ. Washington, Seattle, unpubl. data).

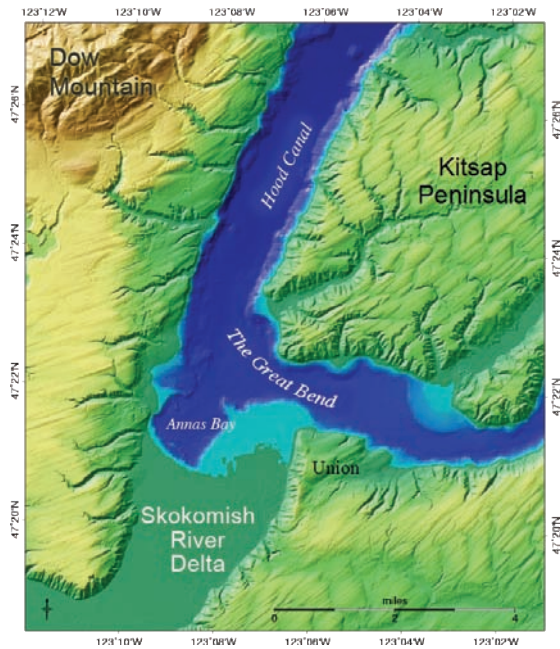


Figure 2.2. Digital elevation model of the Great Bend region of southwest Hood Canal. Data from Finlayson (2006).

with shallow sills at their entrances. For example, the central portion of Puget Sound is more than 300 m deep but shallows to less than 100 m in Admiralty Inlet.

The fourth geomorphic unit is associated with modern erosion processes that have reworked the topography since ice retreat. This is most obvious around the margins of Hood Canal (Figure 2.2). When the ice retreated, it left a landscape that was over-steep, particularly where the troughs cut through the Lowland fill. Without the ice support, the steep coastal bluffs began to collapse. Surface runoff caused rills and then gullies to form on the bluff faces, some of which have developed into proper streams and rivers. Most sediment that eroded from the coastal bluffs appears to have accumulated in small stream delta deposits or in sediment lobes at the base of the steep trough walls. Because the troughs are so deep, they tend to sequester delta sediments and limit the geographic range over which river sediments become incorporated into beach deposits. This can be seen in the Skokomish River delta (Figure 2.2). In this case, the river has cut a wide floodplain through fill and deposited this material (along with material derived from the southern flanks of the Olympics) in a large delta in the Great Bend. However, the delta deposits are basically confined to the deposition area, and there is no obvious influence on the morphology either north or east of the delta. This is generally the case for large river deltas throughout Puget Sound (less so for small stream deltas as will be shown in ensuing discussion).

The final geomorphic unit is the wave-cut platform on which the beaches of Puget Sound are formed. At the scale of Figure 2.2, it is virtually undetectable. This is in contrast to most ocean beaches, which occupy a shallow, gently dipping shelf that can extend for several kilometers offshore (and in some cases can be

seen from space). Instead, the shores of Puget Sound typically occupy a narrow wave-cut shelf notched into the steep walls of the marine basins. The nearshore effectively divides the trough walls into two sections: (1) a submarine section seaward of the nearshore; and (2) a terrestrial section landward of the beach—the coastal bluffs. However, this pattern breaks down in the south Sound, where the sea floor of the inlets is not significantly deeper than the terrace platform. In these locations the lower nearshore grades gently into the sea floor without a significant break in slope. The backshore¹ continues to be dominated by coastal bluffs.

High-resolution maps of the nearshore reveal topography nearly as complex as the upland bluffs. A good example is Piner Pt. on the southwest corner of Maury Island (Figure 2.3). Directly to the east of Piner Pt., Puget Sound is more than 180 m deep. The walls of the basin rise steeply until they reach the nearshore platform at around -4 m to -2 m mean lower low water (MLLW), where there is a distinct break in slope that forms the base of the platform and then the shelf rises more gradually to the base

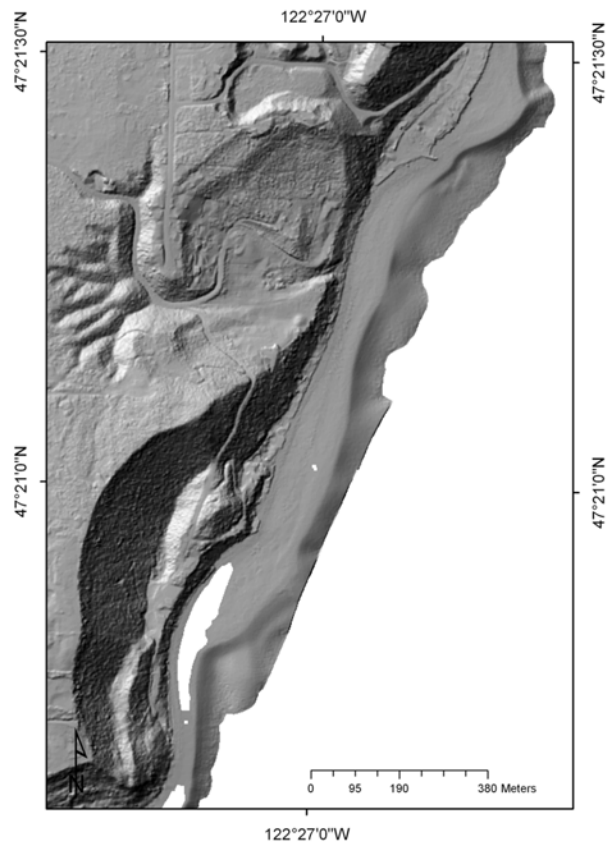


Figure 2.3. Nearshore bathymetry and topography of Piner Pt. on the southwest corner of Maury Island. Data courtesy of Joint Airborne Lidar Bathymetry Technical Center of Expertise (JALBXTX 2003), Puget Sound Lidar Consortium (PSLC 2000–2004).

¹The zone of the beach profile extending landward from the sloping foreshore to the point of development of vegetation or change in physiography (sea cliff, dune field, etc.) (Komar, 1998, p. 47).

of the bluffs between 6 m to 8 m MLLW. The bluffs rise another 100 m over the shoreline to the Lowland plain. One of the most noticeable characteristics of the nearshore platform in Figure 2.3 is the high variability in morphology across the nearshore platform and alongshore. This three-dimensional topography, which is very different from ocean shelves where the topography tends to be uniform alongshore, has implications for the physics of sediment transport on these platforms as well as implications for biological diversity.

The nearshore topography of Brace Pt. just south of the Fauntleroy ferry terminal (Figure 2.4) shares many characteristics of Piner Pt. Here, the side walls of the Sound exceed 25% grade as they rise from a depth of more than 180 m in just 700 m distance. Again, the break in slope occurs at about -4 m to -2 m MLLW where the 100 m wide platform rises up to the foot of the coastal bluffs. Like Piner Pt., the nearshore platform is highly three-dimensional in nature, with variability in the across and longshore directions. Like Piner Pt., Brace Pt. has prevalent arcuate scarps along the coastal bluffs adjacent to the shoreline. These scarps are relicts of landslide activity. Landsliding is an important source of sediment to the nearshore beaches as well as a significant nearshore hazard.

Small coastal streams are another source of sediment to the nearshore, as mentioned previously. High-resolution topography

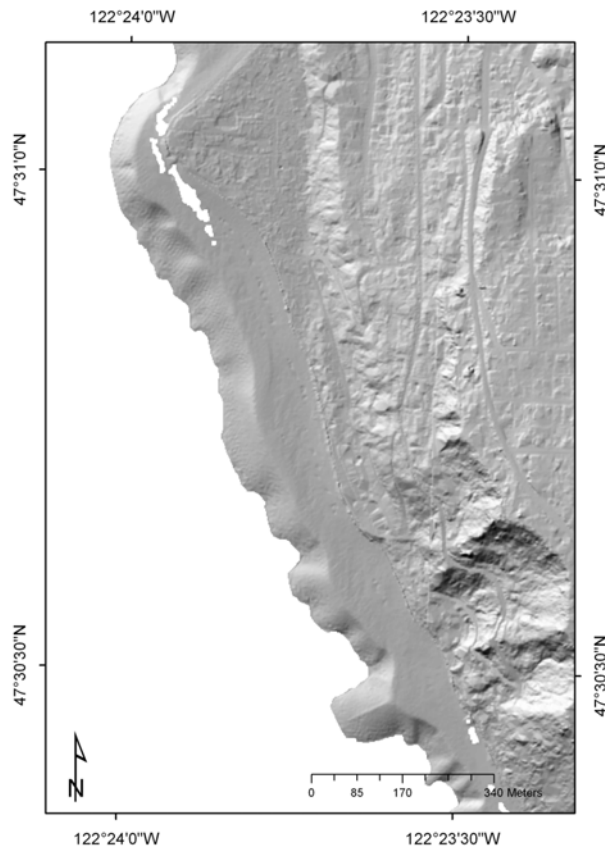


Figure 2.4. Combined bathymetry and topography of Brace Pt. south of the Fauntleroy (Vashon) ferry terminal, Seattle. Data courtesy of JALBXTX (2003), PSLC (2000–2004).

of the Lofall region of northern Hood Canal shows the elevated delta of a small creek formed directly on the nearshore platform (Figure 2.5). The extent to which these sediments are transported onto the nearshore is not known. If the sediments cascade out beyond the bench onto the steep walls of the trough, it is likely that they are permanently lost to the nearshore. Alternatively, if the sediment is swept laterally off the delta onto the terrace, it may play a more important role in supporting the terrace ecosystem. Observations of several small beaches formed on delta deposits are discussed further (Section 5.2).

The nearshore is not always a sink for sediment. Slope failures on the nearshore act as a source of sediment from the nearshore platform down to the lower slope. Marine slope failures occur when shear stresses acting downslope exceed the sediment shear strength and can be triggered by earthquakes, storm waves, extreme tidal excursions, artesian pressures, construction, or gravity.

Two examples of slides demonstrate how the nearshore can act as a sediment source for the deeper portions of the sound. The first occurred at Duwamish Head, Seattle. In 1986, dredging operations associated with the placement of a new sewage outflow triggered a large slope failure off the northwest side of Duwamish Head (Figure 2.6). The slide removed 250,000 m³ of sediment and was up to 15 m deep when first discovered (Sylwester and Holmes 1989). Although this slide was human-induced, modern

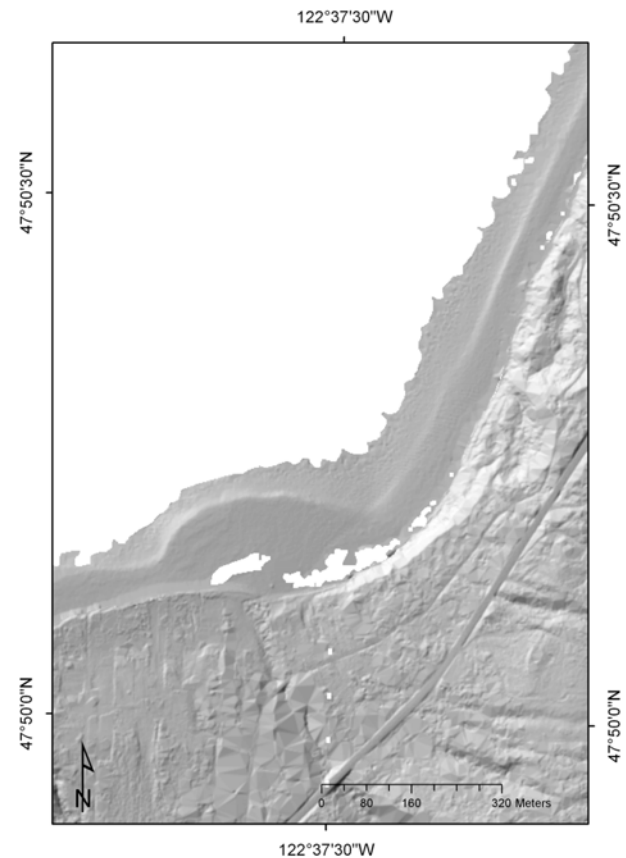


Figure 2.5. A small creek delta near Lofall, northern Hood Canal. Data courtesy of JALBXTX (2003), PSLC (2000–2004).

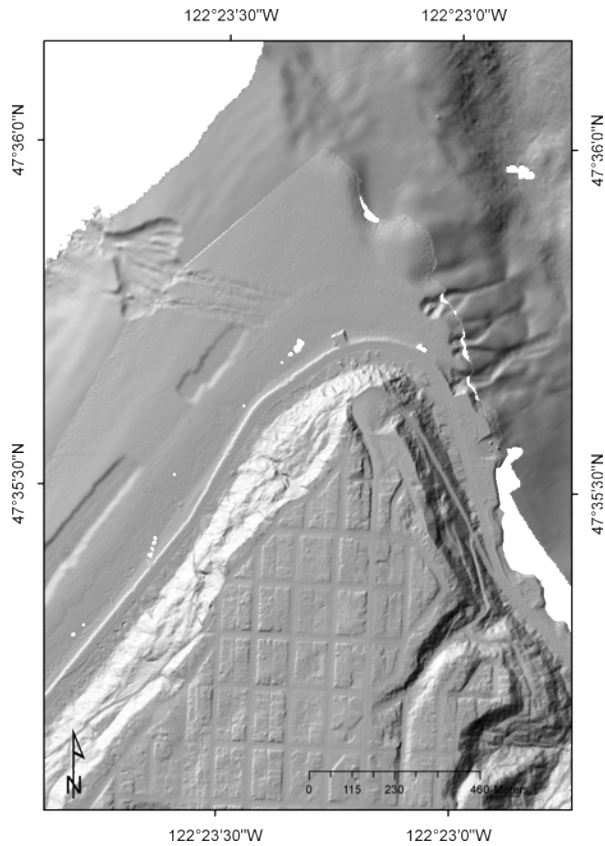


Figure 2.6. Bathymetry and topography of Duwamish Head, Seattle. The large scarp to the northwest of Duwamish Head and the dredge scarps to the west are anthropogenic. The chutes to the northeast of the point appear to be natural. Data courtesy of Gardner et al. (2001), JALBXTX (2003), PSLC (2000–2004).

surveys of the area show that submarine gullies have also formed off Duwamish Head and may act as a pathway for sediment to move from the nearshore platform into Elliott Bay. The second example pertains to the natural submarine canyons off Possession Pt., Whidbey Island (Figure 2.7). Here, a series of deep gullies begin on the nearshore terrace and terminate more than 200 m below in large sediment lobes at the base of Possession Sound. Similar nearshore headscarps found along the eastern side of the main basin (see Figure 2.4), the western side of Camano and Gedney islands, and further north on Whidbey Island may indicate the widespread distribution of this slope failure mechanism. Whether the features on Possession Pt. are relict or remain active is unclear, but these chutes clearly have formed a pathway for sediment to escape to the deep basins of the Sound in the past and may be reactivated under certain conditions.

Finally, barring catastrophic geologic events, humans have become the dominant geomorphic agent on the nearshore platform. The effects of human-induced slope failure on Duwamish Head have already been discussed (Figure 2.6). The same figure also shows the effects of offshore dredging to the west of Duwamish Head. Another example of human-induced modification to the nearshore is the scour caused by ferry prop wash adjacent to the Clinton ferry terminal, Whidbey Island (Figure 2.8). Whether

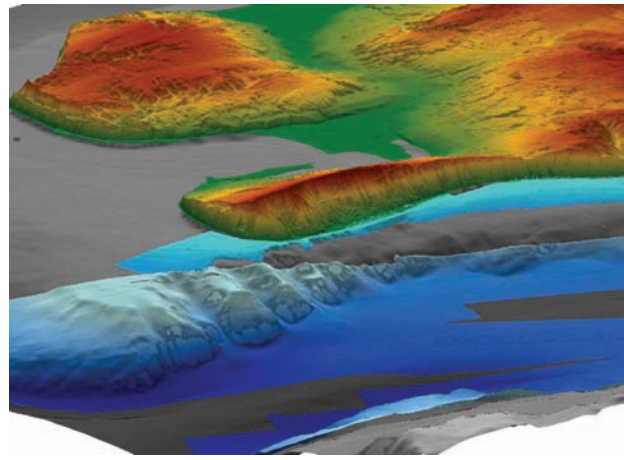


Figure 2.7. Oblique view looking northwest at Possession Pt., southernmost Whidbey Island. A series of deep submarine gullies have formed off the nearshore platform and reach 180 m down into Possession Sound. Sediment lobes at the base of the chutes indicate that sediment has moved from the nearshore into deep water via these pathways in the past. Data courtesy of Gregg and Finlayson (2002), PSLC (2000–2004), and Finlayson (2006).

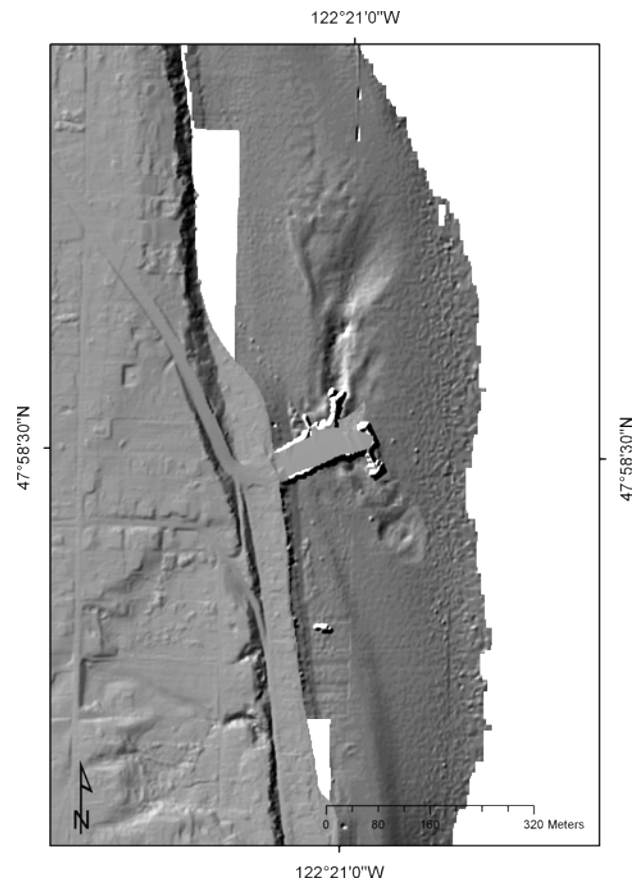


Figure 2.8. The Clinton ferry terminal, Whidbey Island. Prop wash from the docked ferries has scoured out the nearshore adjacent to the ferry terminal. Data courtesy of JALBXTX (2003), PSLC (2000–2004).

these effects are planned or unintended, human machinery and habits have become more effective at moving sediment than natural processes. Harbor maintenance, dredging, and even pleasure boating can and do impact nearshore morphology. Therefore, including anthropogenic factors in beach planning and research is important.

2.2. Sediment Character and Supply

The major source of sediment to the shores of Puget Sound is due to the erosion and reworking of coastal exposures of till, outwash sediments, and glaciomarine and glaciolacustrine deposits. According to the Washington State Department of Ecology, almost 1,000 km of coastal bluff are affected by shallow land sliding (Shipman 2001). In addition, there are 13 mountain rivers which erode the Olympic and Cascade mountains and deliver sediment to Puget Sound at a modern rate of 3.22×10^6 t yr⁻¹ (Downing 1983). Innumerable small creeks also provide sediment to the shoreline, though their mass contribution has never been estimated.

Coastal bluffs in Puget Sound often exhibit a variety of glacio-genic facies simultaneously including clay, silt, sand, and diamicton (Crandell et al. 1958, Easterbrook 1968, Keuler 1988, Booth et al. 2004). Because bluff stratigraphy is unpredictable and rarely continuous over more than a few hundred meters, the character of beach sediments derived from these sources is complex. Sediment grain sizes on beaches range from fine-grained silts to boulders, with pebble gravels and coarse-grained sands being the most prevalent. With few exceptions, beaches in Puget Sound do not have a single source or sink for sediment. Instead, a mosaic of eroding bluffs and accretion shoreforms develops along the entire length of the littoral cell (see Figure 2.9).

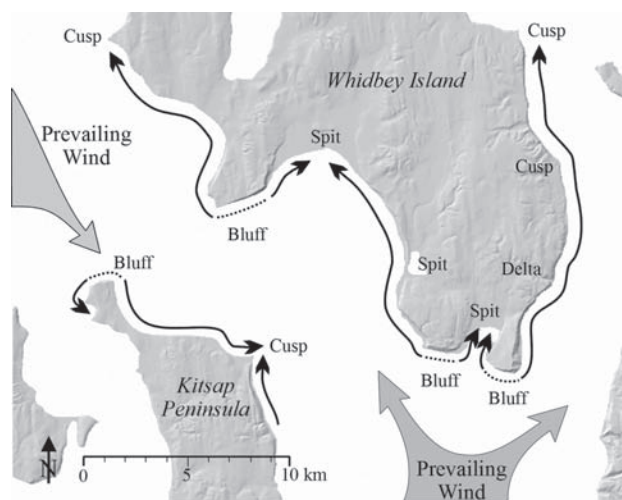


Figure 2.9. Littoral cells and the direction of net shore drift for southern Whidbey Island. Typically, drift cells in Puget Sound are a mosaic of eroding bluffs and accretion shoreforms. Reproduced from Finlayson and Shipman (2003).

The erosion of coastal bluffs occurs by a number of mechanisms that can be broadly classified into wave-induced undercutting and gravity-induced mass wasting. In all cases, however, the balance between downward shear stresses and cohesive forces within the rock and soil determines the fate of the bluff face. Many factors can modify these conditions, including the stratigraphy of the bluff, the presence of vegetation, weathering, perched water tables, and wave attack. Small-scale bluff retreat associated with raveling and sloughing is a relatively continuous process with larger landslides being more episodic (Gerstel et al. 1997).

Shipman (1995) has gathered together available data to estimate erosion rates for coastal bluffs on Puget Sound (Table 2.1). Bluff retreat rates on these sites ranged from 3 cm yr⁻¹ to 150 cm yr⁻¹. The volumetric erosion rates are positively correlated with fetch length, suggesting that wave action is an important catalyst for bluff erosion. Estimates of the total length of unstable shoreline range by county from 3% to more than 50%, with an average of 31% (Shipman 2004).

Several excellent resources are available on the character and geomorphology of the coastal bluffs of Puget Sound including Shipman (2004) and a review of landsliding in particular by Gerstel et al. (1997) and Shipman (2001).

2.3. Sea-Level History and Neo-Tectonics

Holocene sea levels in the Puget Lowland reflect the complicated interaction of glacio-isostatic rebound, eustatic sea-level rise and vertical tectonic land movement (Figure 2.10). Early Holocene sea levels in northern Puget Sound were about 90 m above present levels, rapidly dropped to as much as 10 m below present levels about 8,000 years ago, and have been rising steadily since (Easterbrook 1963, Clague 1983, Thorson 1989, Kelsey et al. 2004). In contrast, relative sea level in south Puget Sound has risen more or less monotonically from about 40 m below present levels (Thorson 1980). By about 5,000 cal yr BP, sea level was within 2 m to 3 m of present and has been rising at a rate of 2 mm yr⁻¹ to 3 mm yr⁻¹ since (Sherrod et al. 2000, Kelsey et al. 2004). The modern marine platform is no more than 5,000 years old throughout the Sound, representing an entirely transgressive sea-level history in the south, while in the north the current platform was previously (if briefly) under wave action 10,000 years ago.

In addition to the gradual sea-level changes associated with isostasy and eustatic sea-level rise, catastrophic co-seismic vertical displacements of the marine platform have been identified at a number of east-west striking faults located throughout Puget Sound. The most dramatic of these is a 5- to 7-m vertical displacement of the marine platform in central Puget Sound that has been dated to around 900 to 930 AD (Bucknam et al. 1992, Atwater 1999). Other displacements on this fault and on Whidbey Island within the past 3,500 years were between 1 m and 2 m (Sherrod et al. 2000, Kelsey et al. 2004). There are ongoing investigations into vertical displacements in other locations.

Table 2.1. Erosion rates of coastal bluffs on Puget Sound (after Shipman 1995). Note that these sites were selected based on available data, and not on the degree to which they represent regional erosion rates. This sample is probably biased towards sites with rapid erosion.

Location	Rate (cm yr ⁻¹)	Fetch (km)	Source
Baby Island, Whidbey Is.	13	15	Keuler (1988)
Maylor Point, Whidbey Is.	15	15	Keuler (1988)
Penn Cove, Whidbey Is.	6.5	5	Keuler (1988)
Mutiny Bay, Whidbey Is.	11	10	Keuler (1988)
S. of Lake Hancock, Whidbey Is.	4	20	Keuler (1988)
Rocky Point, Whidbey Is.	14	> 50	Keuler (1988)
Camano Island, west side	3	10	Keuler (1988)
Smith Island	69	> 50	Keuler (1988)
North Beach, Quimper Pen.	6	> 50	Keuler (1988)
Shannon Point, Fidalgo Is.	20	10	Keuler (1988)
Skagit Co. (mean of 6 sites)	7.6±2.7	—	Keuler (1988)
Skagit Co. (mean of 26 sites)	4.9±3.4	—	Keuler (1988)
Port Williams	30	50	Eckler et al. (1979)
Sequim Bay	6	< 5	Eckler et al. (1979)
Port Angeles	90–150	> 50	Galster and Schwartz (1989)
Port Grey, B.C.	30–50	> 50	van Osch (1990)
Cowichan Head, B.C.	60	> 50	van Osch (1990)

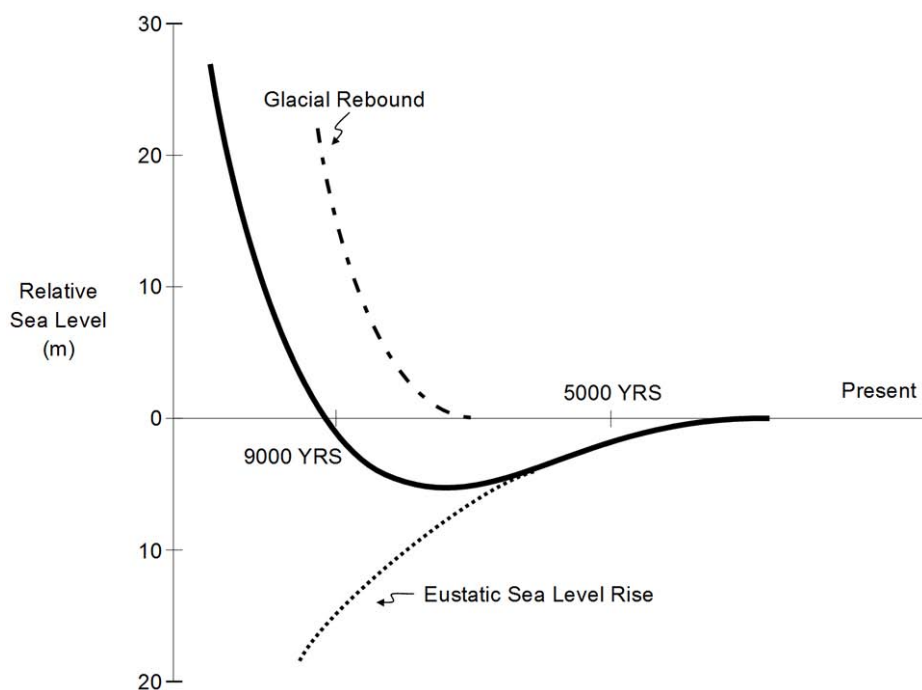


Figure 2.10. Relative sea-level curves for Puget Sound (after Shipman 1989). Northern Puget Sound follows the dark curve while southern Puget Sound follows the dotted line.

3. Waves

Most beaches in Puget Sound and Hood Canal are isolated from the Pacific Ocean by topography. As a result waves in the Sound are generated locally by wind blowing over the irregular channels and basins of the fjord system; they receive little to no swell from the eastern Pacific. Consequently, (1) the waves have limited fetch and low energy compared with incident waves on the Pacific coast, and (2) the wave climate is tightly coupled with local wind patterns. In addition, vessel wakes may be a significant wave energy source, particularly in restricted channels, where large incident waves would not otherwise occur.

Only a few published wave records exist for Puget Sound. They are of short duration and limited to only a handful of locations. Therefore, wave conditions must be inferred from wind climate and, where possible, supplemented with existing wave records.

3.1. Wind Patterns in the Pacific Northwest

The direction of prevailing wind in Puget Sound is south² or southwest during the winter and west or northwest during the summer (Phillips 1968, Overland and Walter 1983). The strongest winds are southerlies resulting from winter storms moving inland from the eastern Pacific. Periodically during the winter, high pressure over the continent and low pressure on the coast can force air down the Fraser River valley and through the mountain passes, resulting in strong northerly winds over Puget Sound. Summer winds are slight to moderate northerlies with diurnal sea and shore breezes.

In general, wind over the Pacific Northwest can be loosely categorized into four patterns (Maunder 1968, Overland and Walter 1983). In late fall and winter, the eastern Pacific high retreats southward, allowing two distinct, low-pressure storm systems to make landfall on the Washington and Oregon coast. In the first type (Figure 3.1), a broad, low-pressure system forms in the Gulf of Alaska, accompanied by a series of rapidly moving cold fronts that sweep counterclockwise around the center. These storms tend to rapidly approach the coast and then weaken over land. The second storm type forms around a disturbance in the central Pacific and moves on a northeast trajectory across the Pacific. These storms can intensify rapidly (so-called “bombs”) into extra-tropical cyclones as they sweep up the West Coast (Bancroft 1999, Allan and Komar 2002). They generally make landfall between Oregon and southern Vancouver Island and can generate hurricane-force winds over large areas of the West Coast, including (infrequently) Puget Sound³. Most severe windstorms in the region are southerlies of this type. The final common winter pattern occurs when a high-pressure ridge develops over north-

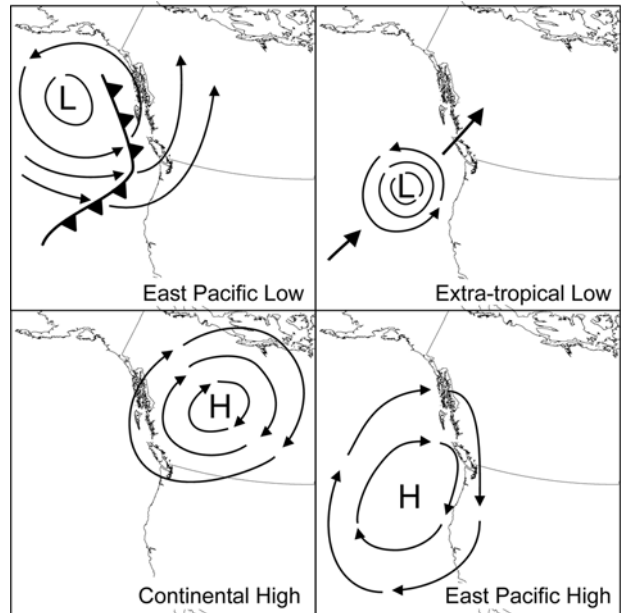


Figure 3.1. Weather patterns of the Pacific Northwest. Typical winter patterns include the east Pacific low pressure system, extra-tropical low pressure system, and the continental high pressure system. The typical summer pattern is an eastern Pacific high pressure system. Redrawn from Overland and Walter (1983).

west Canada, accompanied by low pressure off the Washington coast. The result is clear winter skies, freezing temperatures, and occasionally strong northerly winds blowing down the Fraser River valley and south across the Puget Lowland. During the summer, a high-pressure area is located off the coast of northern California and Oregon. The anti-cyclonic (clockwise) circulation of air around this high results in gentle, westerly-to-northwesterly winds moving onshore throughout the Northwest.

The interaction between the large-scale weather patterns and topography is very important to the wind in Puget Sound (Overland and Walter 1983, Schoenberg 1983). The Olympic and Cascade mountains confine the free movement of air at sea level, which prevents geostrophic adjustment between pressure and wind. The result is that the winds blow predominantly from high to low pressure in a direction dictated by the orientation of sea-level channels. Since Puget Sound and the Strait of Juan de Fuca are at right angles to one another, the topographic control causes the wind patterns over each water body to respond differently to the same synoptic pressure system. For example, high pressure to the east results in easterly (i.e., down-gradient) winds in the Strait of Juan de Fuca and light winds over Puget Sound, while low pressure to the north results in strong southerly winds over Puget Sound and light winds in the central part of the Strait of Juan de Fuca (Overland and Walter 1983). For the same reason, the passage of a weather front through the region will result in a different time sequence of wind speeds and directions in the

²Wind directions in this report will always indicate the direction from which the wind is blowing.

³Mass, C. Windstorms of the Pacific Northwest: the origin and history of the great windstorms of the region. Public lecture series, 2004. University of Washington, Dep. Atmospheric Sciences.

two water bodies (Halladay 1970, Overland and Walter 1983, Schoenberg 1983)—that is, regional wind speeds and directions vary substantially over time.

Topography in Puget Sound also effects the development of local meteorological phenomena, including gap winds, the orographic low-pressure formation in the lee of the Olympic Mountains, the Puget Sound Convergence Zone, and diurnal sea and valley breezes (Overland and Walter 1983).

During the winter, if a cold high-pressure area forms east of the Cascade Mountains with a low-pressure system offshore, a large east–west pressure gradient can develop over the Puget Sound region, leading to a locally strong and at times destructive “gap” wind flowing out of the Fraser River valley down the Straits of Juan de Fuca (strong winds known as “Bora” flow out of the Cascade Passes on similar occasions).

Another locally destructive wind can occur in the lee of the Olympic Mountains. When strong storms move inland from the Pacific, the Olympics split the southerly wind stream, causing a low-pressure area in the lee of the mountains. If this low-pressure area is enhanced by other meteorological phenomena (such as a low-pressure system over Vancouver Island), large pressure gradients can result in severe winds. On February 13, 1979, for example, winds locally in excess of 50 m s^{-1} resulted in the sinking of the Hood Canal Floating Bridge.

During the spring, as the eastern Pacific high moves northward and the predominant winds in Puget Sound begin to transition from southerly to northwesterly, the passage of weather fronts often results in air masses moving northeasterly on both the north and south of the Olympics. This flow pattern results in a convergence zone over northern Puget Sound more important for its effect on enhancing precipitation than for producing strong winds (Mass 1981).

Finally, during the warm summer months, with regional stability provided by the eastern Pacific high offshore, differential heating of land and water result in a daily sea and shore breeze cycle.

To generalize, winter winds in Puget Sound are dominated by meso-scale atmospheric effects covering much of the eastern Pacific; during the summer the eastern Pacific high-pressure area results in regional stability and Puget Sound winds begin to reflect local heating and cooling phenomena in the form of sea and shore breezes. This seasonal pattern is evident in the energy spectra for winds at West Point where winter months are dominated by a 4-day energy peak representing the passage of low-pressure storm systems while during the summer there is a diurnal peak that is the daily sea and shore breeze cycle (Overland and Walter 1983).

3.2. Wind and Wave Observations at Cama Beach

Puget Sound and Hood Canal are isolated from the Pacific Ocean by the Olympic Peninsula, and ocean swell cannot penetrate much beyond Admiralty Inlet. As a result, the wind patterns described in Section 3.1 are the only natural source

of high-frequency wave energy in the Sound. These are classic fetch-limited conditions where the waves are highly variable both spatially and temporally, depending on the geometry of the channels and the local wind conditions. Unfortunately, very few wave observations have been made available and most of these were deployed for only a few days at a time (see Downing 1983, Nordstrom 1992).

From October 2002 to May 2005, wind speed and direction were monitored at Cama Beach from a Davis Vantage Pro wireless anemometer installed on the roof of a large boathouse centrally located on the shoreline of Cama Beach (Figure 3.2). The anemometer recorded mean wind speed and direction at approximately 11 m above MLLW at 15-min intervals throughout the study period.

Between September 2002 and November 2004, a National Institute of Water and Atmospheric Research, Ltd. Dobie-A non-directional wave gage was deployed 12 times to collect wave data sets of between 30 and 90 days each. The gage was mounted vertically to a pipe embedded in a cement platform with the pressure sensor 80 cm above the bed. Between September 2002 and March 2003, the gage platform was located on the southern limb of Cama Beach at approximately -2.7 m MLLW (Figure 3.2). After this date, the gage platform was moved to the northern limb of Cama Beach at -2.6 m MLLW. In both cases, the gage was situated on the landward margin of the low-tide terrace within a dense eelgrass bed. The gage pressure sensor was above all but the longest grass blades.

The wave gage was programmed to sample at 10 Hz for 204.8 s with a burst every 15-min synchronized with the anemometer data logger. The Dobie gage does onboard processing of the raw pressure signal and stores a standard suite of wave statistics as well as the resulting pressure frequency spectrum for each burst, after which the raw pressure signal is deleted to save memory.

The large tidal range and small wave amplitudes at Cama Beach are a challenging environment for the Dobie gage. Attenuation of the pressure signal of high-frequency, short-period waves is significant, particularly at high tides. In order to prevent sensor noise from dominating the wave record, the gage employs two conservative tests to the resulting wave records. The first is based on maximum wave steepness:

$$(kH_s)_{\max} = \frac{2\pi}{7 \tanh(kh)} \quad (3.1)$$

Where k = wave number,
 H_s = significant wave height, and
 h = water depth.

The second test is based on the maximum ratio of wave height to water depth:

$$H_s / \bar{h} = 1 \quad (3.2)$$

If either theoretical value is exceeded then the wave is deemed physically unrealistic and flagged.

In addition to the two wave checks above, the Dobie gage reports a statistic called “penetration” which is defined as follows:

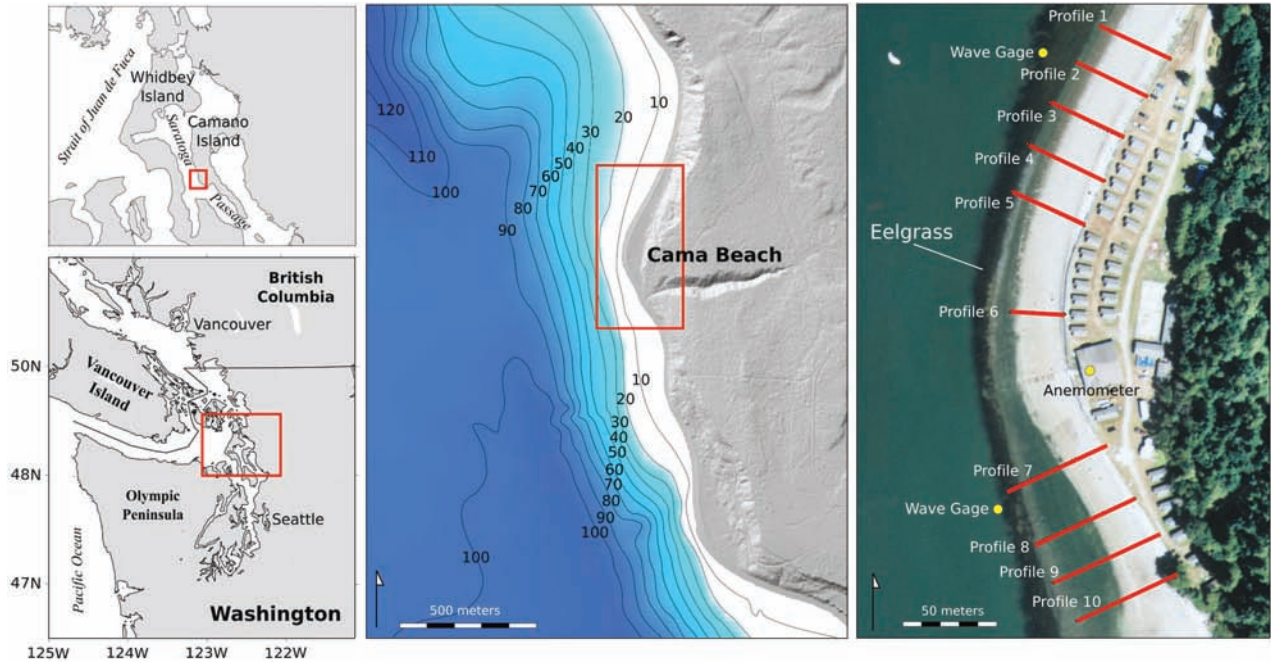


Figure 3.2. Location of Cama Beach, Washington. The central figure shows the offshore bathymetry (depths in m). The right-hand figure shows the location of the 10 survey profiles in this study as well as the permanent location of the anemometer, and the southern and northern deployment locations of the wave gage (the gage was moved from the southern to the northern position in April of 2004). From Finlayson (2006).

$$\frac{\cosh(k(z^* + \bar{h}))}{\cosh(kh)} \quad (3.3)$$

Where z^* is the depth of the Dobie below mean water level. Penetration is an approximate indicator of the fraction of the pressure signal that has been attenuated between the water surface and the level of the Dobie. Low penetration values are associated with low signal-to-noise ratios.

Between October 2002 and May 2005, the 15-min average wind speed at Cama Beach was $2.6 \pm 2.5 \text{ m s}^{-1}$ with peak wind speeds ranging from 10 m s^{-1} to 17 m s^{-1} . The time series of wind observations reveals a strong seasonal cycle to the winds at Cama Beach. During the summer, there is a nearly constant gentle breeze blowing over Saratoga Passage while during the winter, there are periods of calm conditions punctuated by strong wind storms. This pattern is reflected in the seasonal median and maximum wind speed records. The median wind speed peaks in June and then decreases to a minimum in January. However, the maximum wind speeds show two windy periods, the first between October to early January and the second between March and April (Figure 3.3). Speed-weighted wind directions show distinct seasonal regimes as well, with strong winds blowing from the south from October through April and from the north from May to September.

The Dobie wave gage occupied two stations at Cama Beach over 12 deployments. From September 2002 to March 2003, the Dobie was deployed eight times to the southern station where it collected 12,367 bursts. From April 2003 to November 2004, the

Dobie was deployed four times at the northern station where it collected 10,430 bursts. Of the 27,797 total bursts collected, only 3628 (15.9%) recorded significant wave height measurements that passed the checks imposed by Equations 3.1 and 3.2; more than 80% of the time the wave conditions were below the signal-to-noise threshold of the gage. Because the number of valid wave estimates was low and because the two sites occupied similar cross-shore positions, the 12 wave records were aggregated into a single ensemble.

The median significant wave height and period at Cama Beach was $0.24 \pm 0.19 \text{ m}$ and $2.0 \pm 0.8 \text{ s}$, respectively. Wave height and period increased with increasing wind speed until winds exceeded about 10 m s^{-1} , at which point both wave height and period became independent of wind speed (Figure 3.4). The decoupling of wind and waves at 10 m s^{-1} is presumably a result of waves breaking over the gage as well as the fetch-limited conditions on Saratoga Passage.

The distribution of wave height and period at any given wind speed is a function of natural variation in the wave field and sensor noise. Natural variability comes from non-steady wind fields, variations in tide levels and tidal currents, and some variation in sheltering between the two sensor locations aggregated in the ensemble data set. However, the measurements mostly are remarkably well clustered around the median values. The more significant outliers appear to be associated with sensor noise. The range and number of outlier measurements increase as wind speed and the Dobie penetration statistic decrease. This suggests that for winds below about $8\text{--}10 \text{ m s}^{-1}$, the wave-induced

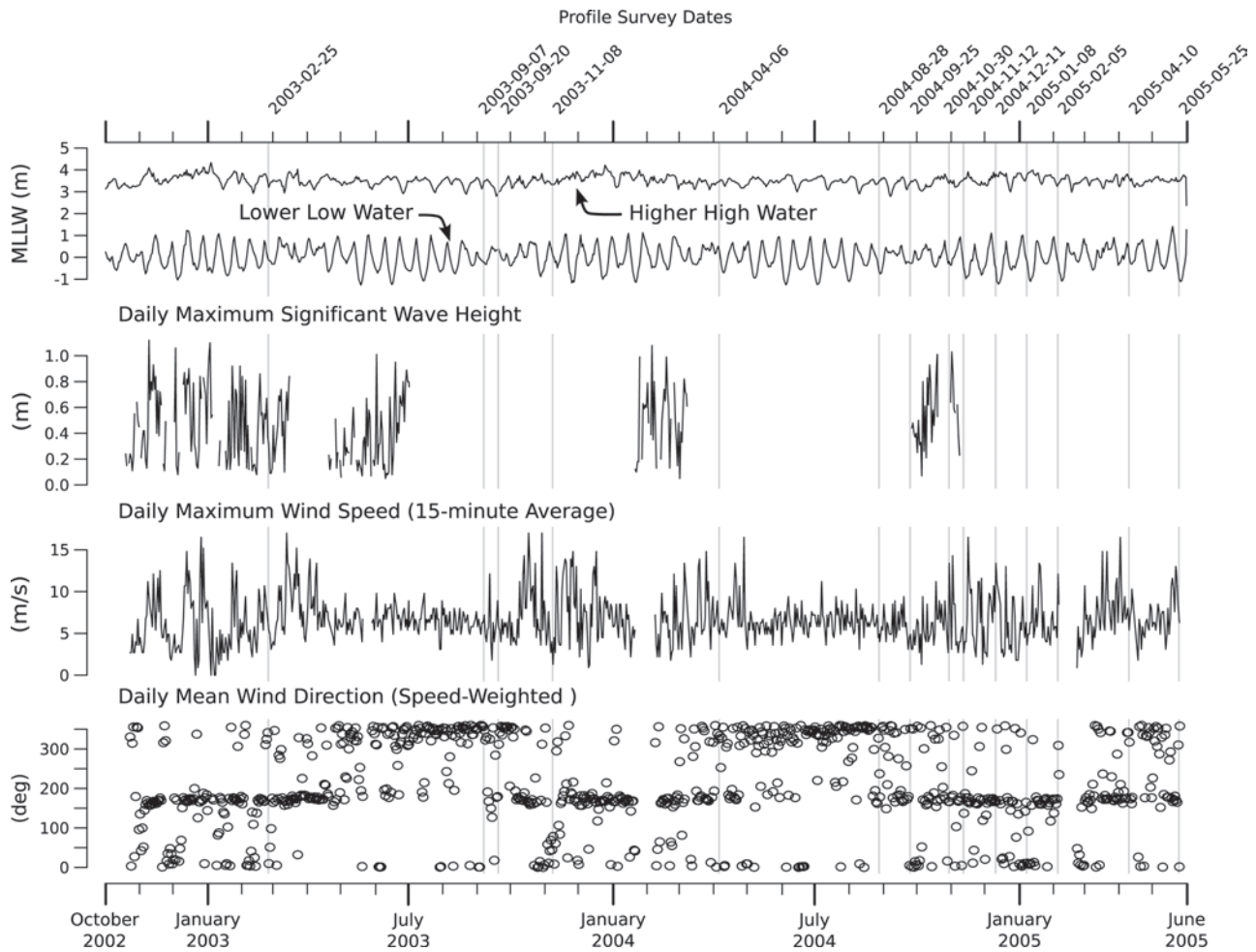


Figure 3.3. Time series of wind and tide observations at Cama Beach for October 2002 to May 2005. From Finlayson (2006).

pressure variations are too attenuated for reliable detection by the Dobie gage, particularly at high tide. The large range of wave measurements shown in Figure 3.4 for low wind speeds at Cama Beach are probably the result of sensor errors.

Whether the waves at Cama Beach are characteristic for other locations in Puget Sound is not known because no other long-term measurements are available for comparison. However, the fetches and wind climate are similar enough that some generalizations should be broadly applicable:

1. Waves in most of Puget Sound (probably excluding Admiralty Inlet) are generated by local winds with little or no energy component from ocean swell.
2. Normal wave conditions are very calm with little or no wave action on the smaller water bodies. Large waves only result during infrequent wind storms
3. Waves are fetch-limited: even during the strongest storms, the topographic confines of Puget Sound set a maximum size (and energy density) beyond which the waves cannot grow.
4. Storm wave heights in most channels are probably simi-

lar to Cama Beach: that is, small ($H_s < 1$ m) with short periods ($T < 4$ s). They are perhaps larger at the ends of the Main Basin where fetches are longest and steady winds will have greater opportunity to transfer energy to the sea.

3.3. Wave Hindcasting

Wave hindcasting entails modeling past wave conditions from historical wind observations. Wave hindcasting also is used to develop wave climate models, which attempt to characterize wave energy on a water body over a long period of time (rather than for a particular event).

Wantz and Sinclair (1981) have produced maps of the mean recurrence interval of annual extreme wind speeds for Washington, Oregon, and Idaho. They concluded that the 50-year, 1-min average wind speed for the Puget Lowland ranged from 22 m s⁻¹ southwest of Tacoma to 28 m s⁻¹ at the northern entrance to Admiralty Inlet. The storm of record for Puget Sound—the Columbus Day cyclone of 1962—had peak wind speeds of 34.2 m s⁻¹ (Read 2004) and all of the top 16 wind storms of the past 50 years have registered peak gusts above 20 m s⁻¹ (Table 3.1). How-

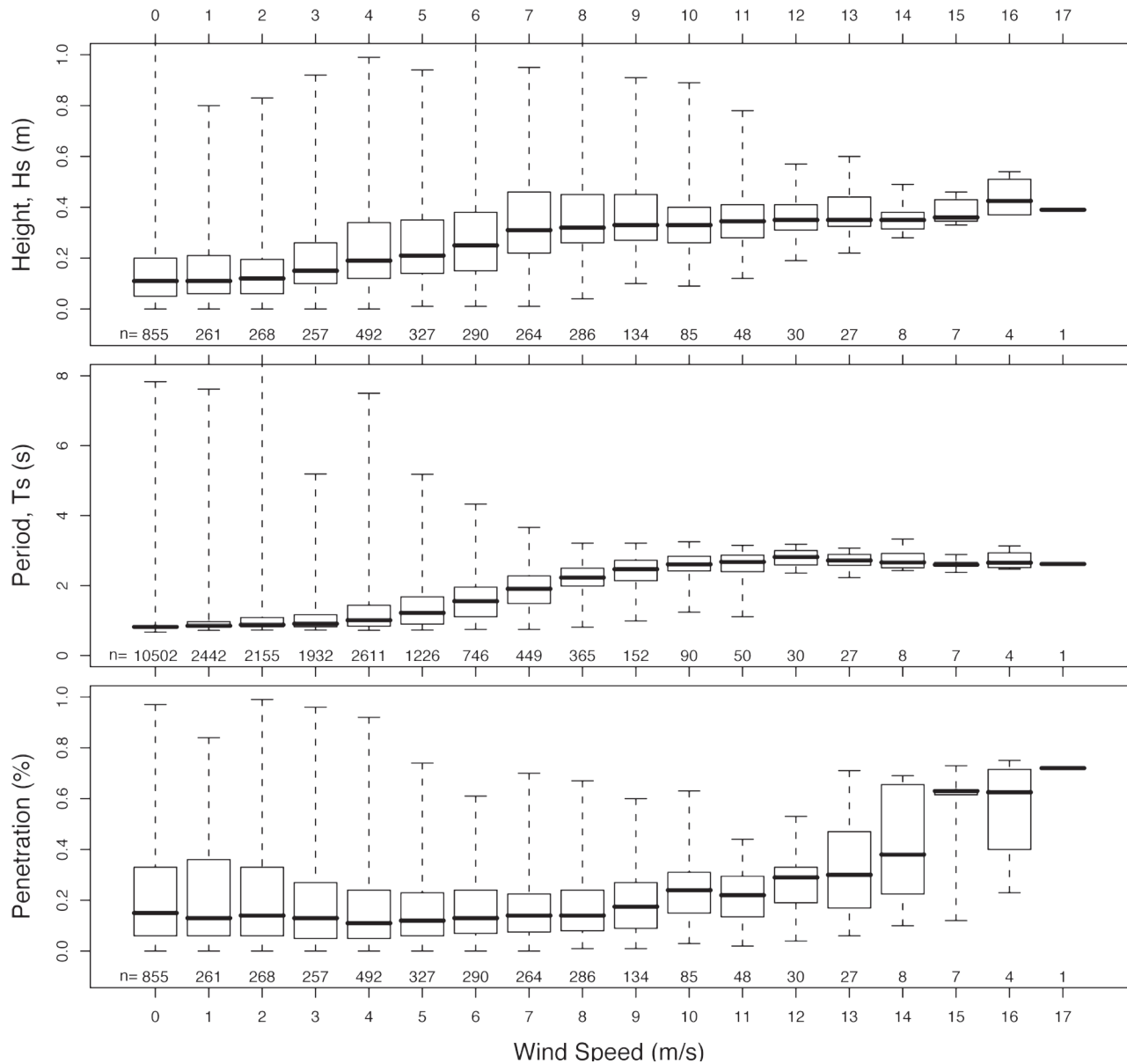


Figure 3.4. Significant wave height, significant wave period, and penetration statistics as a function of wind speed for observations at Cama Beach between September 2002 and November 2004. From Finlayson (2006).

ever, these strong storms are unusual. At the West Point light station (WPOW1), Seattle, the average wind speed since 1984 has been $4.7 \pm 3.2 \text{ m s}^{-1}$ with an annual maximum 1-hr wind speed of $<20 \text{ m s}^{-1}$ (National Data Buoy Center (NDBC) 2003). The annual maximum recurrence interval curve for WPOW1 is shown in Figure 3.5.

It is possible to characterize the wave climate of Puget Sound by hindcasting waves using a simple and efficient wave model adapted from the Shore Protection Manual (SPM) (CERC 1984). This procedure is based on the Sverdrup-Munk-Bretschneider (SMB) methodology and produce deep-water wave-height estimates from three input parameters (fetch length, wind speed, and wind duration). A more sophisticated numerical model for wave propagation is not shown here because of the compu-

tational cost, the lack of comprehensive environmental data to control the boundary conditions of a more sophisticated model, and because the deep water of Puget Sound limits the first-order errors associated with the SMB approach.

The classic SMB wave forecasting equations can be used to quickly estimate the 50-year maximum significant wave height and period in the main basin of Puget Sound (CERC 1984):

$$H_m = 1.616 \times 10^{-2} U_a F^{1/2} \quad (3.4)$$

$$T_m = 6.238 \times 10^{-1} (U_a F)^{1/3} \quad (3.5)$$

where H_m = the fetch-limited significant wave height (m),
 T_m = the significant wave period (s),

Table 3.1. Peak wind speeds (m s^{-1}) from storms of record in the Puget Lowland, 1950–2002 (adapted from Read 2004).

Rank	Date	Everett	Seattle	Boeing	Sea-Tac	Renton	Tacoma	Average
1	12-Oct-62	36	30	30	26	45	39	34.2
2	15-Jan-51	24	31	27	34	-	29	29.0
3	09-Jan-93	30	23	31	29	33	28	28.9
4	09-Jan-53	27	24	24	31	-	23	25.7
5	14-Nov-81	23	29	21	30	31	21	25.7
6	24-Feb-58	21	25	30	29	-	24	25.7
7	24-Nov-83	27	25	24	28	29	21	25.6
8	26-Oct-50	22	24	29	29	-	21	25.2
9	16-Jan-00	27	25	24	23	24	27	24.9
10	13-Feb-79	-	28	21	27	23	24	24.5
11	19-Jan-64	21	25	21	29	26	26	24.7
12	03-Mar-99	26	-	23	27	23	25	24.7
13	26-Mar-71	25	-	21	27	26	25	24.6
14	28-Feb-55	14	28	23	33	-	25	24.6
15	12-Dec-95	26	-	21	27	-	23	24.3
16	15-Nov-81	23	24	21	23	27	-	23.8

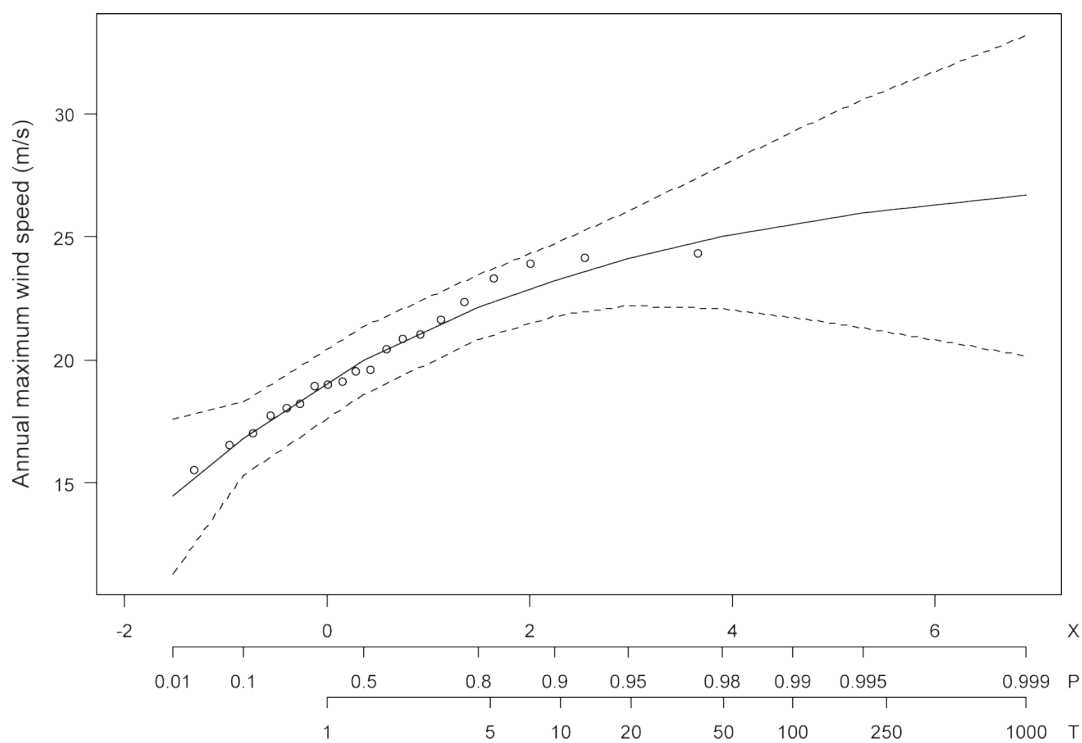


Figure 3.5. Probabilities of annual maximum wind speed at West Point, Seattle. X is the reduced variate $-\ln(-\ln P)$. P is the probability that the annual maximum is less than the value shown. T is the estimated return period in years assuming an exponential distribution of maximum wind speeds. The dotted lines indicate the 95% confidence interval. Wind data courtesy of National Data Buoy Center (NDBC 2003).

U_a = wind-stress factor,
 U = wind speed (m s^{-1}), and
 F = fetch-length (km).

An assumption of $F = 40$ km and $U = 25$ m s^{-1} yields a 50-year significant wave height and period for the main basin of Puget Sound of 3.8 m and 7.1 s, respectively. Few places in Puget Sound have such a large open-water fetch and sustained wind speeds of 25 m s^{-1} are extremely rare, so these waves are about as large as will ever be observed for wind-waves in Puget Sound.

To generalize the preceding results into a wave climate map for all of Puget Sound, we must statistically summarize wind storms across the region. Wind records for 16 coastal stations dating from the mid-1990s through 2004 were obtained from the University of Washington, Department of Atmospheric Sciences. From these data, statistics were generated for each of three wind-event types: (1) a light air (wind speed >0 m s^{-1}), (2) a strong breeze (wind speed >10 m s^{-1}), and (3) a gale (wind speeds >20 m s^{-1}). The data show that a light air (or greater) is present 85% of the time over the waters of Puget Sound, these events are mainly from the south or north, and the winds have steady durations in excess of 4 hours. Raising the minimum wind threshold to a strong breeze (>10 m s^{-1}) results in a drop in the frequency of events to just 4% of the record, southerlies become dominant (36% of the record), and the mean duration of events drops to under 2 h. Gales >20 m s^{-1} are extremely rare. Only 374 measurements >20 m s^{-1} were recorded from all 16 weather stations combined over the 9-year dataset. This represents only 0.05% of the record. As with more frequent winds, gales are predominantly southerlies but the mean duration of gale-force winds is <1 h.

The frequency of windstorms is inversely proportional to the strength of the storm (which is a function of sustained wind speeds and storm duration). However, it is not clear which events do the most work: strong but infrequent events or moderate events that occur more often. In the absence of accompanying long-term beach profile measurements, selecting the most significant storm in terms of geomorphic impact on the beach is impossible to do with certainty. For the following analysis, 10 m s^{-1} was chosen as a “typical” storm event based on the fact that these events occur at least once a year and tend to last for several hours—this choice is somewhat arbitrary. Statistics for winds blowing >10 m s^{-1} are shown in Table 3.2.

In order to make the wave climate model spatially explicit, we automated the SPM algorithms in a geographic information system (GIS). These include delineating fetch (using the arithmetic average of 9-radials centered on the target bearing) and calculating the lesser of fetch-limited, duration-limited or fully arisen wave heights and periods (Equations 3-33a, 3-35a and

3-26a in the SPM). As modified, the hindcasting procedure can be efficiently applied to every water cell in a DEM and produces wave prediction surfaces across the entire water body.

The wave climate characterization consists of calculating the mean duration of wind events (between the years 1996 and 2004) that continuously exceeded 10 m s^{-1} and blew without deviation from each of 16 compass directions. For each direction, a wave hindcast was created using 10 m s^{-1} as the wind speed, the mean duration of events and fetch length (Table 3.2). The resulting rasters of significant wave heights H_s and periods for the 16 individual directions j were then combined to form overall mean significant wave height and period rasters (H_m and T_m) by a weighted mean procedure:

$$H_{m(x,y,j)} = \sum_{j=0}^i H_{s(x,y,j)} \cdot f_j \quad (i = 000^\circ, 022.5^\circ, \dots, 337.5^\circ) \quad (3.6)$$

$$T_{m(x,y,j)} = \sum_{j=0}^i T_{s(x,y,j)} \cdot f_j \quad (i = 000^\circ, 022.5^\circ, \dots, 337.5^\circ) \quad (3.7)$$

where $H_{s(x,y,j)}$ = the significant wave height and
 $T_{s(x,y,j)}$ = the significant wave period calculated at location (x,y) for wind blowing in direction j for the duration shown in Table 3.2, and
 f_j = the relative frequency that the wind blew in the direction j also shown in Table 3.2.

The resulting wave climate map (Figure 3.6) attempts to characterize the wave energy of every location in Puget Sound based on statistics about the frequency and duration of wind storms observed between 1996 and 2000. It does not represent a particular event. Darker areas on the map such as in the narrow inlets of south Sound indicate a high degree of topographic sheltering resulting in low wave energy, while bright areas on the map are an indication of high wave exposure. For example, the southern and western shores of Whidbey Island are much more exposed to wave energy than the northern or eastern shores. Similarly, Hood Canal is more sheltered than the main basin. There are regions of direct wave exposure and sheltering within a few 100 m of one another. One feature that is not well expressed in the map is the progression of the seasons. As the seasonal wind patterns progress throughout the year and the winds shift from strong southerlies during the winter to northerlies during the summer, different parts of the shoreline will become exposed to or sheltered from wave action. Clearly, it is difficult to generalize about the geographic distribution of wave climate without careful consideration of the numerous factors that control wave processes.

Table 3.2. Relative frequency and mean duration of exceedence for wind events in the Puget Lowland from 16 weather stations in Puget Sound for 1996 through 2004 (station locations shown in Figure 3.10). Data courtesy of the Department of Atmospheric Sciences, University of Washington. Note: This table aggregates the data from 14 weather stations located near Puget Sound. Frequency is the relative frequency calculated from the total number of observations that exceeded 10 m s^{-1} and fell within the 22.5 degree direction bin. The duration is the mean length of time wind events blew without deviation from the given direction and without dropping below 10 m s^{-1} .

	Wind direction (degrees east of north)															
	22.5	45.0	67.5	90.0	112.5	135.0	157.5	180.0	202.5	225.0	247.5	270.0	292.5	315.0	337.5	360.0
Frequency (%)	1	1	0	0	1	11	21	36	7	3	2	9	2	1	0	4
Duration (hr)	3.0	1.0	0.1	1.7	1.2	2.7	1.2	3.9	3.0	3.0	0.8	2.7	1.0	1.7	0.4	1.2

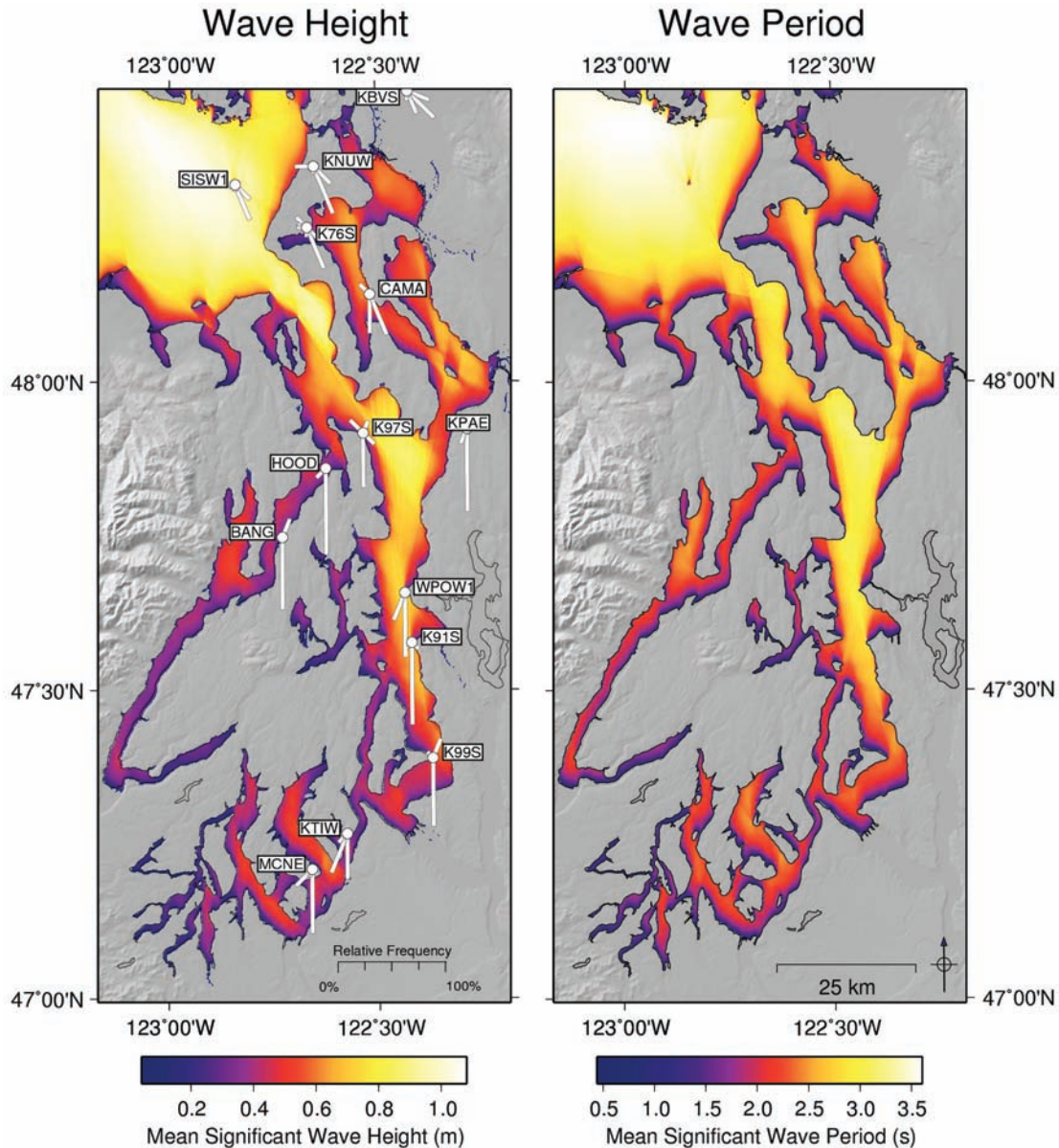


Figure 3.6. Estimated storm significant wave height (left) and period (right) for Puget Sound and Juan de Fuca Strait. Wind roses (directional histograms) on the left figure indicate the relative frequency sustained winds $>10 \text{ m s}^{-1}$ blew from each compass direction between the years 1996 through 2004. The dominance of southerly storms in the Sound and westerly storms in the Strait is reflected in the model. From Finlayson (2006).

4. Water Levels

After waves, tides are the most important natural forcing mechanism on the beaches of Puget Sound. The twice-daily rise and fall of mean water level translates the swash zone⁴ across the beach profile, governing the amount of time each beach elevation is exposed to wave processes. At the same time, the tides raise and lower the beach ground water table. The resulting infiltration and exfiltration through the beach is an important component of swash-zone fluid dynamics and foreshore⁵ sediment transport (Section 5.1.1). In addition, tidal currents can exceed 1 m s^{-1} in some parts of Puget Sound. In combination, wave and tidal currents are often more effective in transporting sediment than either of them alone.

It is important to distinguish between an *observed water level*, which is recorded by a tide gage, and *tide levels*, which are those portions of the observed water level attributed entirely to the gravitational effects of the earth–moon–sun system. This distinction is necessary because the observed water level that varies with time, $X(t)$, comprises three major components:

$$X(t) = Z(t) + T(t) + S(t) \quad (4.1)$$

where $Z(t)$ = the mean sea-level,

$T(t)$ = the tidal part of the variation, and

$S(t)$ = the meteorological surge component (Pugh 1987, p. 17).

Technical descriptions of the tides of Puget Sound can be found in Mofjeld and Larsen (1984), Mofjeld (1989, 1992) and Mofjeld et al. (2002). These resources can be obtained directly from the NOAA Pacific Marine Environmental Laboratory (Seattle) or from the University of Washington Library system. A more general description of tides is provided by Pugh (1987).

The following section describes how these three components of the observed water level are expressed in Puget Sound and suggests how to assess the impact of tides on the beach morphodynamic system.

4.1. Tides

The tidal portion of the observed water level variation in Puget Sound ($T(t)$ in equation 4.1) includes all regular, periodic effects of observed water levels. The dominant contribution comes from the gravitational forces caused by the regular movement of the earth–moon and earth–sun systems. Regular meteorological effects on water levels are also associated with the diurnal cycle as well as predictable seasonal effects due to variations in climate over the course of the annual cycle.

⁴The swash zone is the portion of the nearshore region where the beach face is alternately covered by the run-up of the wave swash and exposed by the backwash (Komar, 1998, p. 47).

⁵The sloping portion of the beach profile lying between the upper limit of wave swash at high tide and the break in slope at the low-tide terrace. Modified from Komar (1998), p. 47.

The tides of Puget Sound are predominantly mixed-semidiurnal with both the diurnal (daily) and semidiurnal (twice-daily) components playing an important role (Mofjeld and Larsen 1984). Because of the nearly 180° phase relationship between the diurnal and semidiurnal components, the typical tidal pattern has two nearly equal high waters but produces a large inequality in low waters (Figure 4.1), except during the short time when the moon is near the equator (Mofjeld and Larsen 1984). The fortnightly spring–neap modulation is dominated by the tropic–equatorial modulations in the diurnal tides. The largest tidal inequalities occur at the solstices (December and June) when the new and full moons occur at the time of large lunar and solar declinations and both the spring and tropic tides occur together. During the equinoxes, small inequalities occur in the spring tides and large inequalities occur in the neap tides. Finally, because of the phase relationships between the tidal constituents in the region, the lowest tides occur at night during the winter and during the day in summer.

The pattern of nearly equal high tides with variable low tides leads to an upward skew in the distribution of water level observations over time (Figure 4.2). Statistically speaking, water levels are more likely to be observed between mean sea level and mean high water than any other part of the tidal range. This is also manifested in the frequency and duration of exposure (or submergence) of any particular elevation of the beach profile. Sediment transport in the swash zone is proportional to the duration the beach is exposed to wave action. The longer or more frequently a portion of the beach profile is exposed to wave action, the greater the potential for sediment transport. In Puget Sound, the upper foreshore of the beach is exposed to more wave action over the course of the year than the low-tide terrace. This conclusion is reinforced by the fact (discussed in Section 4.2) that barometric pressure drops during storms, raising sea level and making it even less likely that extreme low levels on the beach profile will be exposed to strong wave action.

The interaction of the tidal waves with the topography of the basins (both dissipation and reflection) leads to spatial variations in the amplitude and phase of the tidal constituents. This is expressed in the diurnal tidal range of Puget Sound, which increases from 1.9 m at the southern end of Vancouver Island to 4.4 m near Olympia (Figure 4.3) (Mofjeld and Larsen 1984, Mofjeld et al. 2002). The large tidal range of Puget Sound leads to an average tidal prism (defined as the volume between mean high water and mean low water) of 8.1 km^3 , about 4.8% of the total volume of 168.7 km^3 (Mofjeld and Larsen 1984). The largest tidal prism is the southern basin, which exchanges 10.6% of its volume on average, and the smallest is the main basin, with an average exchange of 3.2%. These large exchanges lead to current speeds in excess of 1 m s^{-1} in many channels throughout the region, while in the deeper basins and side inlets the tidal currents are weak or barely detectable (Mofjeld and Larsen 1984). The strongest currents ($>4 \text{ m s}^{-1}$) are found in Deception Pass as a

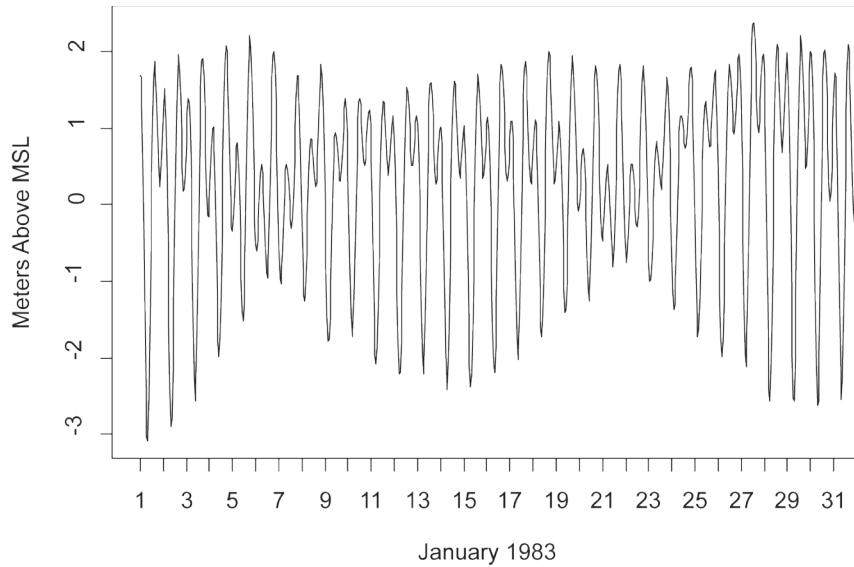


Figure 4.1. An example of mixed semidiurnal tides from Elliott Bay, Seattle. Data courtesy of Center for Operational Oceanographic Services (CO-OPS 1983–2002).

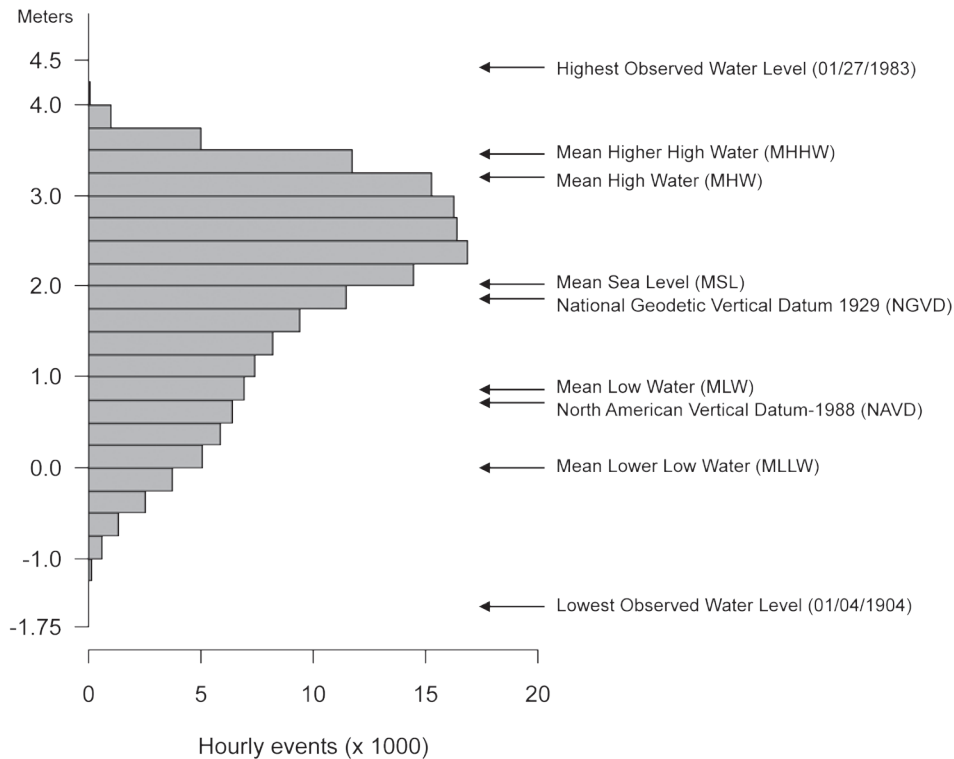


Figure 4.2. Hourly tide-level histogram and associated tidal datum for Seattle between 1983 and 2001 (NOS Station: 9447130). Data courtesy of CO-OPS (1901–2005).

result of the large difference in tide elevations between the Whidbey Basin and the Strait of Juan de Fuca. Strong currents are also found in Admiralty Inlet and most of the narrow channels that connect the subbasins of south Sound and eastern Kitsap Peninsula. Weak currents are found away from the basin entrances, particularly on Hood Canal and the Whidbey Basin. A marked

difference exists in the pattern of tidal currents from north to south. In Admiralty Inlet, large diurnal inequalities occur in the strength of the flood and ebb currents, while in the Tacoma Narrows only the flood currents show inequalities, with ebb currents being nearly equal in strength (Mofjeld and Larsen 1984).

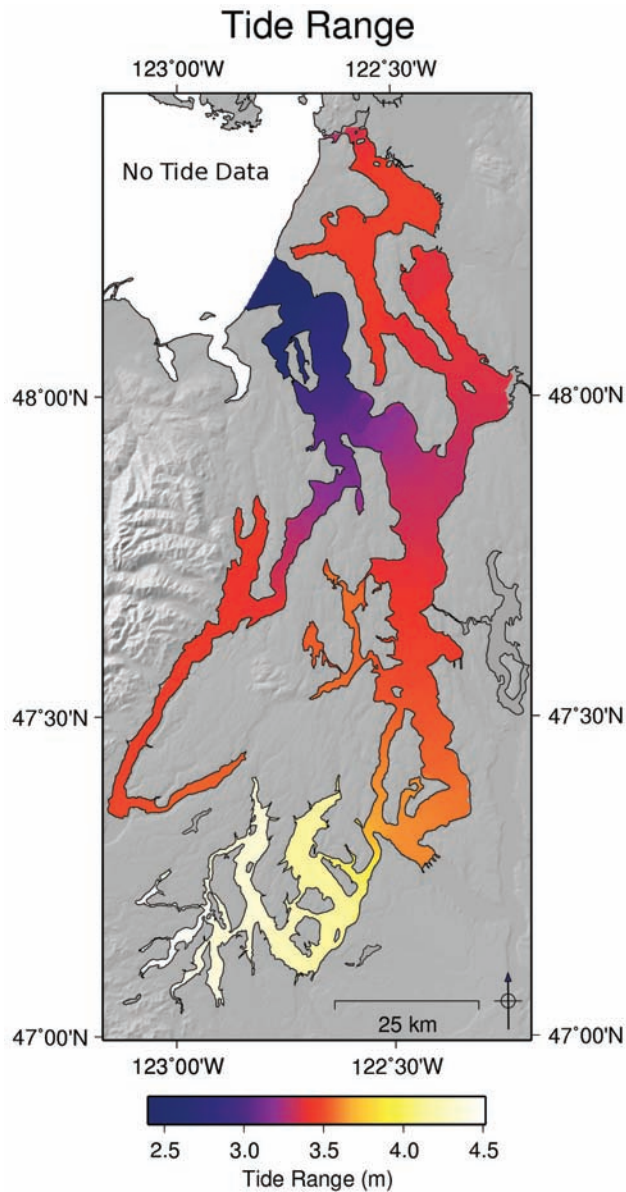


Figure 4.3. Tidal range (mean higher high water–mean lower low water) for Puget Sound and Hood Canal interpolated from the Puget Sound Tide Channel Model. Data courtesy of Mofjeld et al. (2002).

4.2. Surge

Actual water level observations differ from tidal predictions because of the unpredictable atmospheric pressure effects of weather. The non-tidal component, $S(t)$, is the portion of $X(t)$ remaining after mean sea level and the predictable tides have been removed (Equation 4.1). $S(t)$ is called different terms depending on the length of time over which the water level observations take place. Over the course of a single storm, the term is called *storm surge* and refers to the large barometric effect that low-pressure systems have on water levels. Over longer time scales, the term is more commonly called the *non-tidal component* or the *meteorological residual*.

A good example of storm surge in Puget Sound occurred on March 3, 1999, when a large extra-tropical cyclone passed over the Pacific Northwest (Figure 4.4). The cyclone moved north-eastward across the Pacific Coast and into southern Vancouver Island. The storm was accompanied by a 40 mb (1 mb = 100Pa) drop in atmospheric pressure, reaching a low of 968 mb off the coast and 990 mb over Puget Sound. Broad areas of the Pacific Northwest experienced damaging winds. This was the 12th strongest storm for the 52-year period 1950–2002 (Table 3.1).

The atmospheric and tidal records recorded at the West Point Light Station and the Seattle Tide gage respectively are shown in Figure 4.5. As the first front in the storm passed over Seattle (early March 2), air pressure rose to a peak and the tidal surge went negative (water levels below predicted); about 12 h later the low pressure of the storm began to enter the region. Wind speeds rose and pressure dropped rapidly to a low of about 990 mb. Six h after the pressure minimum, the tidal surge peaked at 65 cm above that predicted. This period corresponded with the maximum wind speeds, so it is not clear whether the tide surge was a result of wave set-up, pressure drop, or both (separating these two components of tidal surge is often difficult). As the storm broke up on March 4, pressure returned to normal levels and the tidal surge dropped down to around 20 cm. It was fortunate for Seattle property owners that the period of maximum wind speed and tidal surge occurred during low tide, where the potential damage from storm waves and coastal flooding was minimized.

The effects of weather on water levels are often coherent over the entire Pacific Northwest (Figure 4.6). The variations in subtidal sea-surface levels (SSL) computed using a 72-h filter for several sites in western Washington indicate that SSL changes are highly coherent with each other and with air pressure variations. Mofjeld (1992) found that SSL in Puget Sound could be largely explained by quasi-steady inverse barometer compensation to atmospheric pressure and the propagation of adjusted sea-level fluctuations from the nearby continental shelf, with some local

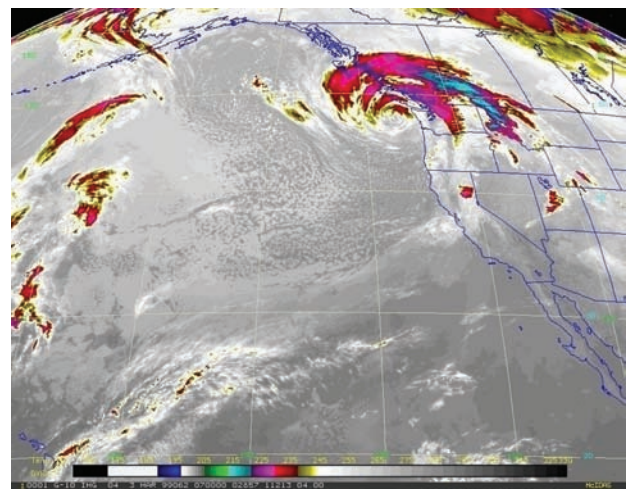


Figure 4.4. Extra-tropical cyclone off the west coast of North America, March 3, 1999. From NOAA–National Environmental Satellite, Data, and Information Service.

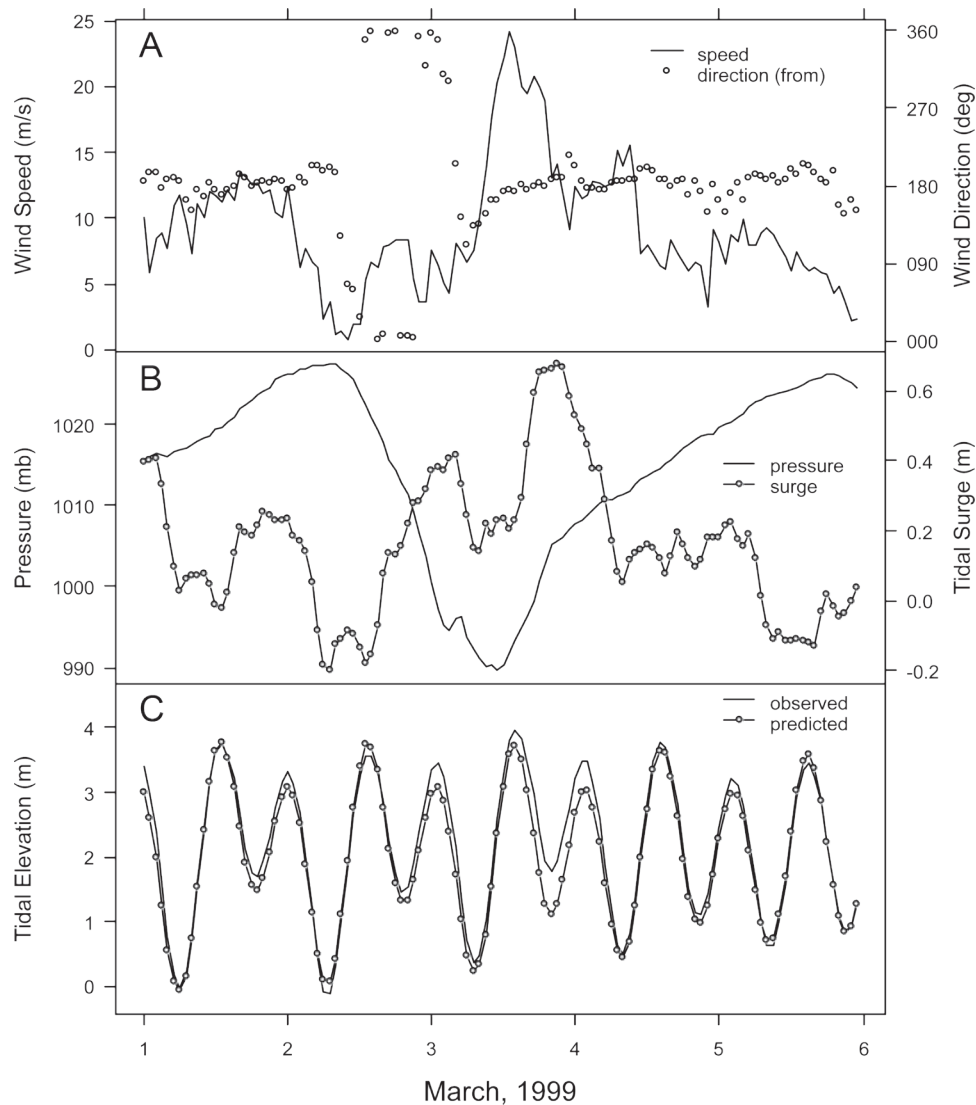


Figure 4.5. Wind, air pressure, and tidal characteristics during an extra-tropical cyclone over the Pacific Northwest between March 1 and 6, 1999. A = the wind speed and direction, B = the relationship between air pressure and the non-tidal residual (surge), C = the observed water levels versus the predicted levels. Wind and air data recorded at West Point Light Station (NDBC 2003); tidal data from Elliott Bay, Seattle (CO-OPS, 1901–2005).

weather forcing in the summer. The value of the inverse barometer effect at Seattle is -19.4 mm mb^{-1} . It is calculated by comparing the relationship between annual mean sea level and annual mean air pressure over a number of years (effectively filtering out the tidal signal) (Figure 4.7; Pugh 1987).

Subtidal SSL in Puget Sound vary seasonally and interannually. Seasonal variations in SSL are driven by annual weather cycles (as shown in Figure 4.6) with the winter months subject to large storm surges. About 99% of surges between December and February are between -40 cm and $+60 \text{ cm}$, while between May and August, 99% of observed surges fell between -30 cm and $+30 \text{ cm}$ (Figure 4.8). Interannual fluctuations in SSL are coupled with climatic cycles that affect the eastern Pacific. Mofjeld (1989) was the first to identify the strong relationship between SSL in Puget Sound and El Niño years (Figure 4.9). This effect is strongest

during the winter months and can lead to a 20-cm rise in SSL for most of the winter. The combination of a high El Niño elevation and a winter storm during early 1983 produced the highest non-tidal peak in sea-level for the 1966–1987 period. Similar water levels peaks occurred during the 1997–1998 El Niño.

Tidal surges in Puget Sound can cause coastal flooding if they occur during spring high tides. Structures built within a meter of mean higher high water (MHHW) are the most vulnerable, but storm waves can throw water well above this elevation during severe weather. Strong El Niño conditions on the eastern Pacific exacerbate the problem by raising SSL an additional 10 cm to 20 cm. Fortunately, over the 19-year period from 1983 to 2002, the highest predicted tides have tended to occur during negative surge conditions (high atmospheric pressure) and not during storms (low pressure). This phenomenon has limited the damage

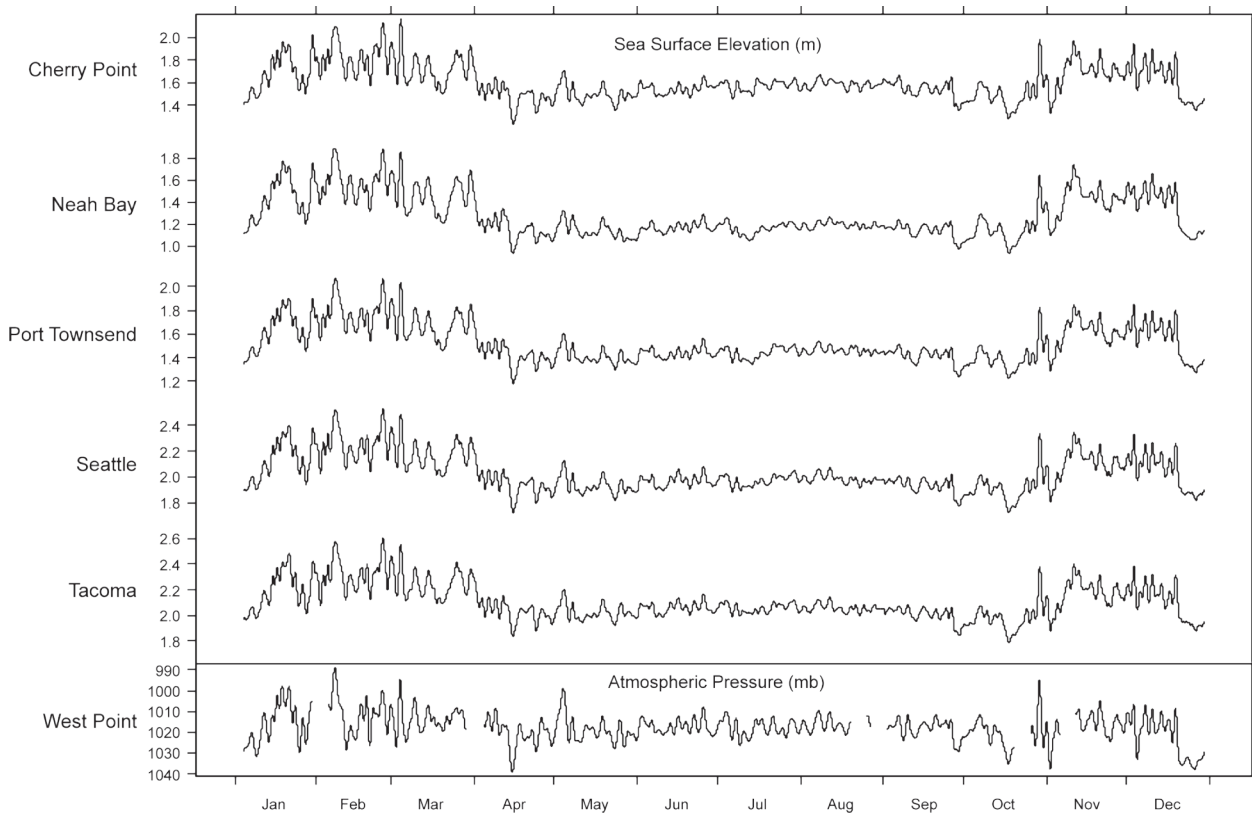


Figure 4.6. Subtidal sea-surface levels (SSL) across western Washington for 1999. SSL was computed from hourly water level observations by passing a 72-h filter over each time series, these were compared with a 72-hr filtered air pressure record from West Point, Seattle. The Y-axis of the air pressure plot has been reversed to emphasize the relationship between air pressure and non-tidal residual. Water levels from CO-OPS (1983–2002); air pressure from NDBC (2003).



Figure 4.7. The relationship between annual mean water levels and annual mean air pressures at Seattle (1984–2003). Water levels from CO-OPS (1983–2002); air pressure from NDBC (2003).

associated with coastal flooding during recent times (as was the case during the March 3, 1999 storm, Figure 4.5). Coastal engineers should factor in the risk of surge while planning low-elevation construction near the shoreline. The long tidal record for Seattle makes it relatively easy to calculate probability curves for water levels around Puget Sound. For example, the 100-year maximum water level expected for Seattle calculated from the 1902–2004 tidal record is 4.4 m above mean lower low water (MLLW; Figure 4.10), a value nearly 1 m above MHHW (3.46 m).

4.3. Mean Sea-Level

The mean sea-level term, $Z(t)$ (Equation 4.1) is written as a function of time because over long periods its value changes. Long-term sea levels in the Pacific Northwest are composed of eustatic (global) and eperiogenic (regional) movements. Eustatic movements are mainly the global rise in sea level associated with the melting of continental ice sheets. Eperiogenic movements include the effects of isostatic adjustment of the landscape after the melting of the Puget Lobe of the Cordilleran Ice Sheet and neotectonic land movements associated with both the Seattle Fault system and the subduction of the Juan de Fuca tectonic plate beneath the North American plate (see Section 2.3).

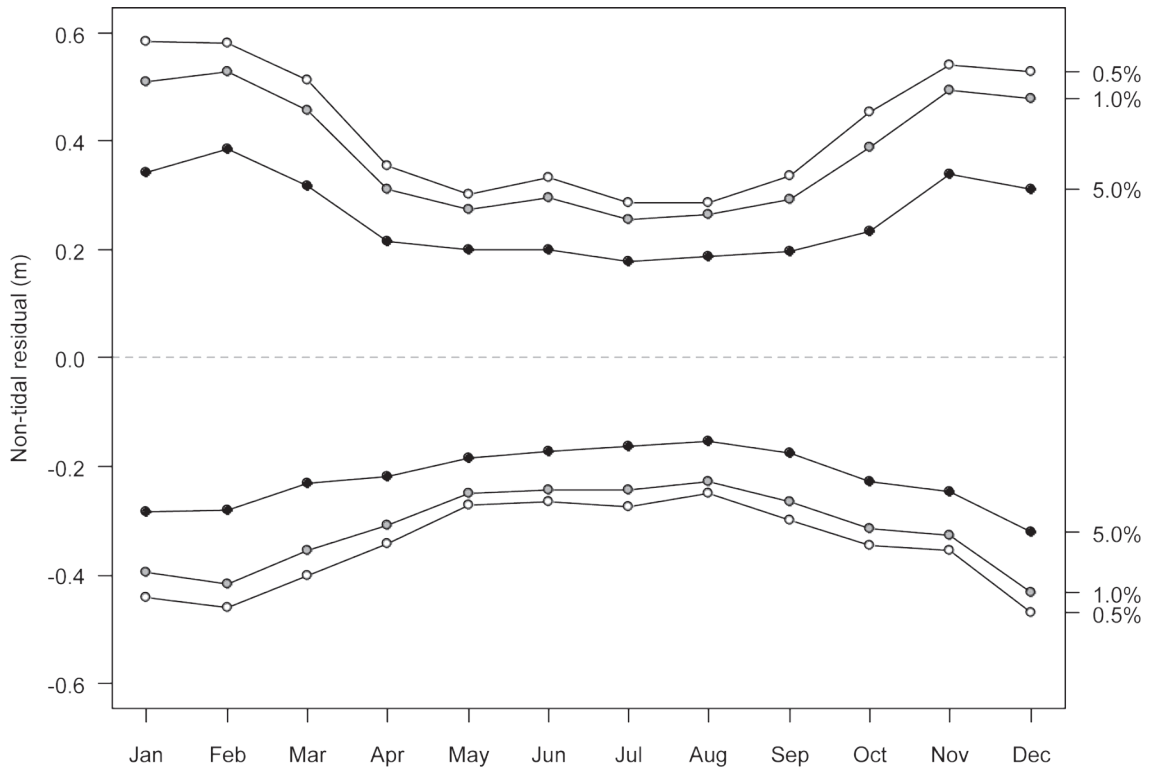


Figure 4.8. Monthly surge probability calculated by subtracting the predicted tide from the observed water level for Seattle over the period 1983–2001. Water levels and predictions obtained from CO-OPS (1983–2002).

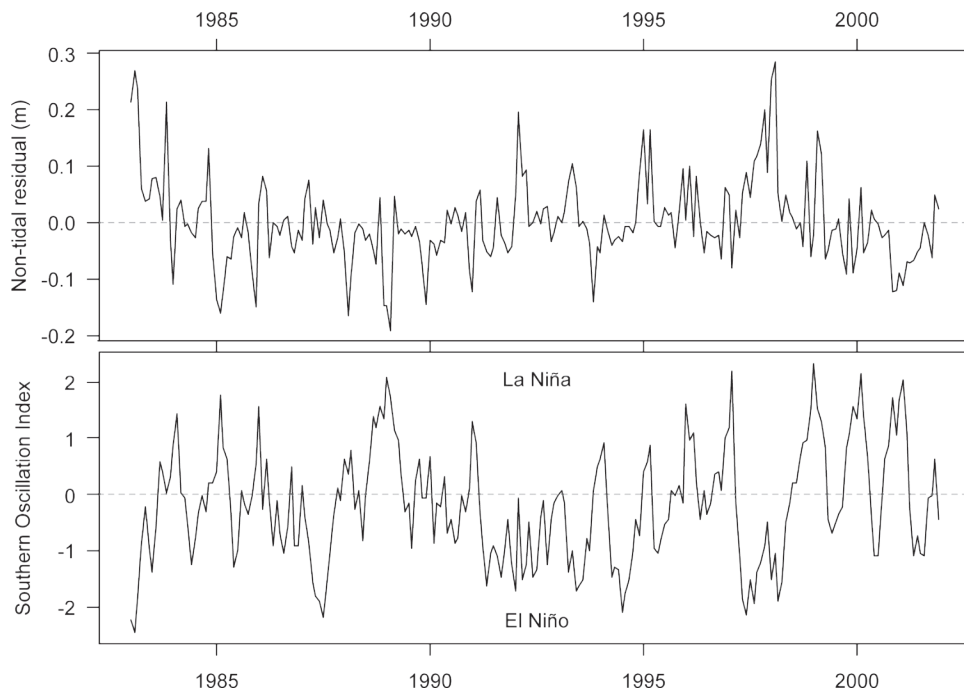


Figure 4.9. Monthly subtidal SSL at Seattle and the Southern Oscillation Index (SOI) for 1983–2001. SOI data courtesy of NOAA-Cooperative Institute for Research in Environmental Studies (2005); water levels and predictions from CO-OPS (1983–2002).

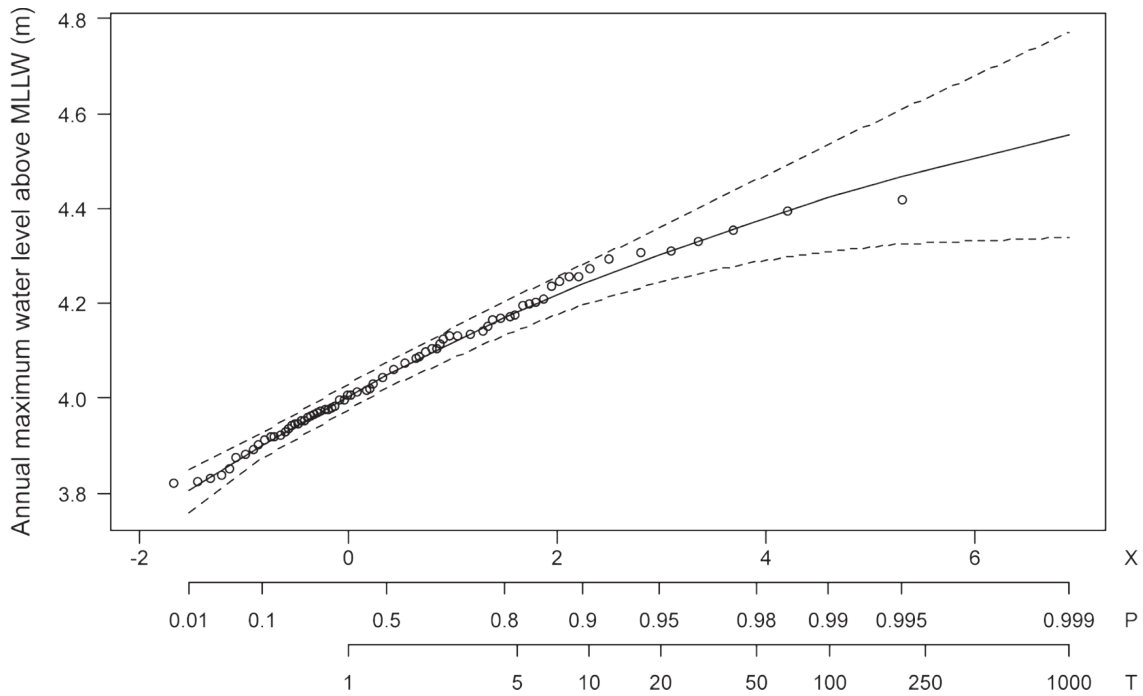


Figure 4.10. Annual maximum water level above mean lower low water (MLLW) for Seattle. X = reduced variate $-\ln(-\ln P)$. P = probability that the annual maximum water level is less than the value shown. T = estimated return period in years assuming an exponential distribution of maximum water levels. ---- = 95% confidence interval. Tide data courtesy of CO-OPS (1901–2005).

The 100-year tide record at Seattle shows that relative sea level is rising at a rate of about $+2 \text{ mm yr}^{-1}$ over the past century (Figure 4.11), Friday Harbor is rising at about $+1 \text{ mm yr}^{-1}$ and Neah Bay is *decreasing* at -1.6 mm yr^{-1} (Mofjeld 1989). Positive values of relative sea level in the Puget Lowlands reflect eustatic sea-level rise, while the negative value at Neah Bay indicates that tectonic forces from the subduction of the Juan de Fuca plate beneath North America are uplifting the Olympic coast at a rate in excess of eustatic sea-level rise.

The extent to which sea-level rise is important to coastal land

management and design depends on the time scale of the particular application. Short-term projects will be exposed to little change in mean sea level (though interannual fluctuations in sea level should be expected; see Section 4.3), but for longer-term projects, sea-level rise may need to be considered during planning. At present rates, sea level is rising in central Puget Sound at $+20 \text{ cm per century}$ (there is much regional variability to this number). Homes and coastal infrastructure located at the lower limit of dry land today may become flooded in the future, particularly when winter storms occur during El Niño years.

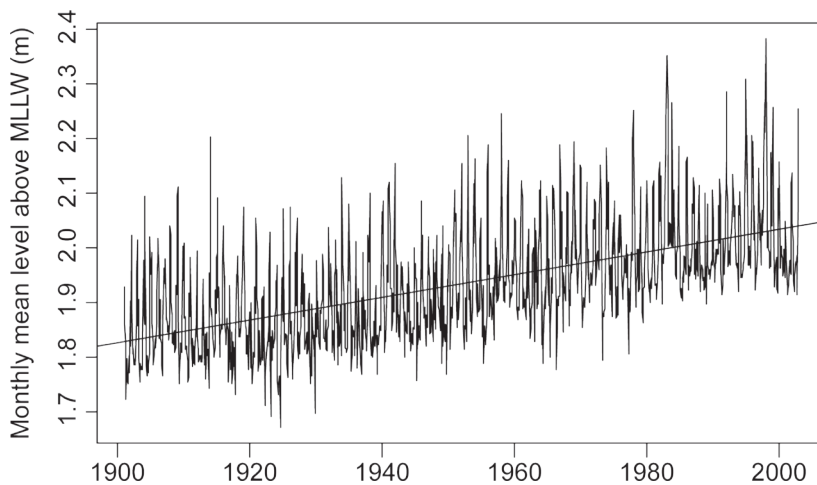


Figure 4.11. Monthly mean sea-level for Seattle (1901–2002). The trend is $+2.08 \text{ mm yr}^{-1}$. Water levels courtesy of CO-OPS (1901–2005).

5. Beaches

5.1. General Characteristics

The beaches of the Puget Lowland exhibit three characteristics simultaneously that are typically treated as separate beach types in the scientific literature: (1) mixed sand and gravel composition, (2) meso- to macro-tidal environments, and (3) low-energy (estuarine) wave environment. Although modern research into beach forms and processes dates back to the Second World War, most of this research has focused on beach environments that have well-sorted sand, and high energy and micro-tidal characteristics. As a result, many conventional beach models are based on assumptions about the wave environment, sediment properties, and transport mechanics that are not appropriate for Puget Sound.

5.1.1. Mixed-Sediment

Mixed-sediment beaches (Figure 5.1) are found where the primary source of sediment to the littoral system contains a mixture of sand and gravel. This beach substrate is common in previously glaciated regions but is comparatively rare on a worldwide basis. As a result, beaches composed of mixed sand and gravel material are under-represented in the scientific literature (Mason and Coates 2001). The term mixed-beach is applied where the substrate comprises a homogeneous mixture of sand and gravel, and also where the foreshore comprises gravel with a sandy low-tide terrace (Pontee et al. 2004). Many gravel beaches may appropriately be considered in this class (also called shingle or coarse-clastic), since gravel is rarely found without a sizable fraction of sand in the substrate.

Most mixed beaches in the literature have a composite profile with a distinct break in slope between the upper foreshore and the low-tide terrace (Mason and Coates 2001, Kulkarni et al. 2004). The break in slope is typically accompanied by a break in sediment grain size, with a pebble-sand mixture found above the



Figure 5.1. Example of a mixed sand and gravel beach foreshore (Cama Beach, Camano Island).

break and mostly coarse sand found below (Figure 5.2). Sediment size is responsible for beach hydraulic conductivity, which in turn, controls the beach profile and groundwater flow.

On gravel beaches, high beach permeability leads to asymmetry of swash zone action, such that swash is stronger during the up-rush than during the backwash. This effect tends to role both gravel and sand shoreward during the up-rush, but only mobilizes finer material seaward during the backwash, effectively stranding gravels higher on the beach with each successive wave. The onshore migration of coarse material continues until the profile steepens to the point that the vertical force of gravity balances the onshore wave forces. The exact mechanism that leads to swash asymmetry on coarse beaches is debatable, with some researchers favoring water infiltration on a permeable foreshore and others favoring increased turbulent dissipation due to the larger clasts (rock fragment or grain resulting from the breakdown of larger rocks) embedded in the beach (Mason and Coates 2001). Either way, the intersection between the saturated lower slope and the intermittently unsaturated upper slope marks a point of divergent sediment transport, with onshore transport (possibly enhanced by infiltration) favored in the upper portion and offshore transport favored in the lower section (Turner 1993).

On mixed sand and gravel beaches, unlike pure gravel beaches, the interstitial space between pebbles and cobbles becomes filled with fine-grained material. This lowers the hydraulic conductivity of the beach without greatly changing its roughness. The result is that the foreshore has the roughness characteristics of a gravel beach with the permeability of a sand beach. According to Mason and Coates (2001), a sand content of around 25% reduces the hydraulic conductivity of a mixed sediment beach to ap-



Figure 5.2. Example of a composite profile with a distinct break in slope and a break in sediment grain size between the upper foreshore and the low-tide terrace (Fay Bainbridge State Park, Bainbridge Island).

proximately that of a sand beach. Since roughness and hydraulic conductivity determine the profile response of a beach, a mixed-sediment beach behaves differently than either a pure sand or pure gravel beach. For example, a mixed-sediment profile will reflect more energy than both a sand beach (due to a steeper gradient) and a gravel beach (due to less energy dissipation through infiltration) (Mason and Coates 2001).

Composite profiles, in and of themselves, can have a dramatic affect on wave hydrodynamics from low to high tide under the same incident wave conditions (Figure 5.3) (Miles and Rus-

sell 2004). At low-tide the waves propagate across the dissipative low-tide terrace. These waves are characterized by spilling breakers, weak undertow, strong longshore currents, and a dominance of infragravity frequencies. At high tide, the waves are not affected by the terrace; instead they break directly on the steep reflective beach, where they are characterized by plunging breakers, large cross-shore variance of the gravity band, and a strong undertow.

The steep slopes of mixed-sediment beaches tend to favor swash-zone over surf-zone transport processes. Horn (2002a)



Figure 5.3. Comparison of high-tide (top) and low-tide (bottom) wind waves. Note that the high-tide photograph shows the waves breaking very near the shoreline at a large angle to the beach while in the low-tide photograph the waves are breaking offshore and moving inshore as less energetic, shore-parallel bores (Cama Beach, Camano Island).

found that studies that compared the contribution of longshore sediment transport of the surf and swash zones indicate that the amount of sediment transported in the swash zone is equal to or greater than the surf zone. Modeling of steep gravel beaches indicates as much as 50–70% of total longshore sediment transport of these beaches takes place in the swash zone.

Efforts to model the erosion and accretion of fine-grained beaches have been quite successful; however, they have been far less successful with coarser sediments, particularly in the inner surf and swash zone. This is probably due in part to a lack of a realistic model for the hydrodynamics and sediment transport in the swash zone (Horn 2002a). The swash zone is complicated because, as Butt and Russell (2000) and Horn (2002a) note:

1. The up-rush and backwash phases do not behave in the same way. During the up-rush the flow is decelerating while during the backwash it is accelerating. Also, the duration of the backwash is typically longer than the up-rush.
2. Sediment concentrations in the swash zone are as much as 3 to 9 times higher than in the surf zone. Because of the very thin water layers, it may be more appropriate to model sediment transport in the swash zone as a single-phase granular fluid flow rather than as the better understood two-phase flows where fluid and sediment can be easily distinguished.
3. Sediment transport in the swash zone is affected by infiltration and exfiltration of water into and out of the beach. This is due to the effects of boundary layer thinning/thickening and surface sediment stabilization/destabilization, which can lead to fluidization.

The effect of the last point has hindered models of mixed-sediment environments because the effects of seepage force and boundary layer thinning tend to oppose one another and have led to contradictory results. High infiltration rates will stabilize surface sediments; however, high infiltration rates will also thin the boundary layer, which increases shear stress and hence increase sediment mobilization.

5.1.2. Large Tides

Beaches exposed to large tidal ranges are affected morphodynamically in two distinct ways: (1) through tidal modulation of wave processes, and (2) through pumping of the beach groundwater system (Turner 1993, Anthony and Orford 2002, Horn 2002a). Large vertical and horizontal tidal excursions modulate wave transport processes by distributing wave energy over a relatively larger area than would have been possible on a micro-tidal beach. By widening the sediment transport zone and reducing the per-unit-area wave energy available for sediment transport, large tides act to reduce or retard morphological change on the beach (Anthony and Orford 2002). Tidal currents also impose a unidirectional and shore-parallel current that can last for several hours per day. Sediment mobilized by oscillating wave currents will adjust to the presence of the tidal current and drift slightly down the beach in response.

Large diurnal tidal ranges lead to large changes in the elevation of the beach groundwater table. The beach groundwater table is an equilibrium surface at which the pore water pressure is equal to atmospheric pressure. Below the water table, pore water pressure is greater than atmospheric pressure; above the water table it is lower. The shape and elevation of the beach water table is a function of beach morphology (mainly permeability), tidal state, wave conditions, rainfall, and terrestrial water sources, but generally, the table surface dips landward during a rising tide and seaward during a falling tide. Observations of the water table have revealed that the water table rises rapidly but drains slowly (Horn 2002a).

The beach groundwater table plays several important roles in shaping beach morphology. First, during flood tides, the swash lens washes over unsaturated sand and water percolates into the beach, attenuating the wave run-up spectrum, which leads to deposition of coarse material high on the swash lens (see also Section 5.1.1). During the ebb tide, the swash lens is acting over saturated sediments. The mean water surface often drops faster than the beach can drain, leading to a decoupling of the mean water surface and the beach groundwater table (Figure 5.4). The positive pore water pressure of the saturated sediments causes exfiltration of groundwater from the water table down to the mean water line. This moving zone is called the seepage face and can lead to sediment mobilization in two different ways: First the exfiltration of groundwater acts to fluidize the surface layer of sediments, decreasing the critical threshold for entrainment (Masselink and Hughes 1998). Second, seepage on the beach face transports fine-grained sediments off the foreshore and onto the terrace even in the complete absence of waves. Sometimes the drainage is sufficient to form small riverlets which carve shallow rills in the upper terrace (Figure 5.4). The role of seepage may be especially important in very sheltered environments where wave energy is rarely a strong geomorphic agent.

5.1.3. Low-Energy

Low-energy beaches are the least well studied of the major beach types (Nordstrom and Jackson 1992, Hegge et al. 1996, Jackson et al. 2002). A “low-energy” beach is defined by Jackson et al. (2002) as a beach where:

1. non-storm significant wave heights are minimal (e.g., <0.25 m);
2. significant wave heights during strong onshore winds are low (e.g., <0.50 m);
3. beach-face widths are narrow (e.g., <20 m in micro-tidal environments);
4. morphologic features include those inherited from higher energy events.

This later point presents problems for researchers attempting to establish a link between beach form and offshore wave climate. In low-energy environments, normal wave conditions may not achieve the critical energy thresholds necessary to mobilize beach sediments, leaving the beach out of equilibrium with the incident wave climate (Hegge et al. 1996, Anthony 1998, Jackson et al. 2002).



Figure 5.4. Beach seepage face, Cama Beach, Camano Island (top) and seep-induced rilling of the low-tide terrace, Kitsap Memorial State Park, Hood Canal (lower). Upper photo by H. Shipman.

In the scientific literature, the term “low-energy” applies to two broad classes of beaches: those that are sheltered from nearby high energy environments, which dissipates wave energy to a fraction of waves on the outer water body (such as lee shores and coastal lagoons), and those that are fetch-limited—that is, where topographic enclosure limits wave generation to the local basin only (Jackson et al. 2002). The key (dynamic) difference is the presence or absence of steady background wave energy. In sheltered water bodies, swell from the external basin propagates into the low-energy basin more or less continuously, while in fetch-limited water bodies, waves do not occur unless there is a local wind disturbance. In western Washington, Willapa Bay, Grays Harbor, and the Strait of Juan de Fuca are sheltered from the Pacific Ocean and so receive significant energy from ocean swell. Alternatively, the main basin of Puget Sound, Hood Canal, Saratoga Passage, and Port Susan are all relatively isolated from the Pacific and each other such that most wave energy is generated by local winds (fetch-limited).

Like mixed-sediment beaches, low-energy beaches often exhibit a composite profile composed of a steep foreshore above a low-gradient terrace (Nordstrom 1992, Jackson et al. 2002). The composite profile, combined with small-incident waves, leads low-energy beaches to exhibit different wave shoaling and breaking behavior than higher energy coasts.

When the tides are high on composite profiles, low-energy waves are not affected by wave shoaling until they are within a few meters of the shoreline, which truncates the surf zone to a meter or two at most before the wave plunges directly onto the beach face (Figure 5.3, top). In addition, short-period waves are less affected by refraction so they have a tendency to approach the shoreline at relatively large angles, increasing the potential for longshore currents for a given wave height (Jackson et al. 2002). Under these conditions, the swash zone is relatively more important as an energy dissipation mechanism than the surf zone. Similarly, sediment transport in the swash zone is a more important

component of the gross sediment transport than in the surf zone (Horn 2002b).

During low tides on composite profiles, the opposite conditions occur. In this case, the large, low-gradient terrace acts to dissipate much of the wave energy as surf before the waves reach the upper foreshore. Refraction may be significant, turning the waves parallel to the shoreline before they break. Suspended-sediment transport mechanisms across the surf zone are a relatively more important component of the bulk sediment transport than the weakened swash zone. In addition, in Puget Sound, the lower foreshore and terrace are often the home of dense communities of flora and fauna (Figure 5.5). These communities can introduce considerable roughness to the bed (shellfish beds for example), increasing fluid turbulence, or in the case of seaweeds and grasses, buffer waves as they cross the low-tide terrace (Fonseca and Fisher 1986, Fonseca and Cahalan 1992). However, the extent to which sea grasses and kelp in Puget Sound are acting to influence wave shoaling and breaking dynamics is not known.

Several studies of seagrasses have demonstrated that dense communities modify current flow, attenuate wave energy, and affect

sedimentation in their environments (e.g., Ward et al. 1984, Fonseca and Fisher 1986, Fonseca and Cahalan 1992, Worcester 1995). However, these effects are reduced when water heights exceed about twice the stem length (Ward et al. 1984, Fonseca and Cahalan 1992), and eelgrass (*Zostera marina*) cannot tolerate bottom currents in excess of 150 cm s^{-1} (Fonseca 1983). Within these limits eelgrass communities may be an important morphodynamic agent as they directly or indirectly affect seabed formation.

In addition to living vegetation, the large accumulation of woody debris found in the Puget Sound nearshore can stabilize or destabilize beach morphology (Figure 5.6). During quiescent periods, logs buried on the beach can act as groins, blocking sediment transport on the foreshore and stabilizing the berm. However, during periods of high tides, even giant logs can be floated and, in the presence of storm waves, act as battering rams against the beach face and any structures on the beach such as sea walls. Logs buried in the storm berm, when floated, tear the berm apart and drag a significant quantity of sediment down onto the beach face.



Figure 5.5. Eelgrass (*Zostera marina*) on the low-tide terrace, Cama Beach (top); oyster (*Crassostrea gigas*) bed on Kitsap Memorial State Park, Hood Canal (bottom). Upper photo by H. Shipman.



Figure 5.6. Large woody debris accumulated on the storm berm at Keystone Spit, Whidbey Island.

Nordstrom and Jackson (1992) have developed a profile change model for sandy beaches with moderate tidal ranges and low wave energy. In this model, two types of cross-shore profile change exist, depending on the orientation of incident waves (Figure 5.7). On beaches where the waves approach normal to the shoreline, sediment transport is cross-shore dominated. Unlike a high-energy beach, however, the exchange of sediment on the upper foreshore is limited to the foreshore itself with relatively little sediment exchange with the low-tide terrace. When wave energy conditions are high, sediment is eroded from the upper beach and deposited at the lower beach face; when conditions are calm, sediment migrates landward. On beaches where the waves approach at highly oblique angles, sediment transport is dominated by parallel foreshore changes. In this case the flux of longshore sediment transport determines whether the beach accretes or erodes. In either case (cross-shore or parallel model), beach slope may not change noticeably.

In regions with larger tidal ranges, the distribution of storm waves across the shoreface is an important control on profile morphodynamics (Finlayson 2006, p. 105). If we assume that storms are a stochastic process unrelated to tide level, then the vertical distribution of storm-wave activity on the shoreface will be proportional to the tide frequency distribution. For typical low-energy waves <0.5 m, the storm waves may be only a small fraction of the tidal range. This has the potential to set up zones of concentrated wave energy, which limit the bulk of sediment transport to the vertical range of elevations most frequented by the tides (see Section 4.1). As a result of this phenomenon, some parts of the shoreface of a low-energy, macro-tidal beach may not be subject to sediment transport on a regular basis (Figure 5.8).

In addition, in mixed-sediment and coarser beach environments, the critical energy thresholds required to mobilize sediments will be higher. Sediment transport will occur primarily in the swash

zone at or above the still-water level. Also, the volume of sediment transported per event will be lower.

On low-energy beaches, the response of the foreshore profile to storm events is proportional to the increase in the wave energy level (Jackson et al. 2002). If large differences exist between storm and non-storm wave energy levels, the recovery time period of the beach may be quite long, particularly if there is a shortage of sediment. In cases where longshore drift is dominant (parallel change model) with restrictions in up-drift sediment supply, the beach profile may not be able to recover.

5.2. Puget Sound Beaches

Most beaches in Puget Sound have a composite profile with a narrow, steep foreshore and a low-gradient, “low-tide” terrace. The break in slope between the upper foreshore and the terrace is typically accompanied by a break in sediment size with coarse-grained sediments found above the break and finer sediments below. The horizontal width of the foreshore is narrow and it often lacks a backshore, especially when abutting a coastal bluff. The width of the low-tide terrace can extend from a few hundred meters to more than a kilometer before a second break in slope marks a distinct drop into deeper water (see Section 2.1).

In an effort to quantify some of these characteristics, Finlayson (2006) surveyed 23 intertidal profiles during the spring and summer of 2004 (see Figure 5.9 for beach locations). In addition to the profiles, sediment and oceanographic parameters were measured (or modeled) for each beach location (Table 5.1). A hierarchical cluster analysis was performed on the (1) foreshore and terrace slope, (2) elevation of the transition point from gravel to sand sediments, and (3) overall profile length. Finally, the sediment and oceanographic parameters were compared with the four profile morphotypes in order to establish what, if

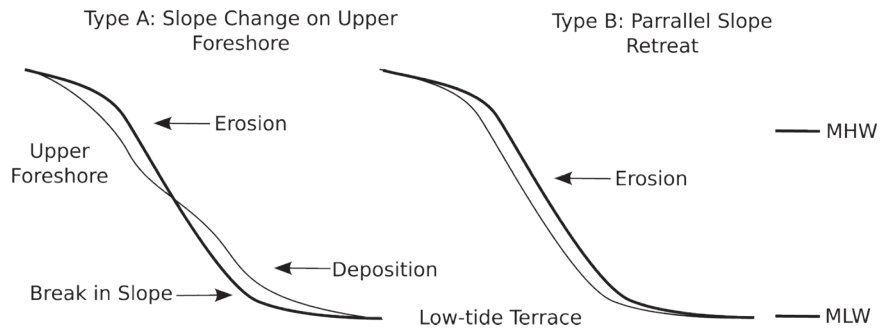


Figure 5.7. Profile change model for low-energy beaches. Redrawn from Nordstrom and Jackson (1992).

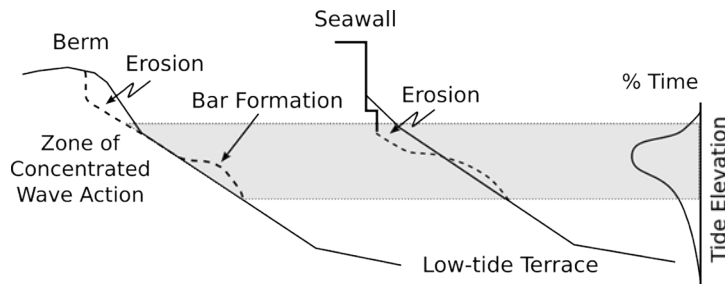


Figure 5.8. Profile response to erosional conditions on macro-tidal, low-energy beaches. Model shown for both natural and modified beaches as observed at Cama Beach, Camano Island. From Finlayson (2006).

any, relationship exists between beach profile shape, sediment size and wave and tidal climate. For further details on the analysis rational and methods, see Finlayson (2006)

The clustering analysis resulted in four profile groups or morphotypes (Figure 5.10): (1) concave with (mostly) low sand-to-gravel transitions, (2) concave with high sand-to-gravel transitions, (3) high-gradient planar with no break in slope (above MLLW), and (4) planar foreshore above low-gradient sand flats (creek-delta beaches). However, no relationship could be established between the beach groups and wave or tidal climate, or between groups and sediment type.

The beaches of Puget Sound are quite distinct from other low-energy beaches studied in the literature. In a comprehensive review, Jackson et al. (2002) identified only 27 beaches where the environment was identified as low-energy. Of these 27 beaches, only 3 had tidal ranges >3.5 m and all of them were composed of sand or finer sediments. Similarly, in Australia, Hegge et al. (1996) examined 50 sheltered beaches (2 of which are included in Table 1 of Jackson et al. 2002) that were all microtidal and composed of fine-grained sediments. On the basis of Hegge et al. (1996), the beaches of Puget Sound clearly have higher tidal ranges and significantly higher sediment sizes in general (Table 5.1).

The beaches in Puget Sound exhibit classic low-energy features including steep, narrow foreshores and dissipative low-tide terraces (Jackson et al. 2002). Sediment size differs by a factor of

8 from the foreshore to the terrace. Compared with the profile morphotypes published for sheltered beaches in Australia, Puget Sound beaches are steeper and have more pronounced concavity; otherwise, the concave, flat and steep divisions proposed by Hegge et al. (1996) seem broadly applicable. However, whether these profile morphotypes are meaningful indicators of morphodynamic processes is another matter. Finlayson (2006) found no correlation between beach morphology and oceanographic characteristics and, in contrast to Hegge et al. (1996), no correlation between morphology and sediment characteristics. Finally, profile morphotype is not a good indication of actual beach appearance, with wide variations in beach sediments, tidal range, and wave exposure in most cases. In fact, only Group 4 (Figure 5.10) shows correlation with an environmental factor identified by Finlayson (2006). Each of the profiles in Group 4 was surveyed on or near a freshwater stream deposit. Hence, the elevated break in slope for these profiles and the low gradient flats that develop in front of them are expressions of delta formation and (assuming the creeks are still supplying sediment) must be controlled by sediment supply.

The near absence of environmental control on these low-energy beaches was anticipated by the results of Hegge et al. (1996) who found no correlation between incident waves and measured beach morphology in low-energy beaches in Australia. They attributed the lack of correlation to the short-time (a few hours) wave measurements recorded for each beach and suggested that longer records that include storm waves might be better cor-

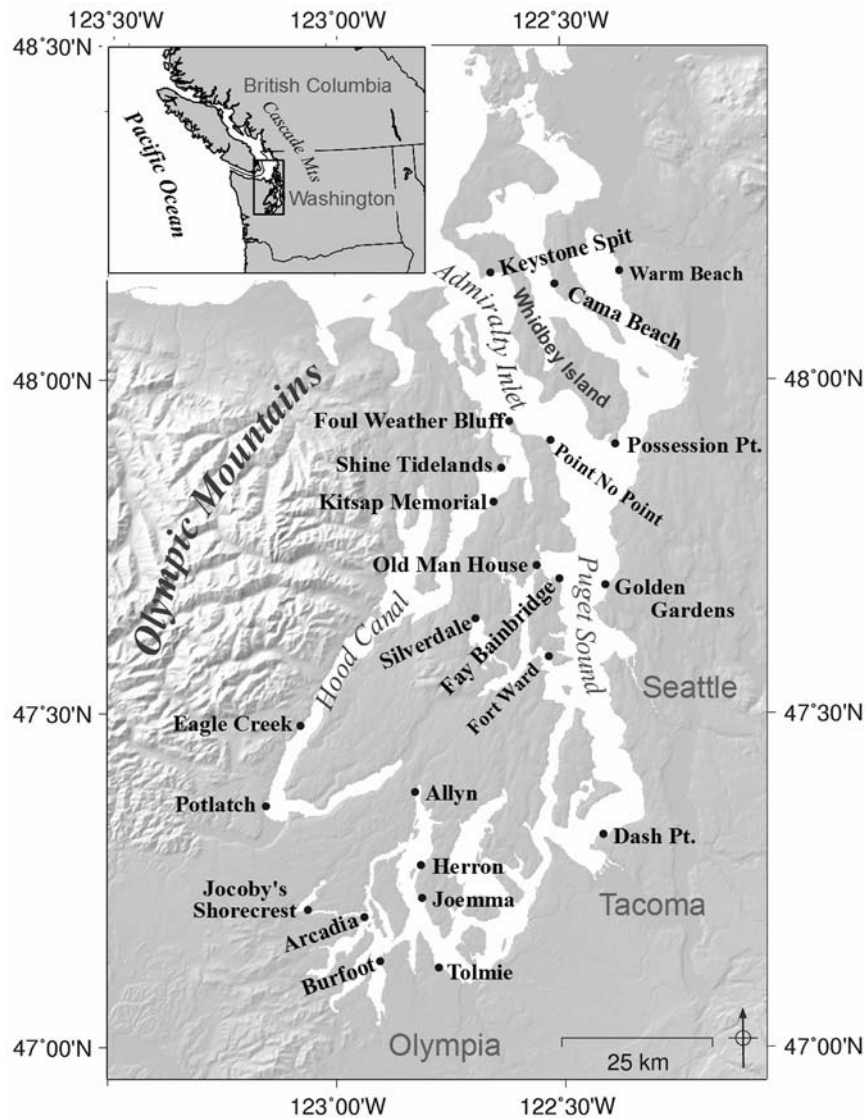


Figure 5.9. Location map of beaches studied in the Puget Lowland (from Finlayson 2006).

related with observed beach morphology. The study of Finlayson (2006) shows that in Puget Sound, at least, neither a 9-year wave climate nor sediment grain size are good predictors of beach morphology. These findings are very similar to the conclusions of Jackson et al. (2005), who found that parametric models (i.e., Wright and Short 1984, Masselink and Short 1993) that emphasize incident oceanographic conditions over geologic control performed poorly in predicting the morphology of high-energy, paraglacial beaches.

If incident oceanographic conditions and sedimentological features are not controlling beach morphology in Puget Sound, what is? First, there is the possibility that Finlayson (2006) did a poor job of characterizing the relevant wave climate. In Puget Sound, strong storms are infrequent and the 9-year record of waves that was employed to develop the wave climate model may not have captured the geomorphically relevant storms. Second, many features of the landscape were not measured, such as beach orientation relative to the waves and proximity to sediment

supply. Either of these seem like likely candidates for future analysis. Finally, geomorphic setting may be more important than modern processes in determining beach shape. Orford et al. (2002) suggest that three geologic factors control gravel barrier beaches: (1) sediment supply rate, (2) volume of sediment available and (3) accommodation space. The association among Group 4 beaches in this study and nearby creeks suggests that sediment supply may also be a controlling factor in low-energy environments in Puget Sound. Future research should attempt to quantify the role of geologic controls such as sediment supply, basement framework (accommodation space), shoreline orientation, and beach stratigraphy.

5.3. Cama Beach

A 2-year study of beach dynamics and profile response at Cama Beach State Park, Camano Island, has produced a time-series of wind and wave observations and profile changes that can be used to evaluate shoreline change models in Puget Sound (see

Table 5.1. Intertidal profile characteristics for 23 beaches in Puget Sound. The ϕ (phi) scale is a representation of sediment grain size where the ϕ grain size D_ϕ is related to the mm grain size D_{mm} by $D_\phi = -\log_2(D_{mm})$.

Site	Foreshore slope	Terrace slope	Profile length (m)	Transition elevation (m)	Tidal range (m)	Wave height (m)	Wave Period (s)	Fetch (km)	Foreshore D_{50} (ϕ)	Foreshore St.Dev. (ϕ)	Foreshore D_{50} (ϕ)	Foreshore St.Dev. (ϕ)
Allyn	0.09	0.05	63	1.46	4.3	0.2	1.5	6	-1.5	2.0	3.0	0.9
Arcadia	0.12	0.09	40	0.43	4.5	0.1	0.9	1	-3.4	1.1	1.9	1.6
Burfoot	0.12	0.03	58	0.78	4.4	0.4	2.1	6	-4.5	0.3	1.7	0.9
Cama Beach	0.15	0.05	50	0.88	3.4	0.3	0.9	12	-1.8	1.7	-2.4	2.8
Dash Point	0.09	0.01	291	3.14	3.6	0.2	0.8	10	-2.4	1.2	1.8	0.8
Eagle Creek Delta	0.09	0.01	226	1.49	3.5	0.3	1.8	9	-3.5	1.5	1.3	1.2
Fay Bainbridge ¹	0.13	0.02	60	0.78	3.4	0.2	1.2	13	-4.7	0.6	2.9	0.7
Fort Ward	0.11	Na	36	Na	3.5	0.4	1.9	6	-1.8	2.0	Na	Na
Foulweather Bluff ²	0.15	0.10	32	2.38	3.1	0.3	1.1	17	-3.1	1.2	-7.6	0.6
Golden Gardens	0.10	0.01	121	1.53	3.4	0.5	1.9	22	-2.5	2.6	1.7	0.5
Herron Ferry	0.13	0.04	70	1.59	4.3	0.3	1.4	8	-2.5	1.2	2.4	0.9
Jacoby's Shorecrest	0.13	0.07	51	2.22	4.5	0.2	1.1	2	-4.1	1.1	1.5	1.4
Joemma	0.13	0.04	79	2.03	4.3	0.5	2.3	7	-2.9	1.2	2.0	0.7
Keystone Spit	0.15	Na	32	Na	2.6	0.6	2.8	23	-3.3	0.8	Na	Na
Kitsap Memorial	0.08	Na	42	Na	3.4	0.5	2.3	6	-1.9	1.5	Na	Na
Old Man House	0.13	0.05	39	0.74	3.4	0.2	1.2	12	-2.5	1.4	2.3	1.1
Point No Point	0.13	0.02	76	1.00	3.2	0.3	1.8	16	1.3	0.7	1.5	0.9
Possession Point	0.10	0.04	60	1.11	3.3	0.6	3.0	24	-3.2	1.0	-0.3	2.8
Potlatch	0.07	0.03	56	0.09	3.6	0.1	1.0	10	-1.6	2.2	1.6	1.3
Shine Tidelands	0.09	0.03	88	1.80	3.2	0.3	1.8	11	-1.8	2.4	2.2	0.7
Silverdale	0.06	0.06	57	0.50	3.5	0.3	1.9	5	-1.6	1.6	2.1	1.4
Tolmie	0.11	0.01	309	2.56	4.3	0.1	0.6	6	-4.3	0.5	2.1	0.7
Warm Beach	0.03	0.01	254	1.07	3.4	0.5	1.8	8	-2.2	2.4	1.6	0.9

¹Foreshore sediment sample calculated from scaled photograph.

²Terrace sediment sample calculated from scaled photograph.

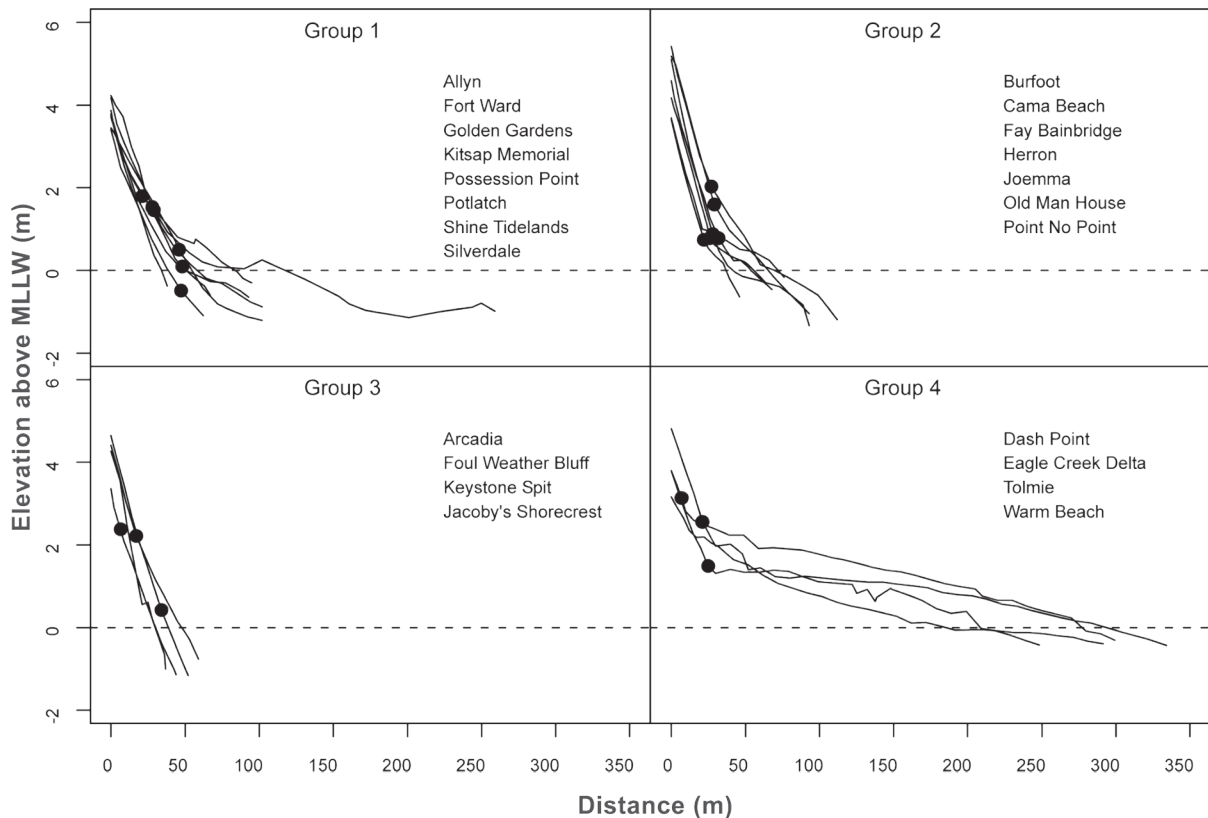


Figure 5.10. Intertidal beach profiles for 23 locations in Puget Sound grouped according to shape characteristics. Each profile is marked by the location of the transition from gravel to sand (small black dot). The classification was based on the beach slope above and below the transition point, the elevation of the transition point, and the overall length of the profile. Note that the classification was performed only to -0.16 m MLLW while the complete profile as collected is shown here (the shallowest profile in the dataset is -0.16 m MLLW). Figure from Finlayson (2006).

Section 3.2.1 for discussion of wind and wave observations; also, the time-series plot shown in Figure 3.3 may be useful as a reference).

Cama Beach is a small cusped foreland (cusped barrier) located on Saratoga Passage (Figure 3.2). Saratoga Passage is completely isolated from the Pacific Ocean, making local winds the only natural source of wave energy to the field site. The direction of prevailing winds over the region are southerly during the winter and northerly during the summer (Phillips 1968, Overland and Walter 1983). The strongest winds are typically (not exclusively) southerlies resulting from winter storms moving inland from the eastern Pacific. The maximum fetch is 7.7 km to the southwest and 4.9 km to the northwest. The tide range between MHHW and MLLW at Cama Beach is 3.46 m with fortnightly spring tides exceeding 5 m.

The portion of the Cama Beach under investigation is approximately 350 m long with an intertidal beach face about 40 m wide on the north-facing limb of the barrier and about 60 m wide on the south-facing limb. The beach is fronted by a narrow low-tide terrace at about -1 m MLLW, which is covered by a dense eelgrass meadow (*Zostera marina*) and the associated benthic fauna (crustaceans, mollusks, etc.). Offshore of the terrace, the water drops off rapidly to >90 m depth. Sediment on the beach is

a mixture of sand, pebbles, and cobbles derived from the erosion of nearby coastal bluffs. These sediments are then reworked by waves and transported into the field area by littoral processes, which have not been observed in detail.

A cement seawall was placed on the upper beach in the late 1950s. In 2005, the seawall footing was exposed on the southern limb of the beach, but the wall was nearly 5 m shoreward of the storm berm on the northern limb of the beach. As a long-term geomorphic indicator of net shore drift, this shows that the northern limb of the beach is accreting and the southern is eroding. South-to-north net drift is consistent with regional maps of drift direction (Keuler 1988).

5.3.1. Beach Sediments

The southern and northern limbs of the beach have distinct sediment textures and unique profile characteristics that appear to be related to long-term erosion and accretion patterns. The northern, accretional limb of the beach has a composite (two-part) profile with a steep, planar foreshore above a low-gradient terrace (Figure 5.11a). There is a well developed pavement of medium pebble gravel at the surface which overlays a nearly homogeneous, matrix-supported, and fine-pebble gravel in a medium sand mixture. The full depth of this layer could not be

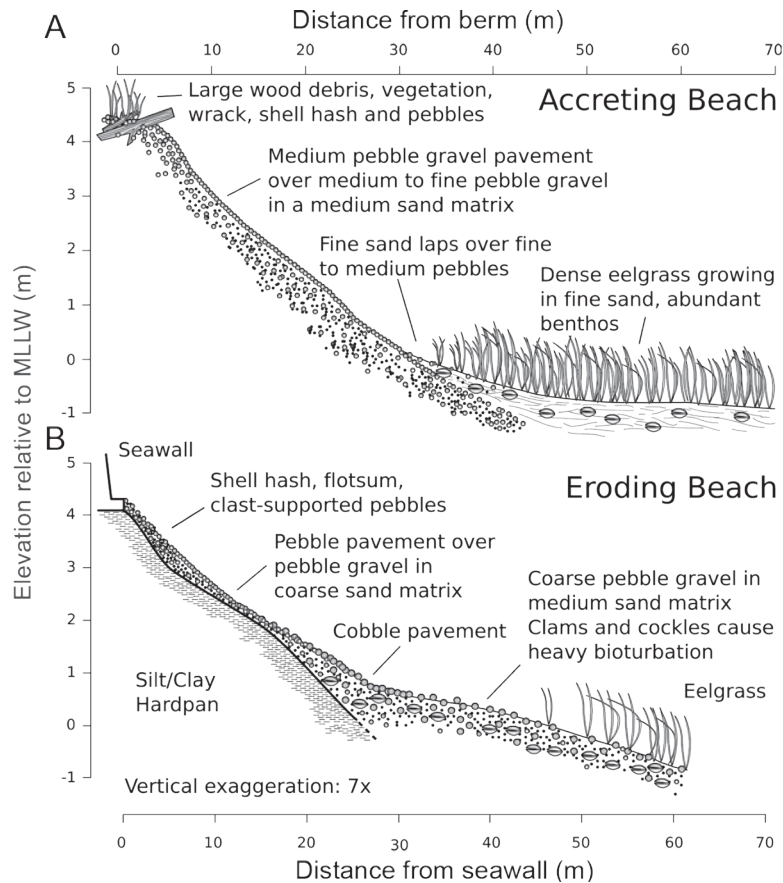


Figure 5.11. Cross-sections of the (A) accretion (north limb) and (B) erosion (south limb) beach segments at Cama Beach. The cross-sections are based on sediment samples and measured trenches dug into the beach during the summer of 2004. Figure from Finlayson (2006).

determined beyond the water table by trenching, but it is at least 1 m thick across the whole beach face. At the top of the profile is a well developed storm berm, which has incorporated large wood debris, vegetation, wrack, shellhash and washed pebbles. Low on the profile (~0 m MLLW), a fine sand laps onto the gravel pavement, marking a transition point between the gravel foreshore and terrace. The upper terrace sands are rilled by flowing water seeping from the beach face and serve as an indication that sediment transport from the shoreface to the terrace can proceed by tidal-induced seepage in the absence of wave activity. Dense eelgrass and abundant benthos occupy the terrace.

The southern, erosional, limb of the beach is also composed of a composite profile, but it is quite distinct from the northern accretional limb (Figure 5.11b). Like the northern limb, a well-developed gravel pavement exists, but it lies over a coarser mix of gravel and sand. The beach deposits are at most 30 cm thick above a silt and clay hardpan that can be exposed during storm conditions. On the upper portion of the beach, the pebble mixture is clast supported with a well-washed appearance. The seawall footing rests directly on the hardpan, well within reach of high-tide wave action. No berm has developed in front of the seawall. Lower on the profile, the pebbles increase in size to cobbles in a coarse sand matrix. The cobbles are encrusted with

seaweed, barnacles, and other organic matter, suggesting seasonal stability at a minimum. Much of the free sand found on the surface of the southern profile is deeply recessed into the interstitial spaces between the cobbles, leading to an overall appearance of a deflated or well-winnowed surface. Eelgrass is sparse on the lower profile and no thick sandy bed has developed.

5.3.2. Beach Changes

Significant elevation changes at Cama Beach were infrequent and confined to the foreshore with little or no change observed on the intertidal portion of the low-tide terrace. The maximum elevation change observed was 0.70 m, but it was more common to see changes <0.15 m. On several surveys the entire profile registered elevation changes beneath the vertical root mean square (RMS) error of the survey technique (approximately ± 6 cm as a result of gravel roughness).

The nature of cross-shore elevation change was a function of longshore position, with the distal limbs of the beach experiencing most elevation changes high on the profile, while the apex of the beach experienced change across most of the foreshore (cf. Figures 3.2 and 5.12). The northernmost profile, Profile 1, has a well-developed storm berm, which shows some variability from

the top of the berm down to about +2 m MLLW. Moving south towards the apex of the beach, more of the foreshore becomes affected until, by Profiles 5 and 6, almost the entire beach face >-1 m MLLW has experienced elevation changes. The southern profiles display a similar pattern in reverse with Profile 7, closest to the apex, showing the most variability on the beach face and Profile 10, the furthest from the apex, showing the least beach-face variability.

For both the northern and southern profiles, the elevation changes are concentrated on the upper portion of the foreshore. On the southern limb, the foot of the seawall rests on glacial hardpan at about +3.5 m MLLW. This is at approximately MHHW and below maximum tide levels during spring tides. Erosional episodes in front of this wall tended to scour out the area in front of the seawall footings, moving the eroded material

a few meters down the beach face into a shore-parallel pile of gravel. The overall effect was to lower the upper beach by as much as 0.70 m, noticeably changing the beach slope within 5 m of the wall. A particularly strong event in late September 2003 resulted in the deepest scour observed in the study, which completely removed all material in front of the wall on Profiles 7, 8, 9 and 10 (this forms the lower-bound on these profiles in Figure 5.12).

In contrast, the northern beach profiles have a well-developed berm of loose pebbles, shellhash, and beach flotsam starting at about +3.5 m MLLW. Erosional episodes here erode a scarp into the berm, redistributing the material on the beach face in much the same manner as on the southern profiles, but notably without scouring or lowering upper beach elevation.

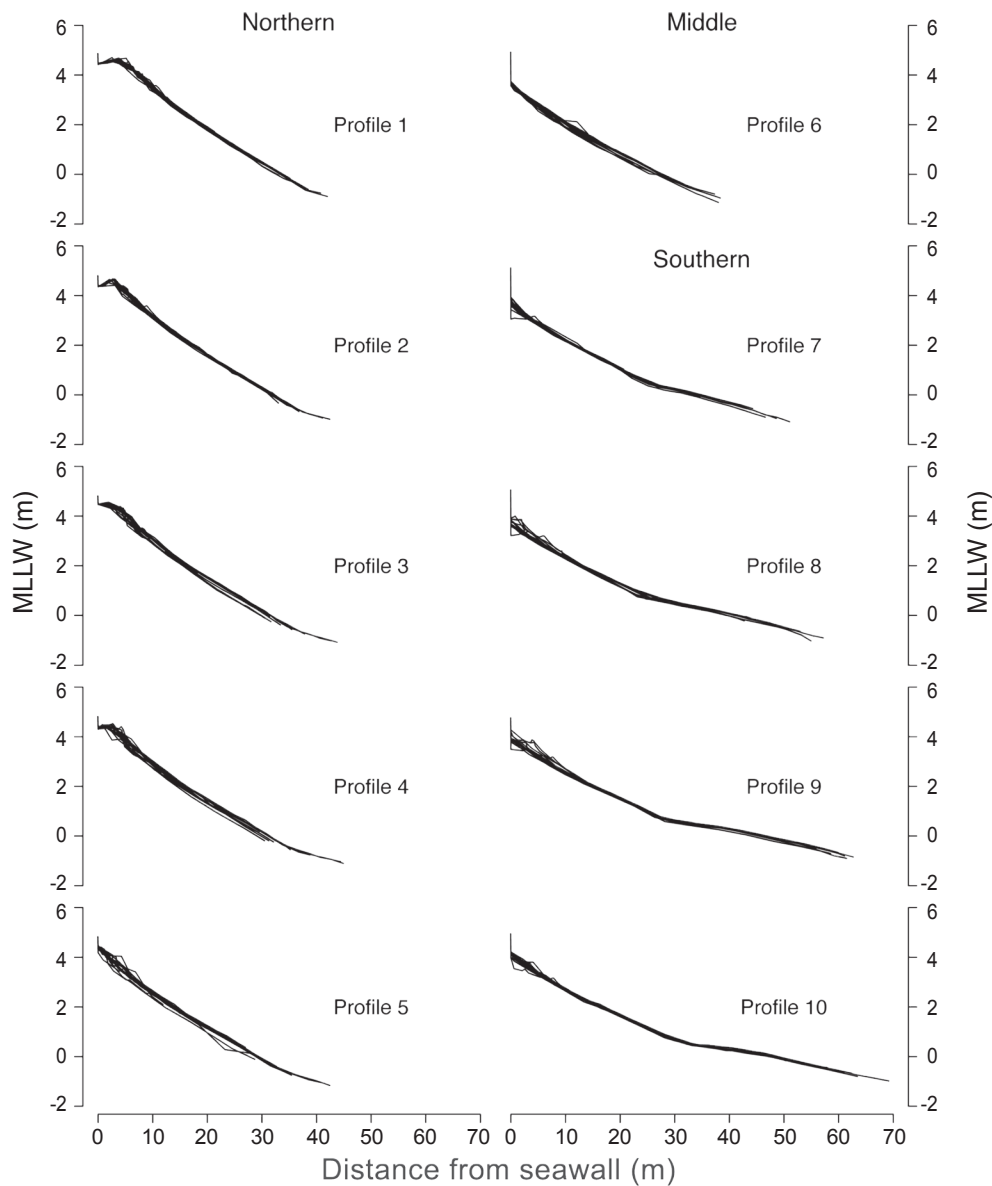


Figure 5.12. Cross-shore profile changes at Cama Beach, August 2002–May 2005. Each profile was surveyed 15 times. From Finlayson (2006).

Both the north and south beaches developed a seepage face as the tide levels decreased below about +2.5 m MLLW. As the water drained from the upper beach sediments, a sheet flow developed over the lower beach face. At the base of the foreshore gravels, the sheet flow was channelized into small rills cut through the sand of the upper terrace. The seepage flow appeared to be an effective means of moving fine sediments from the beach face toward the terrace, even in the complete absence of wave energy. However, the D_{50} grain size of the lower foreshore (-4ϕ) was much larger than elevation changes associated with seepage transport. As a result, no quantitative measurements of the volume of sand transported by this mechanism were attempted.

The cumulative volume change per-unit-area between August 2002 and May 2005 at Cama Beach shows a net loss of material from the southern profiles and a net gain of material on the northern profiles (Figure 5.13). Most of these changes occurred during the fall and winter of 2003–2004 and to a lesser extent to the spring of 2005. The remainder of the surveys showed insignificant volume changes after the vertical RMS errors were removed.

5.3.3. Storm and Recovery

Between September 7 and November 8, 2003—the dates on which beach profile data were collected—a series of strong storms occurred at Cama Beach (see Figure 3.3). These events were the strongest weather observed during the investigation and resulted in the largest changes to the beach profiles (Figure 5.14).

Between August 8, 2002 and September 7, 2003, Cama Beach had built up a large berm on the northern portion of the beach (the green line on Profiles 4 and 5 in Figure 5.14) as well as a more modest berm beneath the seawall on the southern limb (Profiles 7 and 8). The first storms of September 2003 approached from the south. The waves cut into the berm on Profiles 4 and 5 and redistributed the material over most of the upper foreshore. On the southern Profiles 7 and 8, the small berm that had built up beneath the seawall was scoured out and that material was moved into two shore-parallel bars about 1 m and 5 m from the seawall (orange profiles in Figure 5.14).

On October 16–19, 2003, a strong southerly struck the area with 15-min average wind speeds up to 17 m s^{-1} (near-gale conditions

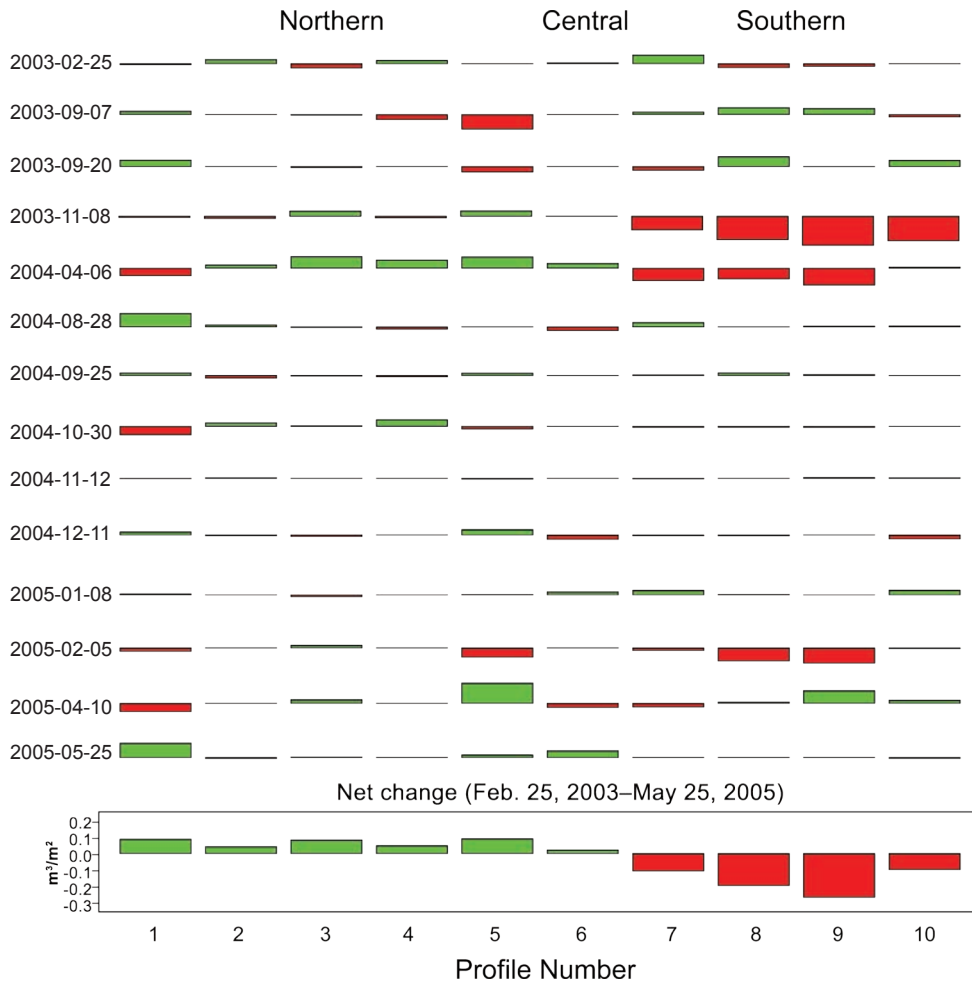


Figure 5.13. Normalized volume change per-unit-area by profile at Cama Beach, August 2002–May 2005. The profiles are arranged from north to south (left to right). Red bars = erosion; green bars = indicates accretion. Volume differences are calculated between adjacent survey dates, which are shown. Figure from Finlayson (2006).

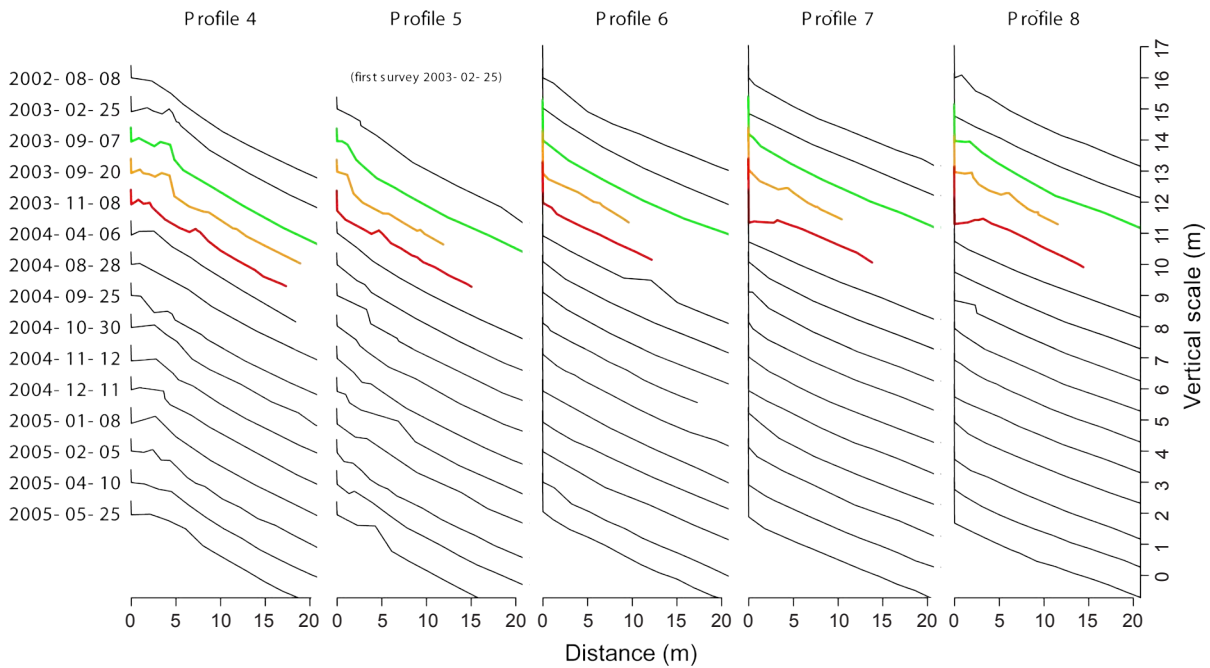


Figure 5.14. Evolution of the upper foreshore at Cama Beach through time. The profiles are truncated beyond 20 m from the seawall. All profiles are to the same scale. The profiles are arranged from August 2002 through May 2005 (top to bottom) and from north to south (left to right). The green profiles represent the pre-storm condition on September 7, 2003; the orange lines are the profiles on September 20, 2003 after the first storm of the season; and the red lines reflect conditions after a major storm on October 15–17, 2003. Note that the first survey on Profile 5 was February 25, 2003. Figure from Finlayson (2006).

on the Beaufort Scale). A detailed time series of wind, wave, and tide conditions during the storm was developed (Figure 5.15). The northern profiles responded to the storm waves by cannibalizing the berm and redistributing the material into a large shore-parallel bar about 5 m down the beach face (the red profiles in Figure 5.14). The southern profiles, with the modest berm already removed during the previous month suffered severe erosion at the foot of the seawall. The entire beach substrate in front of the wall was eroded, exposing both the seawall footing and the glacial hard-pan on which the beach is supported. Some of the material eroded was redistributed across the foreshore, but much of the material appears to have been lost to longshore transport.

An important feature of the October 2003 storm was the relationship between tide levels, storm waves, and beach change. During this storm, the strongest winds occurred during high tides. As a result, the largest waves (based on Figure 3.4) were estimated to have occurred high on the beach foreshore rather than lower on the beach face or terrace. This concentrated erosion and sediment transport into a narrow corridor high on the beach (Figure 5.16).

By April 6, 2004 (6 months after the first large storm), the beach had essentially recovered its pre-storm configuration. On the northern profiles, the shore-parallel bar had migrated up the beach face and welded itself onto the remains of the previous berm, effectively rebuilding the berm. On the southern profiles, the scoured-out region in front of the seawall had filled in and the pre-winter beach slope was reestablished, albeit at a lower overall elevation. The large shore-parallel bar that formed on

Profile 6 was notable. This appeared to be caused by the migration of material eroded from the southern profiles during the winter. The material was redistributed over Profiles 5 and 6 during the following summer.

No other event during the 34 months of observations at Cama Beach had as much impact on the beach form as the storms of Autumn 2003. One factor that may have contributed to the effectiveness of the October 2003 event in mobilizing sediment is that no event of similar intensity had been observed during the previous year. The beach had built up berms during an extended low-energy interval that were unsustainable under higher energy conditions. Strong wind events the year following the October 2003 storm may have had less impact on the beach, in part, because the beach profile had not yet fully recovered its low-energy configuration from the 2003 storms.

These observations may be indicative of an interannual cycle of accretion and erosion. In a high-energy environments, cycles of erosion and accretion are driven by seasonal changes in storm intensity. In contrast, a low-energy beach erosion cycle may be triggered by storms with longer return intervals. A similar interannual phenomenon is observed in temperate forest streams. The dominant flood—that for which the frequency of flow cumulatively transports the most sediment—has a return interval of between 1 and 2 years (Wolman and Miller 1960). Floods larger than this occur infrequently enough that they do not dominate the channel morphology; floods smaller than this carry an insignificant sediment load. Perhaps a similar situation exists for low-energy beaches, where the 2- to 3-year storm event dominates

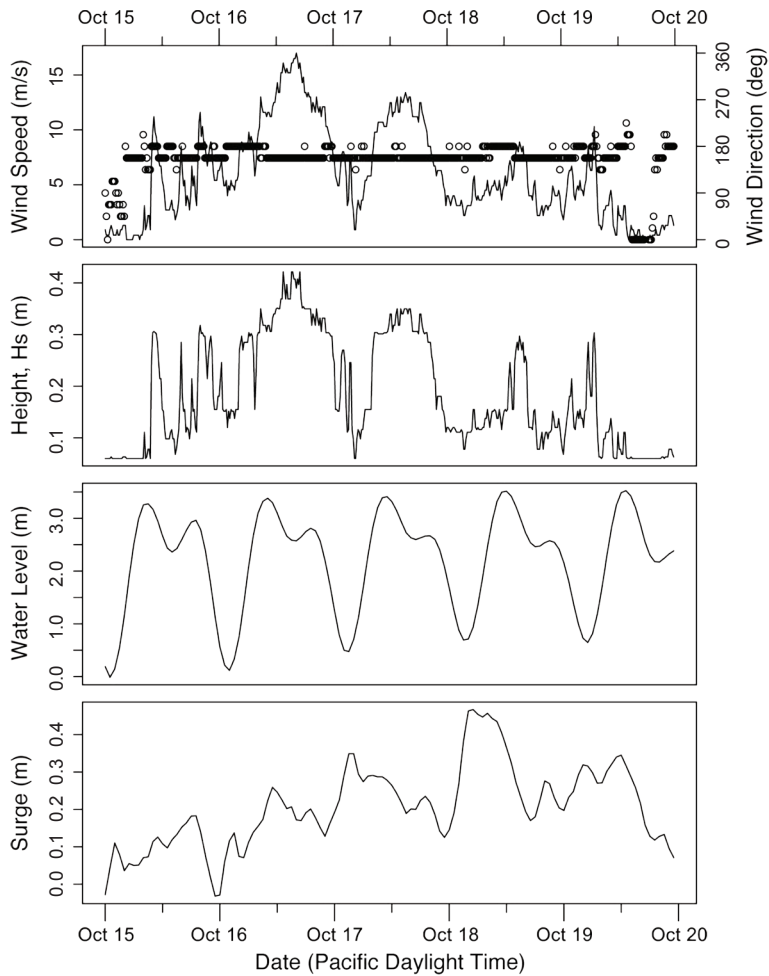


Figure 5.15. Measured wind speed, wind direction, significant wave height, water level, and surge at Cama Beach during near-gale conditions, October 15–20, 2003. Wind speed and direction were measured on site during the storm; tide levels and surge were calculated from NOS station 9447130, and wave heights were estimated from the Seattle Tide gage (CO-OPS 1901–2005). Figure from Finlayson (2006).

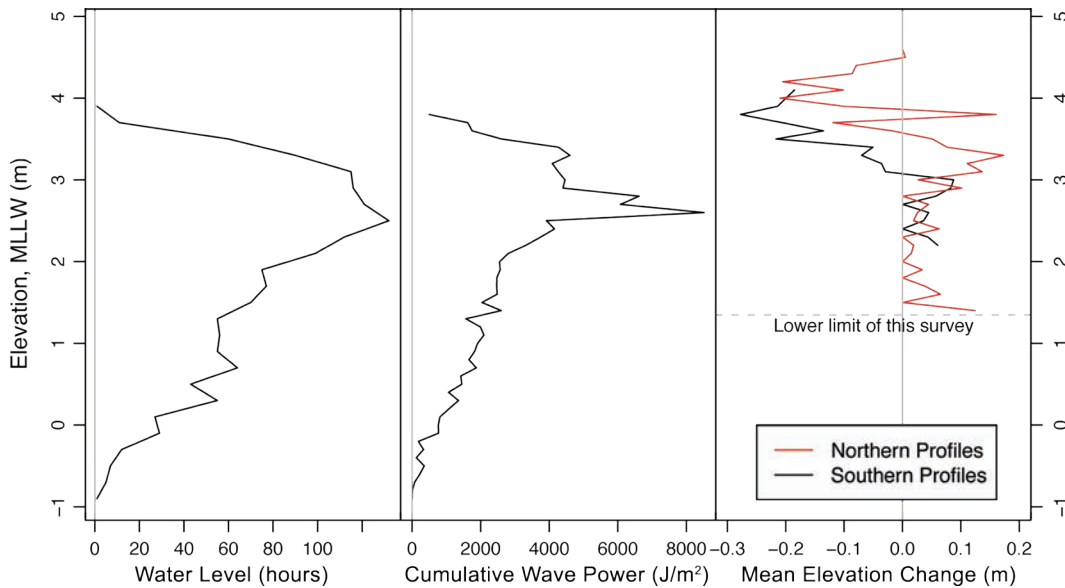


Figure 5.16. Vertical distributions of water level (still water), cumulative wave energy, and profile elevation change from September 7, 2003 through November 8, 2003, at Cama Beach. Wave heights are estimated from Figure 4.5; tide levels are from the Seattle tide gage (CO-OPS 1901–2005). Figure from Finlayson (2006).

beach morphology; that is, its frequency of occurrence cumulatively transports the most sediment on a low-energy beach.

5.3.4. Profile Response Model for Puget Sound

The profile responses to storm waves illustrated in Figures 5.14 and 5.16 suggest that the low-energy profile response model of Nordstrom and Jackson (1992) needs to be modified for Puget Sound. The original model was developed in Raritan and Delaware Bay, New Jersey, where tidal ranges are <2 m and beach sediments primarily constitute sand. Two parts of the model should be adjusted.

First, in a micro-tide environment, wave energy is dissipated across most of the beach face (skewed upward slightly by storm surge). In Puget Sound, however, the large, mixed semidiurnal tides result in about 6–8 h of high tide at or above MHW for every 2–3 h below MLW (see Section 4.1). If we can assume that storms are a stochastic process unrelated to tide level, then most storm-wave activity will be proportional to the tide frequency distribution. In other words, most storm waves will occur at high tide in the Sound.

Second, coarse-grained sediments in (relatively) low-wave energy environments behave differently than in the Nordstrom and Jackson model. Rather than removing sediment from the upper foreshore and delivering it uniformly across the lower foreshore, the profile evolution for Cama Beach (Figures 5.14 and 5.16) suggests that coarse-grained beaches remove material from the upper foreshore to a shore-parallel bar a few meters down the beach face. The bar formation may be an indication that the waves were restricted by tide action to the upper foreshore (as discussed previously), or it may indicate that the process of transporting gravel is different from that for the sandy beaches observed in New Jersey. This distinction is unresolved.

Given the differences in environment, the low-energy response

model of Nordstrom and Jackson (1992) was modified to incorporate the observations seen at Cama Beach (Figure 5.8). The key difference between this model and that shown (schematically) in Figure 5.7 is that the beach modification is restricted to the upper foreshore above mean sea level (MSL). The development of a bar as opposed to accretion of the whole lower beach face may be the result of tidal restriction of the active erosional zone of the beach.

5.3.5. Summary of Observations at Cama Beach

The low-energy beach response model of Nordstrom and Jackson (1992) developed for sandy, micro-tidal beaches does not adequately describe the profile response of the macro-tidal, mixed-sediment beaches common in Puget Sound. A more appropriate model must account for the effects of the tidal distribution in concentrating wave action and hence, sediment transport, to a narrow vertical corridor located above MSL. Sediment transport below this zone may be negligible (on the coarse-grained foreshore, at least).

The most important sediment transport events observed at Cama Beach were associated with dominant storms. Dominant storms are sufficiently strong that they mobilize the beach sediments, but they also occur frequently enough that their cumulative effect on the beach dominates other stronger events. In a low-wave energy environment like Puget Sound, the dominant storm may have a return interval of several years or more.

5.4. Longshore Transport Observations

Qualitative studies of net shore drift along the marine shorelines of western Washington were conducted during the late 1970s and early 1980s (Wallace 1988). From these theses, 26 locations (17 in Puget Sound, Table 5.2) were identified where it was pos-

Table 5.2. Net longshore drift rates for Puget Sound. From Wallace (1988).

Site (county)	Wave approach	Fetch (km)	Cell length (km)	Rate (m yr ⁻¹)
1. Twanoh Park Boatramp (Mason)	SW	6.9	8.1	200
2. Vaughn Bay Spit (Pierce)	S	8.6	3.9	2000
3. Steamboat Island Spit (Thurston)	SW	5.4	4.0	300
4. Cooper Point Spit (Thurston)	S	10.0	7.7	800
5. Zittel's Marina (Thurston)	N	4.8	0.5	100
6. South Foss Tug Jetty (Pierce)	S	1.5	0.6	80
7. North Foss Tug Jetty (Pierce)	S	1.5	0.3	100
8. Carr Inlet Naval Range (Pierce)	SW	6.4	2.8	600
9. Nearns Point Spit (Pierce)	SW	6.4	0.7	90
10. NW Fox Island Bridge (Pierce)	SW	7.6	1.5	30
11. SE Fox Island Bridge (Pierce)	SE	7.6	2.7	50
12. Des Moines City Marina (King)	SW	17.6	2.9	5,000
13. Port Townsend marina (Jefferson)	SE	8.6	6.0	1,000
14. Pope and Talbot Mill Jetty (Kitsap)	SW	8.0	26.0	80
15. Kingston Ferry Terminal (Kitsap)	SE	12.5	1.2	2,000
16. Keystone Harbor (Island)	SW	13.7	9.6	5,000
17. Mariners Cove (Island)	SW	14.3	1.5	200
	Mean	8.3	4.7	1,037

sible to quantify net shore-drift rates. The procedure involved (1) field measurements of sediment accumulation at drift obstructions, (2) extrapolation of spit growth using aerial photography and historical maps, and (3) evaluation of maintenance dredging volumes at navigation channels. The mean drift rate for south Sound locations was $400 \text{ m}^3 \text{ yr}^{-1}$ and for the main basin it was $>2000 \text{ m}^3 \text{ yr}^{-1}$. Overall, the mean cell length was 4.7 km with a mean drift rate of $1037 \text{ m}^3 \text{ yr}^{-1}$.

Wallace (1988) found that mean shore-drift rates were a strong function of mean fetch length in the region. Since longer fetches can produce larger waves, this can be interpreted to mean that larger waves move sediment more rapidly. Wallace (1988) also suggests that mean drift rate is a weak function of drift-cell length, but drift-cell length is no doubt cross-correlated with overall fetch length, so this conclusion may not be relevant.

The aforementioned net shore-drift observations rely on geomorphic indicators of long-term drift directions rather than short-term observations of wind and wave directions. The advantage of this approach is that the results integrate many years of variable wind and wave action. The disadvantage of this is that it does not indicate the magnitude of short-term variability in longshore drift, which may be more important to individual property owners as they make management decisions about their property during unusually stormy years. Observations at Cama Beach (Section 5.3) show that gross annual variability in longshore sediment volumes can be as large as the long-term fluxes.

5.5. Secondary Features

Jackson et al. (2002) identify several secondary features of low-energy beaches. These include the following:

1. longshore and transverse bars and biogenic features on the low tide terrace,
2. swash bars,
3. vegetation and wrack accumulations on the intertidal foreshore,
4. pebbles/shells, and
5. small Aeolian dunes.

Additional features in Puget Sound are cobble lag deposits and pebble armoring.

Whether these features are present or absent is highly dependent on small changes in wave energy and sediment supply. Many of these features are present in Puget Sound and have already been described. However, several interesting features of Puget Sound beaches not mentioned elsewhere bear discussion.

5.5.1. Bars

Longshore bars are often found on the low-tide terraces of low-energy beaches (Jackson et al. 2002, and sources therein). They appear to be stranded features that do not exchange sediment with the beach foreshore, as they would in high-energy systems. Once sediment moves offshore from the foreshore, it is rarely compensated by transport back up the profile. In Puget Sound,

transverse bars have been observed in a number of locations on the low-tide terrace. Prominent bars are located on the southeast shore of Camano Island (Figure 5.17).

Small swash bars, cusps and other rhythmic morphologies are commonly observed on some beaches in Puget Sound. A precondition for these features is a ready supply of mobile sediments that the waves can rework. At Cama Beach, a swash bar developed in the days after a severe wind storm scoured material from the front of the seawall and deposited it about mid-beach. Over the next several days, the swash bar migrated up the beach profile, eventually re-burying the scoured foot of the seawall. The landward migration and welding of gravel ridges to the upper foreshore during flood tides is an important mechanism for building and maintaining the storm berm on mixed-sediment beaches (Pontee et al. 2004).

5.5.2. Cobble Lags and Beach Armoring

Another interesting characteristic of Puget Sound beaches is the distribution of cobbles and boulders. Lag stones are large boulders that have been eroded out of coastal bluffs and deposited on the beach face (Figure 5.18). There is a certain size beyond which no wind-wave generated in Puget Sound can mobilize these



Figure 5.17. Transverse bars off the west coast of Camano Island. Photo by M. Baum.



Figure 5.18. Lag stones at Foulweather Bluff.

stones and they become abandoned in place. The beach simply evolves around them. In some places cobbles are sufficiently dense that they form a nearly continuous surface—a cobble lag deposit. These surfaces may not be completely immobile under storm conditions, but they are stable enough that they tend to be heavily encrusted with marine life. Lag deposits sometimes have a sunken or deflated appearance caused by the fine-grained matrix being well recessed into the interstitial spaces of the larger clasts. This suggests that either (1) the a finer-grained matrix material has partially filled the interstitial spaces between the larger clasts (in-filling); or (2) that the fine-grained matrix has been removed to a depth of about half a cobble diameter (deflation).

Surface armoring is a related phenomenon that is found on many mixed-sediment beaches in Puget Sound (Figure 5.19). An armored surface constitutes a nearly homogeneous layer of gravel. Immediately beneath this surface layer, one finds a much more heterogeneous mixture of sand and gravel. The difference between the surface armor and subsurface is mainly the addition of fine-grained material to the mix rather than a loss of coarse clasts. Various mechanisms have been suggested for armoring including (a) gravel overpassing during the backwash, (b) a process similar to kinetic sieving when the bed is fluidized during the swash cycle, and (c) winnowing of fine-grained materials during the decelerating phase of the backwash (Mason and Coates 2001). As opposed to gravel rivers, there has been almost no research on surface armoring of beaches under oscillatory flow, so determining what effect armoring might have on beach morphodynamics is difficult. Certainly, armoring increases surface roughness and may prevent fine-grained sediment transport during quiescent conditions, but these gravels can be easily mobilized during storm-wave conditions, exposing the main body of the beach to wave action, thereby limiting the protection benefit.

Surface armoring presents a conceptual problem. There is a tendency to describe Puget Sound beaches as gravel beaches based on the characteristic of the surface layer. Pure gravel beaches are permeable and have very different hydrodynamics than a mixed sand-and-gravel beach, which has a permeability determined by the fine-grained fraction (Section 5.1.1). For mixed-sediment beaches with as little as 25% by volume sand, the permeability of the beach is similar to that of a pure sand beach. Hence, most of the gravel literature that focuses on increased permeability as a mechanism for asymmetric run-up must be carefully vetted before applying it to Puget Sound.



Figure 5.19. Surface pavements (armoring) developed on gravel beaches: (A) a pit carved through the surface pavement (Cama Beach), (B) surface gravel pavement and subsurface sand-gravel mixture (Cama Beach), (C) surface gravel pavement and subsurface sand-gravel mixture (Allyn).

6. Conclusions

The purpose of this report has been to describe important aspects about the morphology and dynamic behavior of beaches commonly found around Puget Sound. Although many of the observations presented here should be useful for shoreline managers, scientists, and coastal engineers, two points bear special consideration: (1) the importance of the tidal distribution curve, and (2) the role of extreme storm events in shaping the intertidal morphodynamic system.

6.1. Tidal Distribution Curve

The upward skew in the tidal distribution curve for Puget Sound (Figure 4.2) controls the zone of sediment transport on the foreshore by concentrating wave attack high on the foreshore. The long-term distribution of semidiurnal tides in Puget Sound is always upwardly skewed. The joint probability of a stochastic process (waves) imprinted on a deterministic process (tides) will always take on a distribution reflecting the deterministic curve, given enough time. The most important ramification of this for Puget Sound is the definition of a narrow, high-tide corridor where wave energy is concentrated and sediment transport is most active. Sediment transport of coarse sand or larger particles outside this zone may be negligible (Figure 5.8).

The tidal distribution curve controls more than just wave-energy levels. Desiccation, light exposure, and the beach groundwater system are also directly controlled by the tides. Hence, the character of the vertical distribution of the tides will have an impact on a broad range of intertidal phenomena, either directly or indirectly. Also, the timing of tides may be critical to habitat. For example, during the summer, low tides occur during the

daytime, which exposes lower intertidal habitat to wave energy generated by summertime pleasure craft. Whether this wave energy increase is severe enough to have an impact on the lower intertidal ecosystem is unknown. An appreciation for the tidal distribution curve and its potential affects on the nearshore system is an important step in characterizing the physical controls on the beach.

6.2. Role of Extreme Storm Events

In a high-energy environment, cycles of erosion and accretion are driven by seasonal changes in storm intensity. In contrast, a low-energy beach erosion cycle may be triggered by individual storms with much longer return intervals. At Cama Beach, for example, a storm with an estimated 3 to 5 year return interval dominated observed beach changes. An interannual view of shoreline morphodynamics on the order of 5 years is tenable in the planning community and would give managers a better sense of the dynamic characteristics of a beach. Studies based on shorter timeframes risk never observing the critical hours during which the beach is most active.

Puget Sound is an extraordinary resource to the Pacific Northwest and the beaches of the Sound are an important part of the marine ecosystem. Significant urbanization of the Sound over the coming decades will put development pressure on the shorelines, as well as fundamentally alter upland sediment and water supplies to the beach. If conservation and restoration efforts are going to succeed in preserving a functional littoral system, detailed, quantitative studies of the nearshore morphodynamics will need to become a larger priority than they are at present.

References

- Allan J.C., and P.D. Komar. 2002. Extreme storms on the Pacific Northwest coast during the 1997–98 El Niño and 1998–99 La Niña. *J. Coast. Res.* 18:175–193.
- Anonymous. 1999. Endangered and threatened species: threatened status for three Chinook salmon evolutionarily significant units in Washington and Oregon, and endangered status of one Chinook salmon ESU in Washington; final rule. Tech. rep. National Marine Fisheries Service.
- Anthony, E.J. 1998. Sediment-wave parametric characterization of beaches. *J. Coast. Res.* 14:347–352.
- Anthony, E.J., and J.D. Orford. 2002. Between wave- and tide-dominated coasts: the middle ground revisited. *J. Coast. Res., Spec. Issue* 36:8–15 (ICS 2002 Proceedings).
- Armstrong, J.E., D.R. Crandell, D.J. Easterbrook, and J.B. Noble. 1965. Late Pleistocene stratigraphy and chronology in southwestern British Columbia and northwestern Washington. *Geol. Soc. Am. Bull.* 76:321–330.
- Atwater, B.F. 1999. Radiocarbon dating of a Seattle earthquake to A.D. 900–930 [abstract]. *Seismol. Res. Ltr.* 70:232.
- Ballantyne, C.K. 2002. Paraglacial geomorphology. *Quat. Sci. Rev.* 21:1935–2017.
- Bancroft, G.P. 1999. Marine weather review, north Pacific area, December 1998 through March 1999. *Mar. Weath. Logs* 43:36–43.
- Bauer, W. 1974. The drift sectors of Whatcom County marine shores: their shoreforms and geo-hydraulic status. Tech. Rep. 74. Whatcom County Planning Commission, Bellingham, Washington.
- Bauer, W. 1978. Marine shore resource analysis: shoreline dynamics. Tech. rep. Washington State Dep. Ecology, Shorelands and Coastal Zone Management Program. Olympia.
- Berry H.D., J.R. Harper, T.F. Mumford, Jr. B.E. Bookheim, A.T. Sewell, and L.J. Tamayo. 2001. The Washington State shorezone inventory user's manual. Tech. rep. Washington State Dep. Nat. Res., Nearshore Habitat Program. Olympia.
- Booth, D.B. 1994. Glaciofluvial infilling and scour of the Puget Lowland, Washington, during ice-sheet glaciation. *Geology* 22:695–698.
- Booth, D.B., and B. Hallet. 1993. Channel networks carved by subglacial water; observations and reconstruction in the eastern Puget Lowland of Washington. *Geol. Soc. Am. Bull.* 105:671–683.
- Booth, D.B., K.G. Troost, and J.T. Hagstrum. 2004. Deformation of Quaternary strata and its relationship to crustal folds and faults, south-central Puget Lowland, Washington State. *Geology* 32:505–508.
- Bretz, J.H. 1913. Glaciation of the Puget Sound region. Tech. Rep. Bulletin No. 8. Washington Geological Survey.
- Bucknam, R.C., E. Hemphill-Haley, and E.B. Leopold. 1992. Abrupt uplift within the past 1700 years at southern Puget Sound, Washington. *Science* 258:1611–1614.
- Butt, T., and P.E. Russell. 2000. Hydrodynamics and cross-shore sediment transport in the swash zone of natural beaches: a review. *J. Coast. Res.* 16:255–268.
- Clague, J.J. 1983. Glacio-isostatic effects of the Cordilleran ice sheet, British Columbia, Canada. Pages 321–343 in D.E. Smith, and A.G. Sawson (eds.), *Shorelines and Isostasy*. Institute of British Geographers.
- CERC (Coastal Engineering Research Center). 1984. *Shore Protection Manual*, Vol. 1, 4th ed. U.S. Army Corps of Engineers, Washington, D.C.
- CO-OPS (Center for Operational Oceanographic Services). 1983–2002. Verified and historical water level data—9447130 Seattle, Puget Sound, Washington. Computer file. Available: <http://tidesandcurrents.noaa.gov/>.
- Crandell, D.R., D.R. Mullineaux, and H.H. Waldron. 1958. Pleistocene sequence in southeastern part of the Puget Sound Lowland, Washington. *Am. J. Sci.* 256:384–397.
- Crandell, D.R., D.R. Mullineaux, and H.H. Waldron. 1965. Age and origin of the Puget Sound trough in western Washington. Prof. Pap. 525-B. U.S. Geological Survey, Denver, Colorado.
- Downing, J. 1983. *The Coast of Puget Sound: Its Processes and Development*. University of Washington Press, Seattle.
- Easterbrook, D.J. 1963. Late Pleistocene glacial events and relative sea-level changes in the northern Puget Lowland, Washington. *Geol. Soc. Am. Bull.* 74:1465–1483.
- Easterbrook, D.J. 1968. Part I: Pleistocene stratigraphy of Island County. Pages 1–34 in *Water Supply Bulletin No. 25*. Washington State Dep. Water Resources. Olympia.
- Ecker, R.M., D.W. Mayer, and S.M. Brown. 1979. Littoral processes—Sequim Bay and adjacent Strait of Juan de Fuca shoreline. Tech. rep. Battelle Northwest Laboratories, Richland, Washington.
- Finlayson, D.P. 2006. The geomorphology of Puget Sound beaches. Ph.D. dissertation. University of Washington, Seattle. 216 p.
- Finlayson, D.P., and H. Shipman. 2003. Puget Sound drift cells: The importance of waves and wave climate. *Puget Sound Notes* 47:1–4.
- Fonseca, M.S. 1983. The role of current velocity in structuring eelgrass (*Zostera marina* L.) meadows. *Est. Coast. Shelf Sci.* 17:367–380.
- Fonseca, M.S., and J.A. Cahalan. 1992. A preliminary evaluation of wave attenuation by four species of seagrass. *Est. Coast. Shelf Sci.* 35:565–576.
- Fonseca, M.S., and J.S. Fisher. 1986. A comparison of canopy friction and sediment movement between four species of seagrass with reference to their ecology and restoration. *Mar. Ecol. Prog. Ser.* 29:15–22.

- Galster, R.W., and M.L. Schwartz. 1989. Ediz Hook—A case history of coastal erosion and rehabilitation. *In* M.L. Schwartz and E.C.F. Bird (eds.), *Artificial Beaches*. *J. Coast. Res.*, Special Issue 6.
- Gardner, J.V., E.J. Van Deen Ameele, and P. Dartnell. 2001. Multibeam mapping of the major deltas of southern Puget Sound, Washington. Open File Rep. R-1-01-WA. U.S. Geological Survey, Coastal and Marine Geology, Menlo Park, California.
- Gerstel, W.J., M.J. Brunengo, W.S. Lingley, Jr., R.L. Logan, H. Shipman, and T.J. Walsh. 1997. Puget Sound bluffs: the where, why and when of landslides following the holiday 1996/97 storms. *Wash. Geol.* 25:17–31.
- Goldstein, B. 1994. Drumlins of the Puget Lowland, Washington State, USA. Pages 299–311 *in* *Subglacial Processes, Sediments and Landforms*, Vol. 91. Elsevier, Amsterdam.
- Gregg M., and D.P. Finlayson. 2002. Swath bathymetry of Possession Sound. University of Washington, Seattle (Cruise TN146 & TN147).
- Halladay, N.E. 1970. Local-area forecaster's handbook. Tech. rep. Naval Weather Service Environmental Detachment.
- Hegge, B., I. Eliot, and J. Hsu. 1996. Sheltered sandy beaches of southwestern Australia. *J. Coast. Res.* 12:748–760.
- Hewitt, A.T., and D.C. Mosher. 2001. Late Quaternary stratigraphy and sea floor geology of eastern Juan de Fuca Strait, British Columbia and Washington. *Mar. Geol.* 177:295–316.
- Horn, D.P. 2002a. Mesoscale beach processes. *Prog. Phys. Geol.* 26:271–289.
- Horn, D.P. 2002b. Beach groundwater dynamics. Pages 121–146 *in* 29th Binghamton Geomorphology Symposium; Coastal Geomorphology, Vol. 48. Elsevier, Amsterdam.
- Jackson, D.W.T., J.A.G. Cooper, and L. del Rio. 2005. Geologic control of beach morphodynamic state. *Mar. Geol.* 216:297–314.
- Jackson, N.L., K.F. Nordstrom, I. Eliot, and G. Masselink. 2002. “Low energy” sandy beaches in marine and estuarine environments: A review. *Geomorphology* 48:147–162.
- Jacobsen, E.E., and M.L. Schwartz. 1981. The use of geomorphic indicators to determine the direction of net shore-drift. *Shore and Beach* 49:8–42.
- JALBXTX (Joint Airborne Lidar Bathymetry Technical Center of Expertise). 2003. Puget Sound CHARTS survey, fall 2003. Computer Files. Under contract: U.S. Army Corps of Engineers.
- Kelsey, H.M., B. Sherrod, S.Y. Johnson, and S.V. Dadisman. 2004. Land-level changes from a late Holocene earthquake in the northern Puget Lowland, Washington. *Geology* 32:469–472.
- Keuler, R.F. 1979. Coastal zone processes and geomorphology of Skagit County, Washington. Master's thesis. Western Washington University. Bellingham.
- Keuler, R.F. 1988. Map showing coastal erosion, sediment supply, and longshore transport in the Port Townsend 30- by 60-minute quadrangle, Puget Sound region, Washington. Misc. Invest. Ser., Map I-1198-E. U.S. Department of Interior, U.S. Geological Survey.
- Komar, P.D. 1998. *Beach Processes and Sedimentation*. Second Edition. Prentice Hall, Upper Saddle River, New Jersey. 544 p.
- Kulkarni, D.C., F. Levoy, O. Monfort, and J.R. Miles. 2004. Morphological variations of a mixed sediment beachface (Teignmouth, UK). *Cont. Shelf Res.* 24:1203–1218.
- Mason, T., and T.T. Coates. 2001. Sediment transport processes on mixed beaches: a review for shoreline management. *J. Coast. Res.* 17:645–657.
- Mass, C. 1981. Topographically forced convergence in western Washington State. *Month. Weath. Rev.* 110:170–183.
- Masselink, G., and M. Hughes. 1998. Field investigation of sediment transport in the swash zone. *Continent. Shelf Res.* 18:1179–1199.
- Masselink G., and A.D. Short. 1993. The effect of tide range on beach morphodynamics and morphology: A conceptual beach model. *J. Coast. Res.* 9:785–800.
- Maunder, W.J. 1968. Synoptic weather patterns in the Pacific Northwest. *Northw. Sci.* 42:80–88.
- Miles, J.R., and P.E. Russell. 2004. Dynamics of a reflective beach with a low tide terrace. *Continent. Shelf Res.* 24:1219–1247.
- Mofjeld, H.O. 1989. Long-term trends and interannual variations of sea level in the Pacific Northwestern region of the United States. Pages 228–230 *in* *Proceedings, Oceans '89 Conference*, Seattle, Washington, September 18–21, 1989, Vol. 1. Marine Technology Society, IEEE Publication Number 89CH2780-5.
- Mofjeld, H.O. 1992. Subtidal sea level fluctuations in a large fjord system. *J. Geophys. Res.* 97:20191–20199.
- Mofjeld, H.O., and L.H. Larsen. 1984. Tides and tidal currents of the inland waters of western Washington. NOAA Tech. Memo. ERL PMEL-56. NOAA Fisheries, Pacific Marine Environmental Laboratory. Seattle.
- Mofjeld, H.O., A.J. Venturato, V.V. Titov, F.I. Gonzoález, and J.C. Newman. 2002. Tidal datum distributions in Puget Sound, Washington, based on a tide model. NOAA Tech. Memo. OAR PMEL-122. NOAA, Pacific Marine Environmental Laboratory. Seattle.
- NDBC (National Data Buoy Center). 2003. Station WPOW1—West Point, Washington, continuous winds data (1996–2002). Computer File. Available: <http://www.ndbc.noaa.gov>.
- NOAA—Cooperative Institute for Research in Environmental Studies Climate Diagnostics Center. 2005. Southern Oscillation Index (SOI). Boulder, Colorado.
- NOAA—National Environmental Satellite, Data, and Information Service. 1999. GOES western US sector color enhanced infrared image.
- NearPRISM. 2000. Proposal. Washington Sea Grant program 2001–2003: Development of a spatially-explicit, biophysical model of Puget Sound nearshore processes.
- Nordstrom, K.F. 1992. *Estuarine Beaches: An Introduction to the Physical and Human Factors Affecting Use and Management of Beaches in Estuaries, Lagoons, Bays and Fjords*. Elsevier Applied Science, London.
- Nordstrom, K.F., and N.L. Jackson. 1992. Two dimensional change on sandy beaches in meso-tidal estuaries. *Zeitsch. Geomorph.* 36:465–478.

- Orford, J.D., D.L. Forbes, and S.C. Jennings. 2002. Organisational controls, typologies and time scales of paraglacial gravel-dominated coastal systems. Pages 51–85 in *Proceedings of the 29th Binghamton Geomorphology Symposium: Coastal Geomorphology*, Woods Hole Institute, Massachusetts, November 1998. Elsevier, Amsterdam.
- Overland, J.E., and B.A. Walter, Jr. 1983. Marine weather of the inland waters of western Washington. NOAA Tech. Memo. ERL PMEL-44. NOAA, Pac. Mar. Environ. Lab. Seattle.
- Phillips, E.C. 1968. Washington climate for these counties: King, Kitsap, Mason and Pierce. Tech. Rep. E.M. 2734. Washington State University.
- Phillips, R.C. 1984. The ecology of eelgrass meadows in the Pacific Northwest: a community profile. Tech. Rep. FWS/OBS-84/24. U.S. Fish Wildl. Serv., National Coastal Ecosystems Team, Div. Biological Services, Research and Development.
- Pontee, N.I., K. Pye, and S.J. Blott. 2004. Morphodynamic behaviour and sedimentary variation of mixed sand and gravel beaches, Suffolk, UK. *J. Coast. Res.* 20:256–276.
- Porter, S.C., and T.W. Swanson. 1998. Radiocarbon age constraints on rates of advance and retreat of the Puget Lobe of the Cordilleran ice sheet during the last glaciation. *Quat. Res.* 50:205–213.
- PSLC (Puget Sound Lidar Consortium). 2000–2004. Lidar bare earth DEM. Computer file. Available: <http://rocky2.ess.washington.edu/data/raster/lidar/>.
- Pugh, D.T. 1987. *Tides, Surges and Mean Sea-Level*. John Wiley & Sons, Chichester.
- Read, W. 2004. Seattle's strongest windstorms 1950–2002. Table. Available: <http://oregonstate.edu/~readw/SeattleBigStorms.html>.
- Schoenberg, S.A. 1983. Regional wind patterns of the inland waters of western Washington and southern British Columbia. NOAA Tech. Memo. ERL PMEL-43. NOAA, Pac. Mar. Environ. Lab. Seattle.
- Schwartz, M.L. 1971. Shannon point cliff recession. *Shore and Beach* 39:45–48.
- Schwartz, M.L., R.S. Wallace, and E.E. Jacobsen. 1989. Net shore-drift in Puget Sound. Tech. Rep. Bull. 78. Washington State Dep. Nat. Res., Div. Geology and Earth Resources. Olympia.
- Sherrod, B.L., R.C. Bucknam, and E.B. Leopold. 2000. Holocene relative sea level changes along the Seattle Fault at Restoration Point, Washington. *Quat. Res.* 54:384–393.
- Shipman, H. 1989. Vertical land movements in coastal Washington: Implications for relative sea level changes. Tech. Rep. PV-11. Washington State Dep. Ecology, Shorelands and Coastal Zone Management Program. Olympia.
- Shipman, H. 1995. The rate and character of shoreline erosion on Puget Sound. In E.R. Strickland (ed.), *Puget Sound Research '95 Proceedings*. Puget Sound Water Quality Action Team. Seattle.
- Shipman, H. 2001. Coastal landsliding on Puget Sound: A review of landsliding occurring between 1996 and 1999. Tech. Rep. 01-06-019. Washington State Dep. Ecology, Shorelands and Environmental Assistance Program. Olympia.
- Shipman, H. 2004. Coastal bluffs and sea cliffs on Puget Sound, Washington. Pages 81–94 in M.A. Hampton, and G.B. Griggs (eds.), *Formation, Evolution, and Stability of Coastal Cliffs—Status and Trends*, Prof. Pap. 1693. U.S. Geological Survey. Denver.
- Sylwester, R.E., and M.L. Holmes. 1989. Marine geophysical evidence of a recent submarine slope failure in Puget Sound Washington. Pages 1524–1529 in *Offshore Technology Conference*, Vol. 5. Seattle.
- Thorson, R.M. 1980. Ice-sheet glaciation of the Puget Lowland, Washington, during the Vashon Stage (late Pleistocene). *Quat. Res.* 13:303–321.
- Thorson, R.M. 1989. Glacio-isostatic response of the Puget Sound area, Washington. *Geol. Soc. Am. Bull.* 101:1163–1174.
- Transboundary Georgia Basin–Puget Sound Environmental Indicators Working Group. 2002. *Georgia Basin–Puget Sound ecosystem indicators report*. Tech. Rep. 02-01-002. Washington State Dep. Ecology and Georgia Basin Ecosystem Initiative. Olympia.
- Turner, I. 1993. Water table outcropping on macro-tidal beaches: A simulation model. *Mar. Geol.* 115:227–238.
- van Osch, E. 1990. Coastal bluff erosion in the Strait of Georgia region: geomorphology and management. Master's thesis. Simon Fraser University, Vancouver. British Columbia.
- Wallace, R.S. 1988. Quantification of net shore-drift in Puget Sound and the Strait of Juan de Fuca, Washington. *J. Coast. Res.* 4:395–403.
- Wantz, J.W., and R.E. Sinclair. 1981. Distribution of extreme winds in the Bonneville Power Administration service area. *J. Appl. Meteor.* 20:1400–1411.
- Ward, L.G., W.M. Kemp, and W.R. Boynton. 1984. The influence of waves and seagrass communities on suspended particulates in an estuarine embayment. *Mar. Geol.* 59:85–103.
- Wells, R.E., C.S. Weaver, and R.J. Blakely. 1998. Fore-arc migration in Cascadia and its neotectonic significance. *Geology* 26:759–762.
- Wolman, M.G., and J.P. Miller. 1960. Magnitude and frequency of forces in geomorphic processes. *J. Geol.* 68:54–74.
- Worcester, S.E. 1995. Effects of eelgrass beds on advection and turbulent mixing in low current and low shoot density environments. *Mar. Ecol. Prog. Ser.* 126:223–232.
- Wright, L.D., and A.D. Short. 1984. Morphodynamic variability of surf zones and beaches: A synthesis. *Mar. Geol.* 56:93–118.
- Youngmann, C. 1977–1980. Coastal zone atlas of Washington. Report DOE Report 77-21-1 through 77-21-12. Washington State Dep. Ecology.

PSNERP and the Nearshore Partnership

The Puget Sound Nearshore Ecosystem Restoration Project (PSNERP) was formally initiated as a General Investigation (GI) Feasibility Study in September 2001 through a cost-share agreement between the U.S. Army Corps of Engineers and the State of Washington, represented by the Washington Department of Fish and Wildlife. This agreement describes our joint interests and responsibilities to complete a feasibility study to

“... evaluate significant ecosystem degradation in the Puget Sound Basin; to formulate, evaluate, and screen potential solutions to these problems; and to recommend a series of actions and projects that have a federal interest and are supported by a local entity willing to provide the necessary items of local cooperation.”

The current Work Plan describing our approach to completing this study can be found at:

<http://www.pugetsoundnearshore.org/documents/StrategicWorkPlanfinal.pdf>

Since that time, PSNERP has attracted considerable attention and support from a diverse group of individuals and organizations interested and involved in improving the health of Puget Sound nearshore ecosystems and the biological, cultural, and economic resources they support. The Puget Sound Nearshore Partnership is the name we have chosen to describe this growing and diverse group, and the work we will collectively undertake that ultimately supports the goals of PSNERP, but is beyond the scope of the GI Study.

Collaborating with the Puget Sound Action Team, the Nearshore Partnership seeks to implement portions of their Work Plan pertaining to nearshore habitat restoration issues. We understand that the mission of PSNERP remains at the core of our partnership. However restoration projects, information transfer, scientific studies and other activities can, and should occur to, advance our understanding, and ultimately, the health of the Puget Sound nearshore beyond the original focus and scope of the on-going GI Study. As of the date of publication for this Technical Report, our partnership includes participation by the following entities:

Interagency Committee for Outdoor Recreation
King Conservation District
King County
National Wildlife Federation
NOAA Fisheries
Northwest Indian Fisheries Commission
People for Puget Sound
Pierce County
Puget Sound Action Team
Salmon Recovery Funding Board
Taylor Shellfish Company
The Nature Conservancy
U.S. Army Corps of Engineers
U.S. Environmental Protection Agency
U.S. Geological Survey
U.S. Fish and Wildlife Service
U.S. Navy
University of Washington
Washington Department of Ecology
Washington Department of Fish and Wildlife
Washington Department of Natural Resources
Washington Public Ports Association
Washington Sea Grant
WRIA 9

PUGET SOUND NEARSHORE PARTNERSHIP



RESTORING OUR
ECOSYSTEM HEALTH